A THREE PHASE ALL SIC PWM RECTIFIER FOR INDUSTRY APPLICATIONS

A THESIS SUBMITTED TO
THE GRADUATE SCHOOL OF NATURAL AND APPLIED SCIENCES
OF
MIDDLE EAST TECHNICAL UNIVERSITY

BY

CEM YOLAÇAN

IN PARTIAL FULFILLMENT OF THE REQUIREMENTS
FOR
THE DEGREE OF MASTER OF SCIENCE
IN
ELECTRICAL AND ELECTRONICS ENGINEERING

DECEMBER 2019

Approval of the thesis:

A THREE PHASE ALL SIC PWM RECTIFIER FOR INDUSTRY APPLICATIONS

submitted by **CEM YOLAÇAN** in partial fulfillment of the requirements for the degree of **Master of Science in Electrical and Electronics Engineering Department, Middle East Technical University** by,

Prof. Dr. Halil Kalıpçılar
Dean, Graduate School of **Natural and Applied Sciences** _____

Prof. Dr. İlkay Ulusoy
Head of Department, **Electrical and Electronics Eng.** _____

Prof. Dr. Muammer Ermiş
Supervisor, **Electrical and Electronics Eng., METU** _____

Examining Committee Members:

Assist. Prof. Dr. Ozan Keysan
Electrical and Electronics Eng, METU _____

Prof. Dr. Muammer Ermiş
Electrical and Electronics Eng., METU _____

Assist. Prof. Dr. Emine Bostancı
Electrical and Electronics Eng, METU _____

Assoc. Prof. Dr. Murat Göl
Electrical and Electronics Eng, METU _____

Prof. Dr. Işık Çadırcı
Electrical and Electronics Eng, Hacettepe University _____

Date: 13.12.2019

I hereby declare that all information in this document has been obtained and presented in accordance with academic rules and ethical conduct. I also declare that, as required by these rules and conduct, I have fully cited and referenced all material and results that are not original to this work.

Name, Surname: Cem Yolaçan

Signature:

ABSTRACT

A THREE PHASE ALL SIC PWM RECTIFIER FOR INDUSTRY APPLICATIONS

Yolaçan, Cem
Master of Science, Electrical and Electronics Engineering
Supervisor: Prof. Dr. Muammer Ermiş

December 2019, 104 pages

In this thesis work, a three phase PWM Rectifier for industry applications will be designed by using SiC Power MOSFETs and its laboratory prototype will then be implemented. The topology of the PWM rectifier is the three phase full bridge topology to convert three phase 400 V AC line-to-line voltage to desirable voltage levels between 500V and 1000V. The PWM Rectifier has the capability of permitting the flow of active power in both directions. The new technology SiC Power MOSFETs can operate at higher frequencies than IGBTs which provide higher efficiency because of lower switching losses and comparable conduction losses. Furthermore, operation at higher frequencies also provides us much lower acoustic noise levels and less harmonic distortion in line current waveforms during the operation of the rectifier. The theoretical results will be verified by experimental work.

Keywords: PWM Rectifier, SiC Power MOSFET

ÖZ

ENDÜSTRİYE YÖNELİK UYGULAMALAR İÇİN BÜTÜNÜYLE SİC GÜÇ MOSFET TEKNOLOJİSİNE DAYALI ÜÇ FAZ PWM DOĞRULTUCU

Yolaçan, Cem
Yüksek Lisans, Elektrik ve Elektronik Mühendisliği
Tez Danışmanı: Prof. Dr. Muammer Ermiş

Aralık 2019, 104 sayfa

Bu tez çalışmasında, endüstriye yönelik uygulamalar için SiC Güç MOSFETleri kullanılarak 3 faz PWM Doğrultucu tasarlanacak ve bire bir boyutlarda laboratuvar prototipi gerçekleştirilecektir. PWM Doğrultucu 3 faz tam köprü topolojisine sahip olup, 3 faz 400 V AA voltajını 500-1000 arası DA voltajına çevirmektedir. PWM Doğrultucu iki yönde de aktif güç akışı kabiliyetine sahiptir. Yeni teknoloji SiC Güç MOSFET'leri günümüzde kullanılan IGBT'lere göre daha yüksek frekanslarda çalışabilmekte bu da düşük anahtarlama kayıpları ve kıyaslanabilir iletim kayıplarından dolayı daha yüksek bir verim sağlamaktadır. Ayrıca, daha yüksek frekanslarda çalışmak, doğrultucunun operasyonu sırasında çok daha düşük bir akustik gürültü seviyesi ve hat akımı dalga şeklinde daha az harmonik bozunum sağlamaktadır. Teorik sonuçlar, laboratuvar ortamındaki deneysel çalışmayla doğrulanacaktır.

Anahtar Kelimeler: PWM Doğrultucu, SiC Güç MOSFETi

To my family

ACKNOWLEDGEMENTS

I am truly grateful to my supervisor Prof. Dr. Muammer ERMİŞ, who has been an exceptional advisor to me with his guidance, insights, encouragement and patience throughout this study and it was a privilege to work with during my time in the department.

I would like to show my gratitude to Prof. Dr. Işık Çadırcı as well for her valuable advice and remarks.

I also would like to thank Doğan Yıldırım for his valuable guidance and support. I am lucky to have worked with such a hardworking and experienced engineer.

I wish to thank my friends, Hakan Akşit, Serkan Öztürk, Behrang Aghdam and Tevfik Pul for their contributions in my experimental study.

I also would like to thank ASELSAN UGES for its financial support to make the experimental setup possible.

I wish to thank my friends Caner Sağlam, Özgün Çokgezen and Özgür Hamat for their support and motivation.

Lastly, and most importantly, I am very grateful to my family for their endless support, patience and understanding.

TABLE OF CONTENTS

LIST OF TABLES

TABLES

LIST OF FIGURES

FIGURES

CHAPTER 1

INTRODUCTION

Rectifiers are utilized in many areas from small electronic appliances to high power applications such as converting AC to DC for high-voltage direct current power transmission. Depending on the application, types are varied such as diode, thyristor or PWM rectifiers.

Application areas of rectifiers which have transistors as switching elements are expanding with the advancement of semiconductor technology, due to the need for high efficiency, unity power factor, bidirectional operation and output voltage with high controllability. Three Phase PWM Rectifiers with IGBT switching elements are one of the most common type of rectifiers in industry where the features above are required to utilize.

1.1. SiC Power MOSFET Technology

Conventional Si based power MOSFETs and IGBTs were widely used switching elements in power electronics applications. In the last decade with the emerge of the SiC based Power MOSFETs with wide band-gap [1], the application of power electronics with SiC MOSFETs in low and medium power levels started to increase. Reason for that is, SiC Power MOSFETs have better material properties when compared to Si IGBTs [2]–[4]. Studies have shown that converters with SiC based switching elements are able to reach over 99% efficiency [5]. The transition to SiC based switching elements first occurred with IGBT-SiC Schottky Diode hybrid systems [6]. Then, all SiC MOSFETs, which consist of SiC MOSFET and SiC Schottky body diode started to widen.

Technical properties of SiC material in power semiconductors in comparison with Si and GaN materials are already described in [1] as given in Figure 1-1.

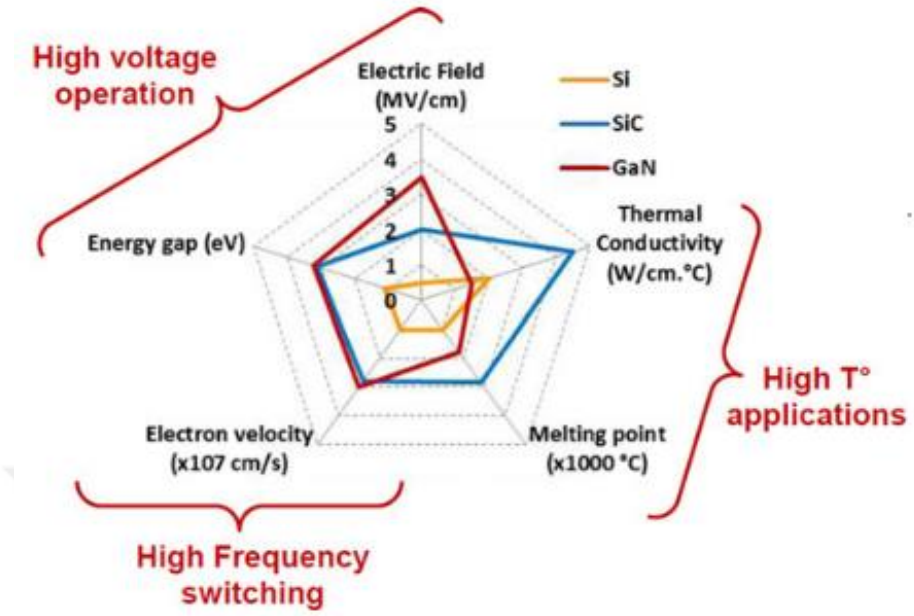

Figure 1-1 Summary of Si, SiC, and GaN relevant material properties [7]

A comparison of SiC Power MOSFETs with HV-IGBTs can be made as follows:

- Operating at higher junction temperatures
- In medium power applications, as a wide bandgap device, SiC power MOSFETs can be switched at higher frequencies (a few tens of kHz) in comparison with Si IGBTs. They have lower turn-on and turn-off losses which decrease the switching loss of the system, thus illustrating higher efficiency at the same switching frequency [1], [8].
- Comparable or lower on-state resistance and hence conduction loss
- Higher switching frequency also ensures reduced sized filtering elements, thus makes the converter reduced weight and size [9].
- At the present time, they are more costly

1.2. Three Phase PWM Rectifier Topology

For AC-DC conversion there are various topologies that are widely used in the industry such as line commutated with diode and thyristors, or with power factor correction such as Vienna, boost or regenerative rectifiers [10], [11].

Although many have advantages in different applications, regenerative three phase two level voltage source rectifier is the one with the abilities suitable for our work.

Three phase two level voltage source PWM Rectifier topology is given Figure 1-2. This PWM Rectifier topology when implemented by the use of SiC Power MOSFETs will have the following features in industry applications:

a. Simple and cheap
b. Ease in control
c. More reliable and
d. Minimum component count

Further than these

e. Unity power factor operation on ac side
f. Nearly harmonic-free line current waveforms on grid side owing to high switching frequency.

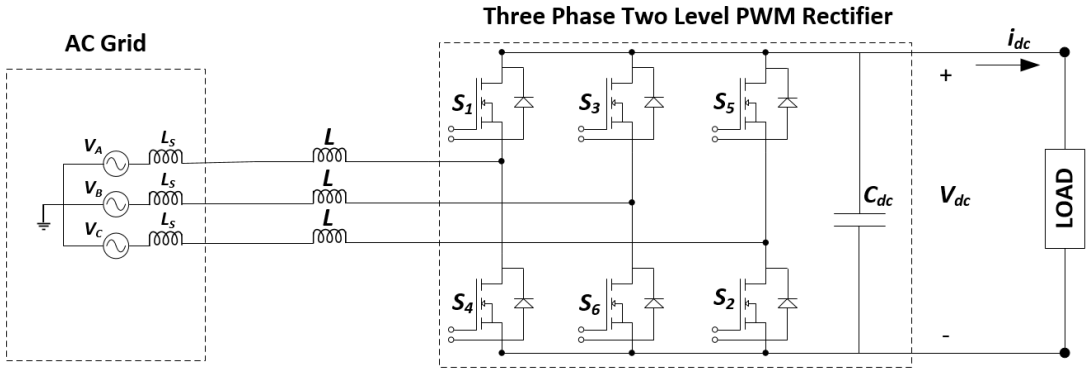

Figure 1-2 Three phase two level voltage source rectifier topology

In today's technology most of the Regenerative PWM Rectifiers are implemented with IGBT switching elements which have smaller than 5kHz switching frequencies at high power levels because the increasing switching losses as the frequency gets higher. In this work, Three Phase PWM Rectifier will be implemented with SiC Power MOSFETs to obtain efficiencies around 99% and accomplish an AC-DC converter with high power density, smaller volume.

1.3. The Scope of This Work:

The starting point of this work is to create a variable, controlled DC voltage level in the laboratory, which is constructed for designing and testing new technology traction converters. Due to this reason, in Traction Systems R&D Laboratory, a 400V, 50 Hz grid connected All SiC Three Phase PWM Rectifier with 225kW rated power is designed and implemented. For the All SiC Three Phase PWM Rectifier in Traction Systems R&D Laboratory a previous work conducted, in which, PWM Rectifier topologies are compared, selection criteria for the components used in PWM Rectifier are explained, Si IGBT and SiC MOSFETs are compared with respect to losses, control strategies and modulation techniques are inspected [12].

The structure of the laboratory test system in Traction Systems R&D Laboratory is explained in [13].

In Chapter 2, Industrial applications of All SiC PWM Rectifier is discussed.

Operation principles and modes, control of the rectifier, simulations at the different voltage levels and implementation of the rectifier are presented in Chapter 3.

In Chapter 4, description of the load system in the laboratory is conducted. Then, experimental results at various output DC voltage and load levels are shown. Efficiency analysis and comparison with theoretical values are clarified. Finally, the harmonic spectrum of the input AC voltages is investigated.

In Chapter 5, Conclusion of the work and possible future improvements are discussed.

CHAPTER 2

INDUSTRIAL USE OF PWM RECTIFIER

In this chapter, industrial applications of PWM Rectifier are discussed. Among these application, there are published work about AC Motor Drive, Battery Charger and Supercapacitor Energy Storage Systems for All SiC Three Phase PWM Rectifier. Resistive Furnaces, DC Motor Drives, Synchronous Motor Field Exciters are not commercially available and do not have published work with this system.

2.1. Resistive Furnaces; Electric Heating

Conventional methods consist of Diode and Thyristor Rectifiers for the application of resistive furnaces and electric heating systems [14]. However, these systems cause high harmonic current components on the grid side. Reactive power variations occur due to the nature of these systems. DC Choppers are also used for reducing THD and increasing power factor for high power applications. [15]

All SiC Three Phase PWM Rectifiers can be suitable for these systems at medium power levels. By using Three Phase PWM Rectifier, the unity power factor operation is accomplished and low THD input is obtained. In this application output DC voltage is adjustable and the power flow is unidirectional. However, it would be more expensive to implement than conventional methods and bidirectional capabilities will not be used.

In Figure 2-1 the structure of the system is shown. All SiC PWM Rectifier is connected directly to grid or via a transformer for galvanic isolation.

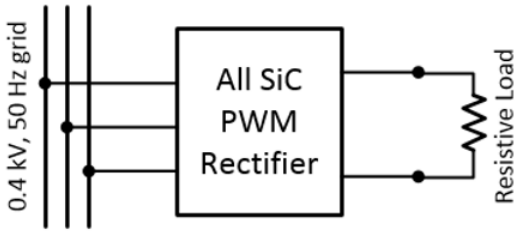

(a)

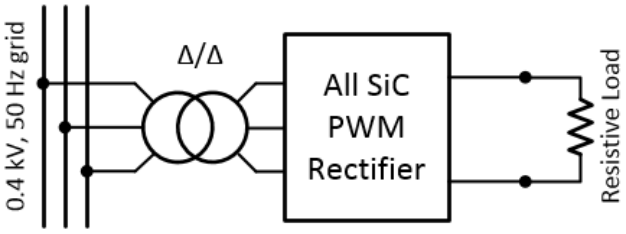

(b)

Figure 2-1 Resistive load fed by All SiC PWM Rectifier (a) directly from grid (b) Δ/Δ transformer

2.2. DC Motor Drive

2.2.1. All SiC PWM Rectifier as a Field Exciter

A separately excited medium power DC Motor can be supplied by a SiC PWM Rectifier as a field exciter. PWM Rectifier will have variable output voltage in order to control the field current. The schematic is given in Figure 2-2.

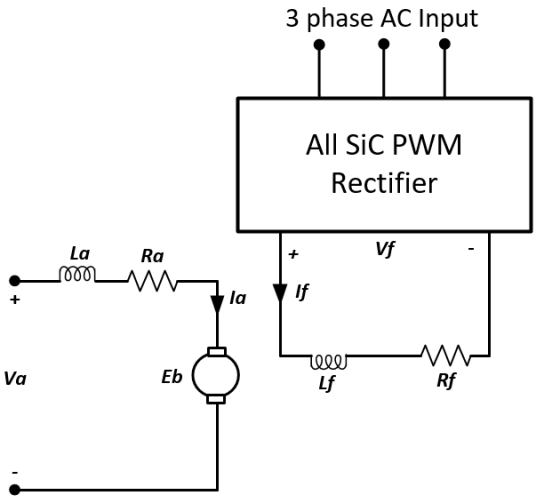

Figure 2-2 Electric equivalent circuit - All SiC PWM rectifier as field exciter

If we neglect the effects of armature reaction and saturation, and keep the armature current constant, the motor equations become as follows:

$$T_d = K * \phi * i_a \tag{2.1}$$

As the armature current is constant, the torque equation becomes:

$$T_d = K' * i_f \tag{2.2}$$

Transfer function is:

$$R_f i_f + L_f(\frac{di_f}{dt}) = v_f \tag{2.3}$$

$$\frac{Jd\omega}{dt} + \mathrm{B} * \omega = K' * i_f \tag{2.4}$$

B is friction coefficient; J is inertia of the motor. The Laplace Transform of the equations are:

$$(L_f s + R_f) I_f(s) = V_f(s) \tag{2.5}$$

$$(\mathrm{Js} + \mathrm{B})\omega(\mathrm{s}) = K' * I_f(s) \tag{2.6}$$

As we simplify these equation:

$$\frac{\omega(\mathrm{s})}{V_f(s)} = \frac{K'}{(L_f s + R_f)(\mathrm{Js} + \mathrm{B})} \tag{2.7}$$

$$\frac{\omega(\mathrm{s})}{V_f(s)} = \frac{K_m}{(T_f s + 1)(\mathrm{T}_m \mathrm{s} + 1)} \tag{2.8}$$

Where,

$$K_m = \frac{K'}{i_f R_f} \tag{2.9}$$

$$T_f = \frac{L_f}{R_f} \tag{2.10}$$

$$T_m = \frac{J}{B} \tag{2.11}$$

In large DC motors time constant T_f is high. In other rectifier types such as diode rectifier, the field current cannot be changed suddenly. Therefore, the stability can be lost. In order to accomplish high response, the All SiC PWM Rectifier would be a better choice. In other words, with All SiC PWM Rectifier, field current can be changed in short time, therefore the motor reacts to changes quickly and there will not be stability issues.

The output of the PWM Rectifier can be decreased so that the field winding would have higher voltage than the output of PWM Rectifier. Then, rectifier will start to operate in inversion mode and current flows toward the rectifier.

2.2.2. Armature Supplied by All SiC PWM Rectifier

Applied armature voltage is adjusted for speed control purpose. It provides 2 quadrant operation (motoring and regenerative breaking) in the case where the field excitation is fixed. The resulting DC Motor Drive can be operated in all 4 quadrants of the speed-torque plane by reversing the field current and adjusting its magnitude. It exhibits nearly harmonic-free operation at unity power factor on the grid side.

Schematic of the system is presented in Figure 2-3.

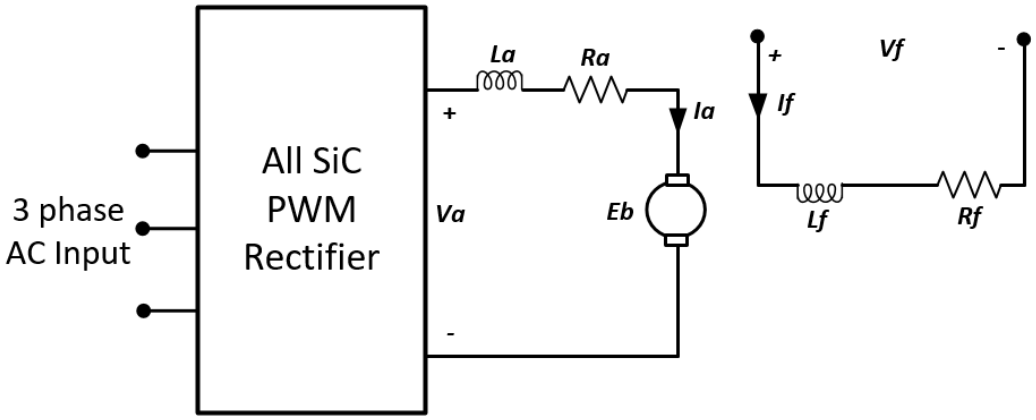

Figure 2-3 Electric equivalent circuit – armature supplied by All SiC PWM Rectifier

Torque equation of the DC Motor is as follows:

$$T_d = K * \phi * i_a \tag{2.12}$$

As an armature controlled DC motor if keep the field current constant i.e. the magnetic field is constant, the torque equation becomes:

$$T_d = K_t * i_a \tag{2.13}$$

The angular velocity, ω and the back emf, Eb relation of the DC Motor is given as:

$$E_b = K_e * \omega \tag{2.14}$$

Motor torque constant, K_t and back emf constant K_e are taken equal as K. From the equivalent circuit of the DC motor following equations are derived.

$$\frac{Jd\omega}{dt} + \mathrm{B} * \omega = K * i_a \tag{2.15}$$

$$R_a i_a + L_a \left(\frac{di_a}{dt}\right) = v_a - K\omega \tag{2.16}$$

If we apply the Laplace Transform, the equation become:

$$(\mathrm{Js} + \mathrm{B})\omega(\mathrm{s}) = K * I_a(s) \tag{2.17}$$

$$(L_a s + R_a) I_a(s) = V_a(s) - K\omega(\mathrm{s}) \tag{2.18}$$

Then, we eliminate $I_a(s)$ between equations above and obtain the open loop transfer function.

$$\frac{\omega(\mathrm{s})}{V_a(s)} = \frac{K}{(L_a s + R_a)(\mathrm{Js} + \mathrm{B})} \tag{2.19}$$

$$\frac{\omega(\mathrm{s})}{V_a(s)} = \frac{K_m}{(T_a s + 1)(\mathrm{T}_m \mathrm{s} + 1)} \tag{2.20}$$

Where $\frac{L_a}{R_a} = T_a$ is electrical time constant

$\frac{J}{\mathrm{B}} = T_m$ is mechanical time constant

In the transfer function above, the rotational speed, ω is considered the output and the input of the system is armature voltage V_a, which is the output of the All SiC PWM Rectifier. DC motor can be controlled by changing the output of rectifier. By decreasing the output, rectifier will start to operate in inversion mode and armature current will flow towards the rectifier.

DC Motor can also be driven by a Buck Type PWM Rectifier which would be connected to the armature of the motor[16].

2.3. Synchronous Motor Field Exciter

SiC PWM Rectifier can be used as a field exciter of directly grid connected large synchronous motors. It provides adjustable field current with boosting action. Power flow is bidirectional. It maintains stability of the synchronous motor against fluctuations in the supply voltage since field excitation can be controlled more rapidly in comparison with diode and thyristor based field exciters. It exhibits nearly harmonic-free operation at unity power factor on the grid side.

The electric equivalent circuit of All SiC PWM Rectifier as a field exciter can be observed in Figure 2-4.

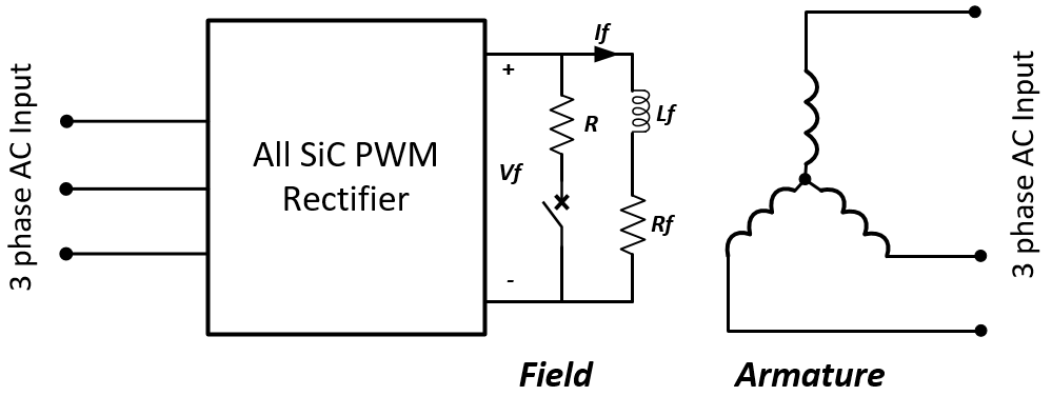

Figure 2-4 SiC PWM rectifier as field exciter for synchronous motor

2.4. Battery Charger

All SiC PWM Rectifier can be used as fast and ultrafast battery charger in many configurations [17]. It provides variable output voltage with unidirectional power flow in off-board battery chargers of all electric vehicles. The rectifier can be connected directly to the battery if the voltage rating of the battery is around dc output voltage level of the SiC PWM Rectifier. In our case output is between 600V-1000V. Nearly harmonic-free operation is accomplished at unity power factor on the grid side. The battery charger diagram can be seen in Figure 2-5. SiC PWM chargers can also be connected in parallel to speed up the charging time.

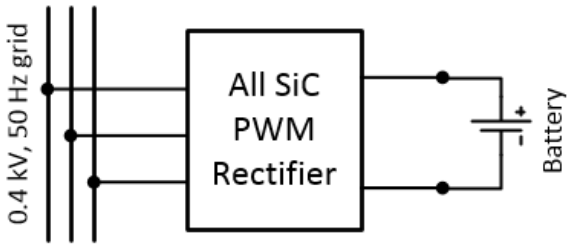

Figure 2-5 Battery charger topology by PWM Rectifier fed from the grid

2.5. Supercapacitor/Battery Energy Storage Systems

Supercapacitors can be directly connected to the output of the All SiC PWM Rectifier if its voltage rating matches the output voltage range of the PWM Rectifier as it can be seen in Figure 2-6. PWM Rectifier will be controlled in variable output voltage level. It provides controllable and bidirectional power flow between the utility grid and the energy storage system.

Other alternative is to connect a DC/DC converter between the PWM Rectifier and the supercapacitor as in Figure 2-7. This time the output of the PWM Rectifier can be a fixed voltage value as DC/DC converter will control the charge or discharge as a buck/boost converter.

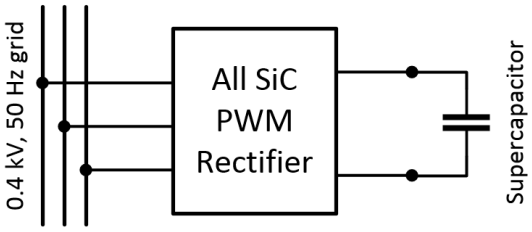

Figure 2-6 Supercapacitor energy storage system topology with PWM Rectifier fed from the grid

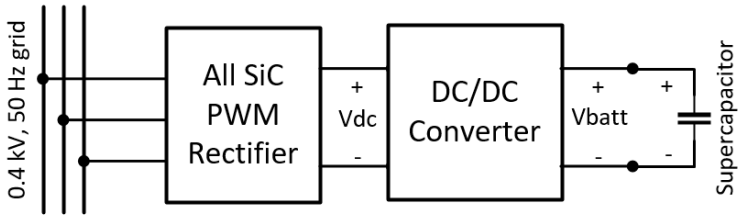

Figure 2-7 Supercapacitor energy storage system topology with DC/DC Converter

2.6. Variable Frequency AC Motor Drives

PWM Rectifier acts as the active front end converter of the AC Motor Drive and provides bidirectional power flow. The resulting motor drive is a 2-quadrant drive with regenerative breaking ability. It can operate as a 4-quadrant motor drive by reversing the phase sequence of inverter output voltages. It exhibits nearly harmonic-free operation at unity power factor on the grid side.

Advantages of supplying the inverter with All SiC PWM Rectifier compared to other types such as diode or thyristor based rectifier specified as follows:

- Due to bidirectional operation of both PWM rectifier and inverter, when the AC Motor operates in regenerative mode, the power can be transferred to grid. Instead of dissipating the power on a resistor at dc-link, the power is recovered with this operation.
- Because the dc voltage and supplied current is nearly pure dc, no need for filtering element at the input of the inverter.
- PWM Rectifiers in these systems can supply variable output voltage.
- Nearly harmonic-free operation at unity power factor on the grid side.

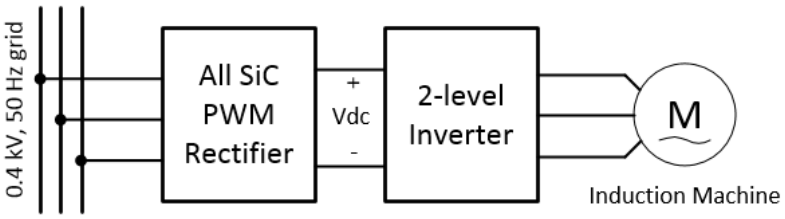

Figure 2-8 AC Motor Drive topology 2-level inverter fed by PWM Rectifier

Depending on the power rating of SiC PWM Rectifier, more than one AC Motor or PMSM can be supplied as it is shown in Figure 2-9.

A squirrel cage induction machine connected to a traction inverter which is supplied by All SiC PWM Rectifier is studied in detail in [13].

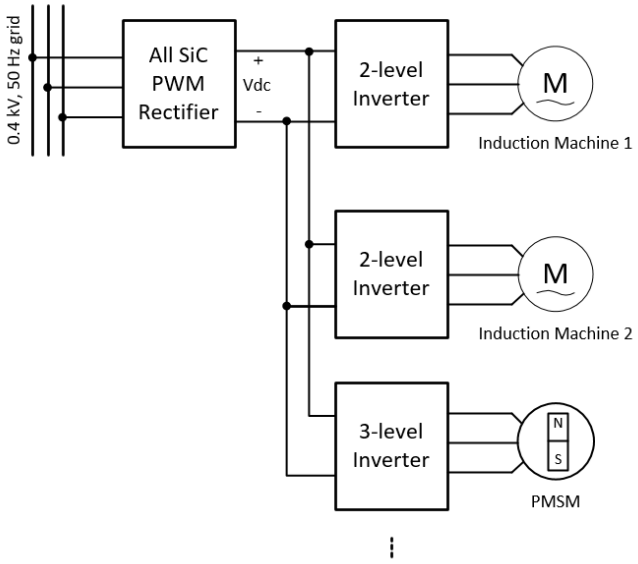

Figure 2-9 Multiple load motor connected All SiC PWM Rectifier

CHAPTER 3

OPERATING PRINCIPLES AND MODES OF PWM RECTIFIER

In Chapter 3, operation modes and control structure of All SiC Three Phase PWM Rectifier is studied. Effects of SPWM and SVPWM modulation techniques on input current THD is investigated. After that switching frequency choice is made based on thermal limits and power capacity of PWM Rectifier. Efficiency and THD is analyzed by changing the switching frequency, output power and output voltage parameters. Finally, simulations for various output levels are conducted and implementation of All SiC Three Phase PWM Rectifier is discussed.

3.1. Operation Modes of PWM Rectifier

The main operation modes discussed in this chapter is for unity power factor operation. Therefore, for rectification, it is transferring active power from the AC side to the DC side of the rectifier.

In Figure 3-1, at given AC supply side voltage and current waveforms, the operation instance is marked with dotted line while the PWM Rectifier is in rectification. This line corresponds to the time instant where Vb and Vc are positive and Va is negative. Therefore, Ib and Ic are conducting at positive direction and Ia current is in negative direction.

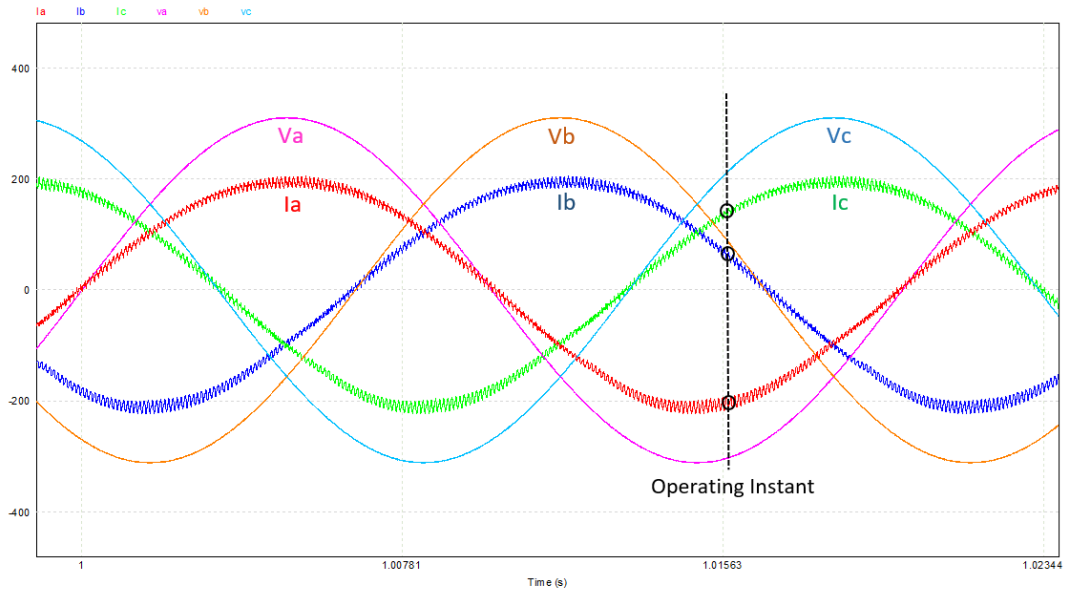

Figure 3-1 Operating Instance on given AC side current and voltage waveforms PSIM power electronics software

A switching pattern is given in Figure 3-2 as an example. This represents the gate signals sent to the high side of the SiC MOSFETs. Therefore, the opposite signals are applied to the low side of the corresponding MOSFETs. The aim of these switching patterns is to create purely sinusoidal current waveform at the AC side of the rectifier at steady state and this is achieved by changing the width of the pulses in each step. The switching frequency for this operation is set to 10 kHz.

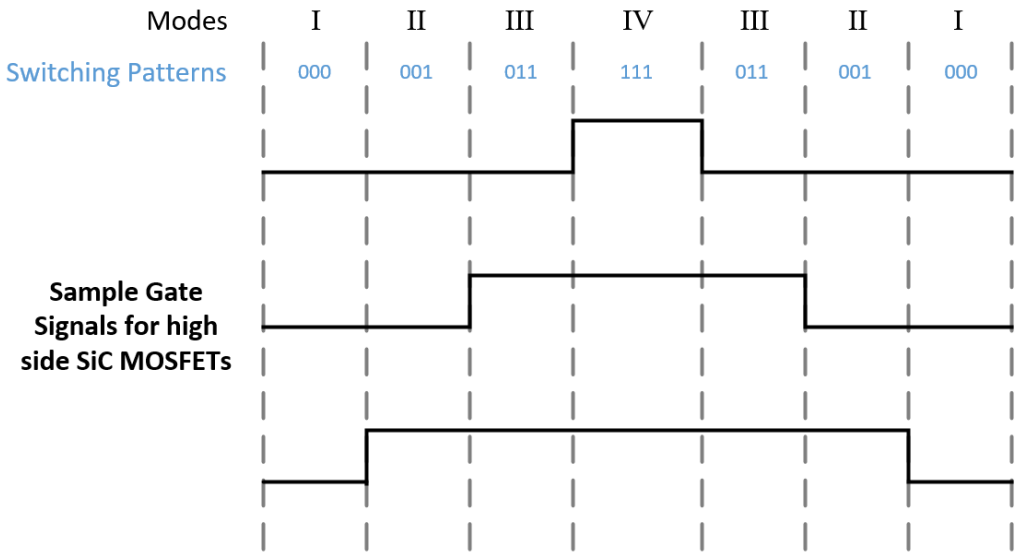

Figure 3-2 High side MOSFET gate signals as an example

According to this time instant, the cases of which switches are conducting is presented in Figure 3-3. During the cases (a) and (d) the load is supplied only by the capacitor. In these periods, the boost inductor is charging. In case (b) and (c) rectification occurs and the load is supplied by the source. Therefore, in cases (a) and (d) capacitor voltage is decreasing whereas in (a) and (d) capacitor voltage is rising.

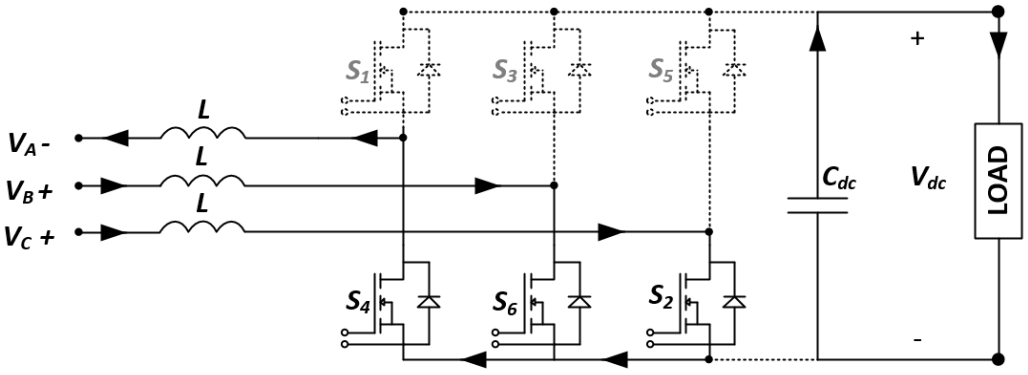

(a)

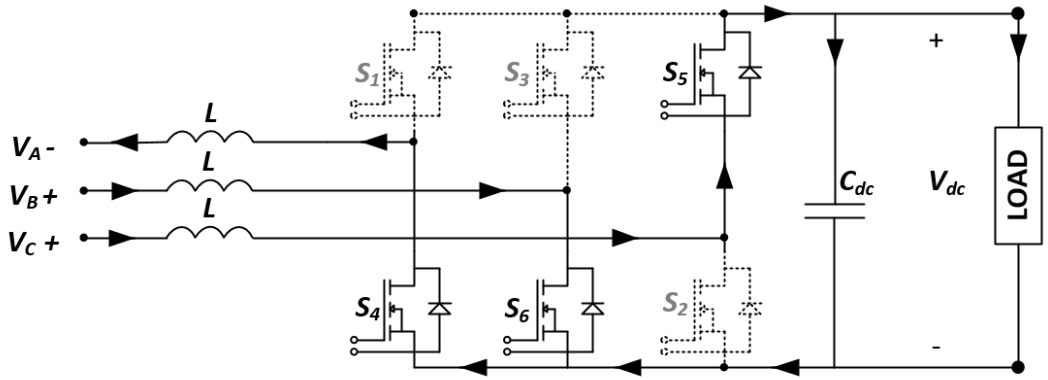

(b)

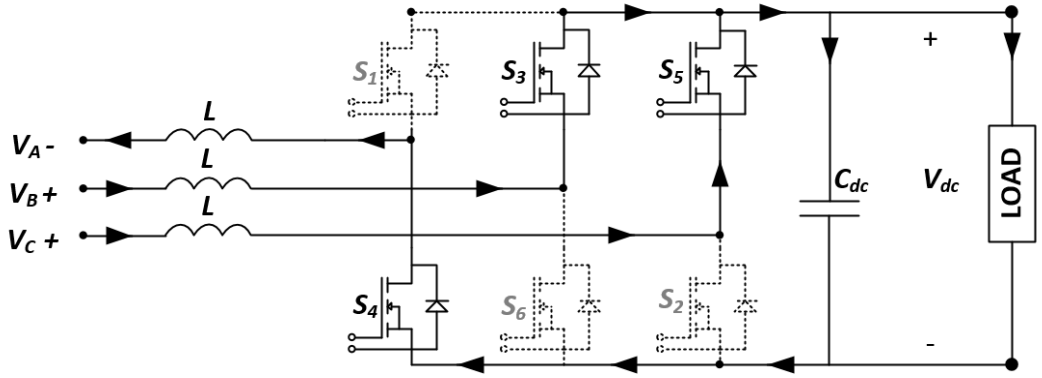

(c)

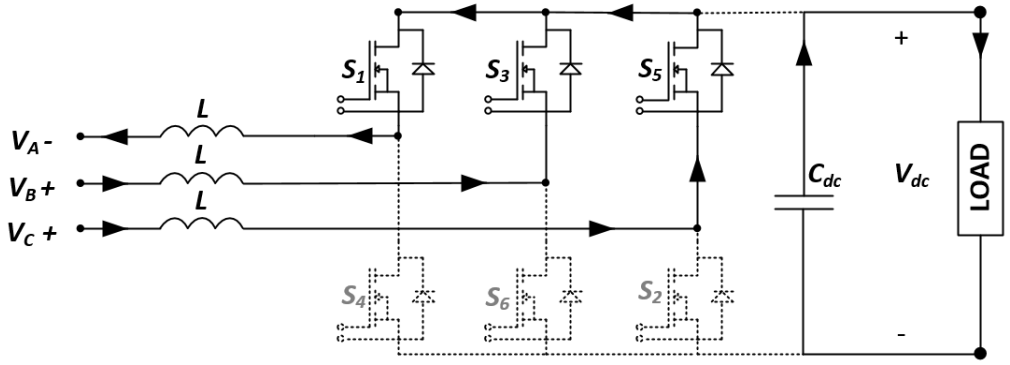

(d)

Figure 3-3 Rectification operation on the switching cases for (a) 000 (b)100 (c)110 (d)111

3.2. Control structure of All SiC Three Phase PWM Rectifier

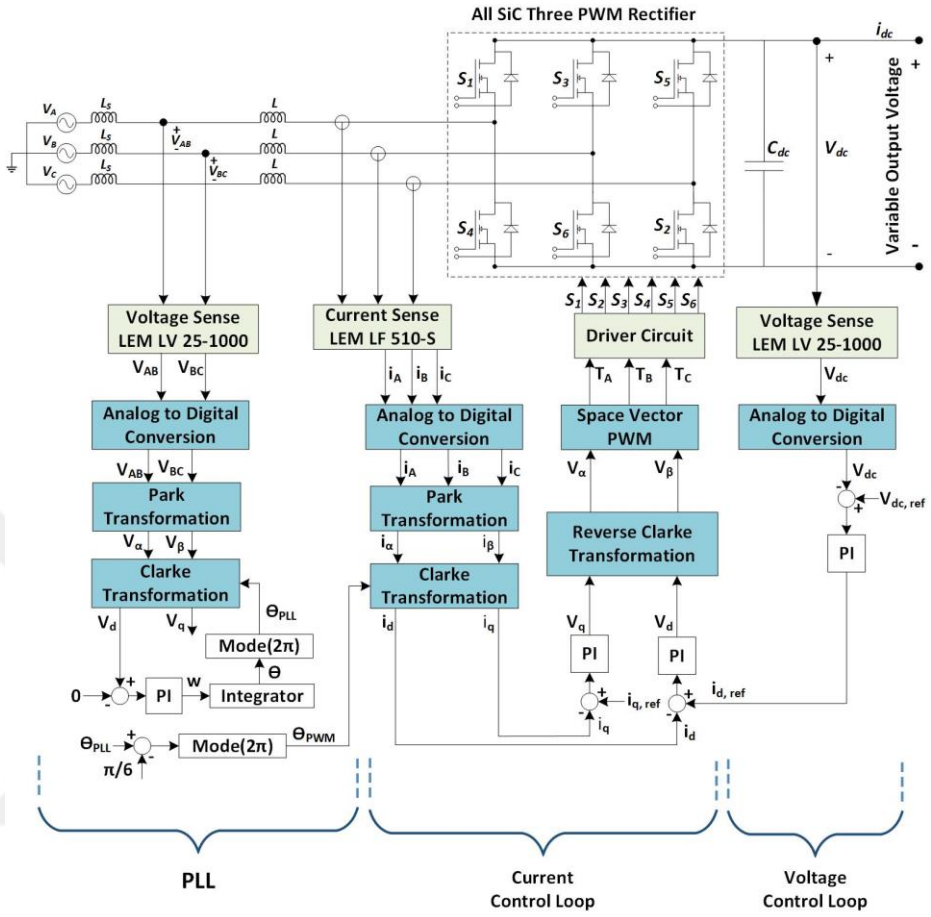

Figure 3-4 Control structure of All SiC Three Phase PWM Rectifier

In Figure 3-4, the control structure used in the scope of this work for the All SiC Three Phase PWM Rectifier is presented. Control of the rectifier implemented in Texas Instruments TMS320F28377D DSP.

At the input of the rectifier voltage between phase A and phase B (V_{ab}) and voltage between phase B and phase C (V_{bc}) are measured with LEM LV 25-100 voltage transducer. Then, the sensed voltages are converted to digital from analog with the control board. The converted V_{ab} and V_{bc} values are processed with Phase Lock Loop (PLL) and the phase angle Θ_{PLL} is acquired. This value is obtained putting the output of Park and Clarke transformations to PI integrator loop. Because this Θ_{PLL} is for line-

to-line voltages, π/6 is subtracted from this value to be able to use it in current loop. This final Θ angle is called Θ_{PWM}.

At the output of the rectifier dc link voltage value V_{dc} is measured with LEM 25-1000 voltage transducer and it is converted to digital. The desired output value which is between 625V and 1000V in this work is fed to the system as $V_{dc,ref}$. Outer voltage control loop is implemented by subtracting V_{dc} from $V_{dc,ref}$, then feeding to result to the PI controller. The output of the PI is called $i_{d,ref}$ and it will be used in inner current control loop.

Input line currents are sensed with LEM LF 510-S and converted to digital values. After these converted input currents go through Park and Clarke Transformations with using Θ_{PWM} angle, their outcomes i_d and i_q are subtracted from reference values of $i_{q,ref}$ and $i_{d,ref}$. In order to achieve zero reactive power, this $i_{q,ref}$ reference current should be set to zero. The results of the subtractions then passed through PI controller, thus the V_d and V_q values are obtained. V_d and V_q are converted to alpha-beta reference frame with Reverse Clarke Transformation and fed to Space Vector PWM modulation block. Output of SVPWM is called T_a, T_b, T_c signals which are the input of the SiC MOSFET driver board. The short description of Clarke and Park transformations are mentioned below.

3.2.1. Clarke transformation (abc to αβ):

It transforms the abc three phase signals to alpha-beta two phase 90 degree apart reference frame.

$$i_\alpha = \frac{2}{3} * (i_a - \frac{1}{2} * i_b - \frac{1}{2} * i_c) \quad (3.1)$$

$$i_\beta = \frac{2}{3} * (\frac{\sqrt{3}}{2} * i_b - \frac{\sqrt{3}}{2} * i_c) \quad (3.2)$$

3.2.2. Park transformation (αβ to dq):

It transforms the alpha-beta two phase 90-degree apart reference frame to dq reference frame which is dc values.

$$i_d = i_\alpha * \cos(\omega t) + i_\beta * \sin(\omega t) \tag{3.3}$$

$$i_q = -i_\alpha * \sin(\omega t) + i_\beta * \cos(\omega t) \tag{3.4}$$

3.2.3. Inverse Clarke Transformation (αβ to abc):

It transforms the alpha-beta two phase reference frame to abc three phase reference frame.

$$i_a = i_\alpha \tag{3.5}$$

$$i_b = -\frac{1}{2} * i_\alpha + \frac{\sqrt{3}}{2} * i_\beta \tag{3.6}$$

$$i_c = -\frac{1}{2} * i_\alpha - \frac{\sqrt{3}}{2} * i_\beta \tag{3.7}$$

3.2.4. Inverse Park Transformation (dq to αβ):

It transforms the dq reference frame to alpha-beta two phase 90-degree apart reference frame.

$$i_\alpha = i_d * \cos(\omega t) - i_q * \sin(\omega t) \tag{3.8}$$

$$i_\beta = i_d * \sin(\omega t) + i_q * \cos(\omega t) \tag{3.9}$$

3.3. Comparison of SPWM and SVPWM

Sinusoidal PWM and Space Vector PWM are two modulation methods that can be used for generating signals for the gate drive circuits. Although SPWM method is simpler and depends on the comparison of transformed Va, Vb, Vc signals with a triangular wave at a fixed frequency, SVPWM is better due to less harmonic content thus smaller THD. Furthermore, switch transitions are smoother, i.e. one switch state changes at a time, therefore a system with SVPWM has less switching loss compared to SPWM.

In Figure 3-5, phase A input current waveform for Three Phase PWM Rectifier with SVPWM is given. In Figure 3-6, SPWM modulation is applied for the same circuit. It can be observed that the one with SVPWM has less harmonic content. THD values are also presented in the figures which are 9.94% for SVPWM and 22.4% for SPWM. Simulations are performed at 2kHz switching frequency so that the difference can be more visible. The output power is 50kW and rectifier is fed by 400V grid voltage.

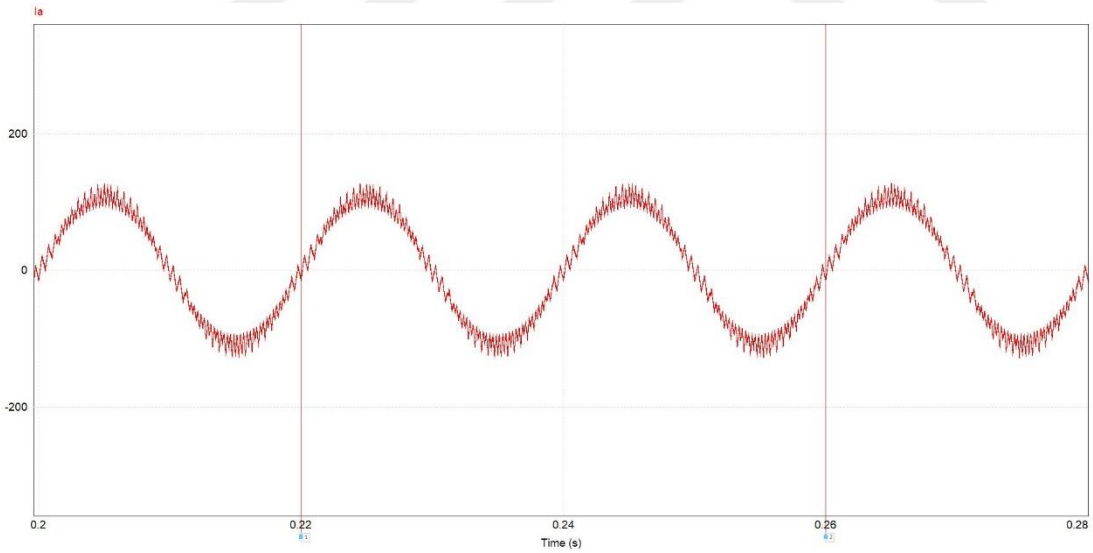

	x1	x2	Δ	THD
Time	2.20000e-001	2.60000e-001	4.00000e-002	freq=50
Ia	-1.41793e+001	-1.35814e+001	5.97890e-001	9.94389e-002

Figure 3-5 Phase A Input current waveform and THD for SVPWM at 2kHz switching frequency

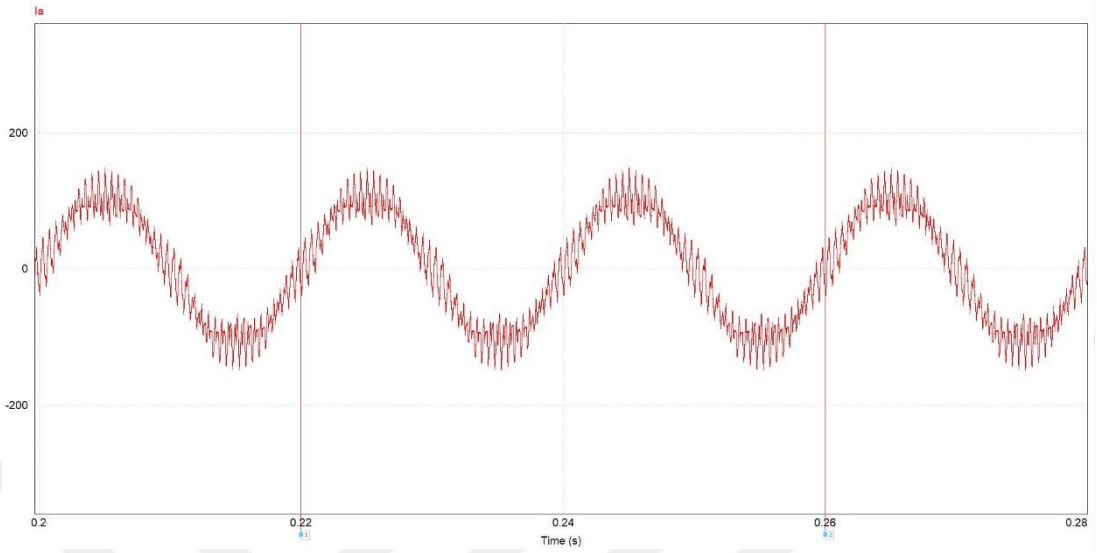

	x1	x2	Δ	THD
Time	2.20000e-001	2.60000e-001	4.00000e-002	freq=50
Ia	-2.42202e+001	-2.40658e+001	1.54458e-001	2.24235e-001

Figure 3-6 Phase A Input current waveform and THD for SPWM at 2kHz switching frequency

Effect of different frequencies on these modulation techniques should also be studied. In Figure 3-7 and Figure 3-8, the simulations at 1kHz and 20kHz switching frequency for SPWM are conducted respectively. In Figure 3-9 and Figure 3-10, the same simulations are performed for SVPWM at 1kHz and 20kHz. The output power for the simulations are 50kW. THD of all simulations conducted for various switching frequency levels are summarized in *Table 1*. It can be concluded that as the frequency increases, the harmonic content of the input current decreases for both modulation techniques and SVPWM gives better results on every frequency level compared to SPWM.

The values in *Table 1* shows that the THDs of frequencies 10kHz and above are in small range and close to each other. When deciding the switching frequency of the system, the values 1 kHz, 2kHz, 5kHz would not be suitable due to their high harmonic contents. 10kHz and above is better choice because of their lower THD level.

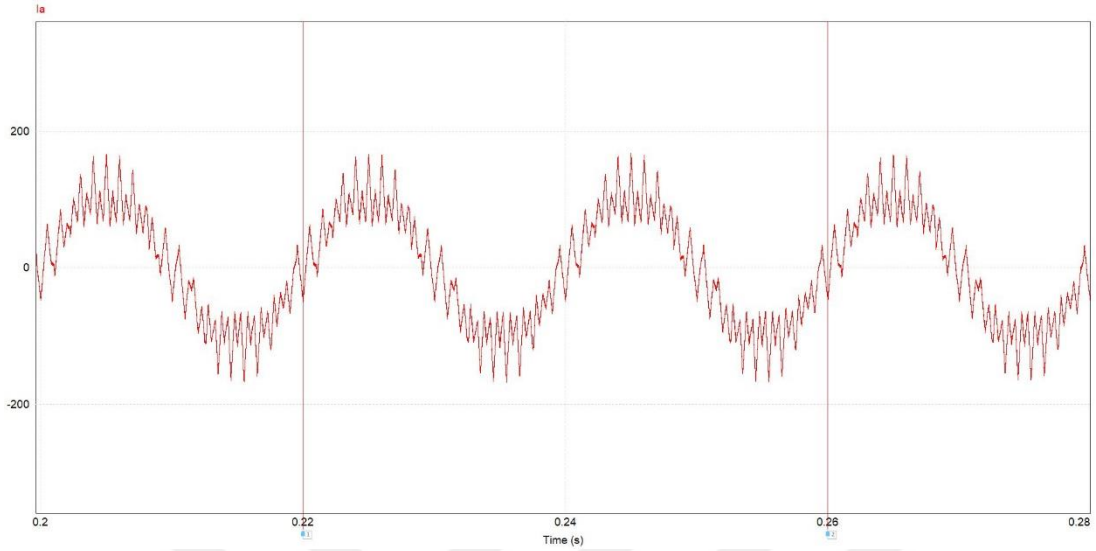

	x1	x2	Δ	THD
Time	2.20000e-001	2.60000e-001	4.00000e-002	freq=50
Ia	-4.59332e+001	-4.60615e+001	-1.28345e-001	2.98549e-001

Figure 3-7 Input current waveform and THD for SPWM at 1kHz switching frequency

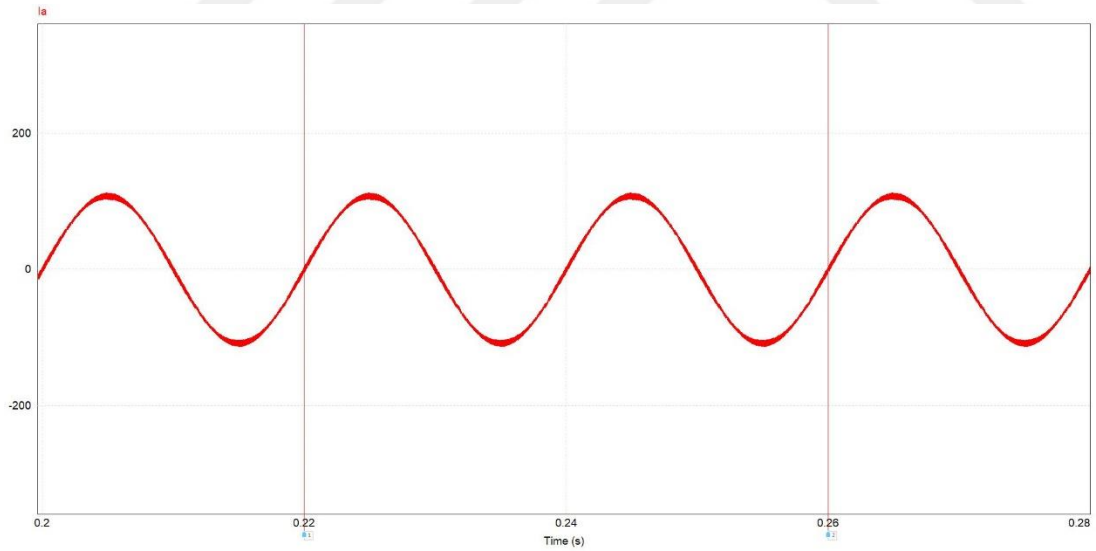

	x1	x2	Δ	THD
Time	2.20000e-001	2.60000e-001	4.00000e-002	freq=50
Ia	-4.29690e-001	-4.29690e-001	3.20789e-007	2.28728e-002

Figure 3-8 Input current waveform and THD for SPWM at 20kHz switching frequency

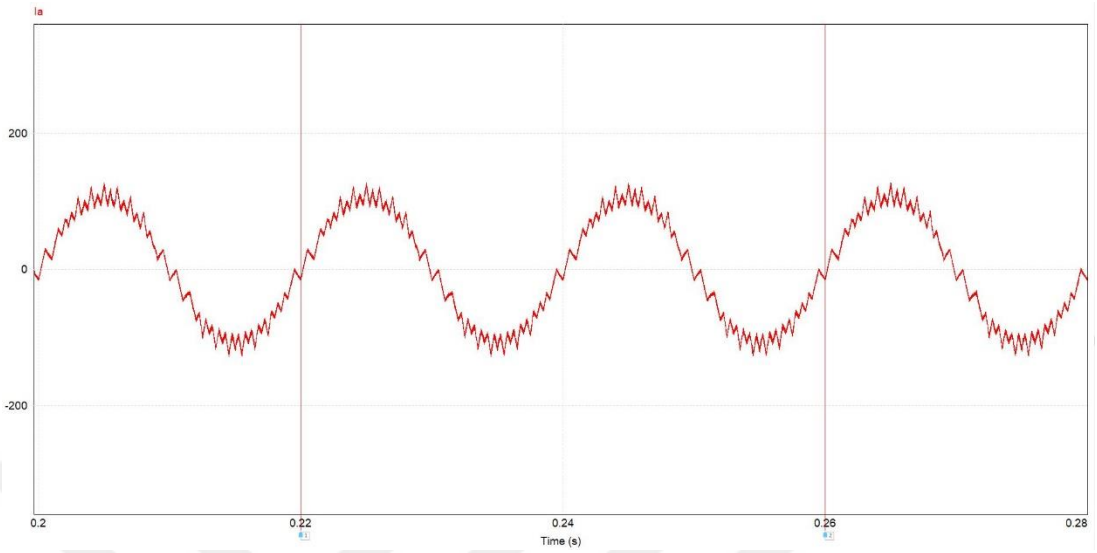

	x1	x2	Δ	THD
Time	2.20000e-001	2.60000e-001	4.00000e-002	freq=50
Ia	-1.48166e+001	-1.40715e+001	7.45084e-001	1.03898e-001

Figure 3-9 Input current waveform and THD for SVPWM at 1kHz switching frequency

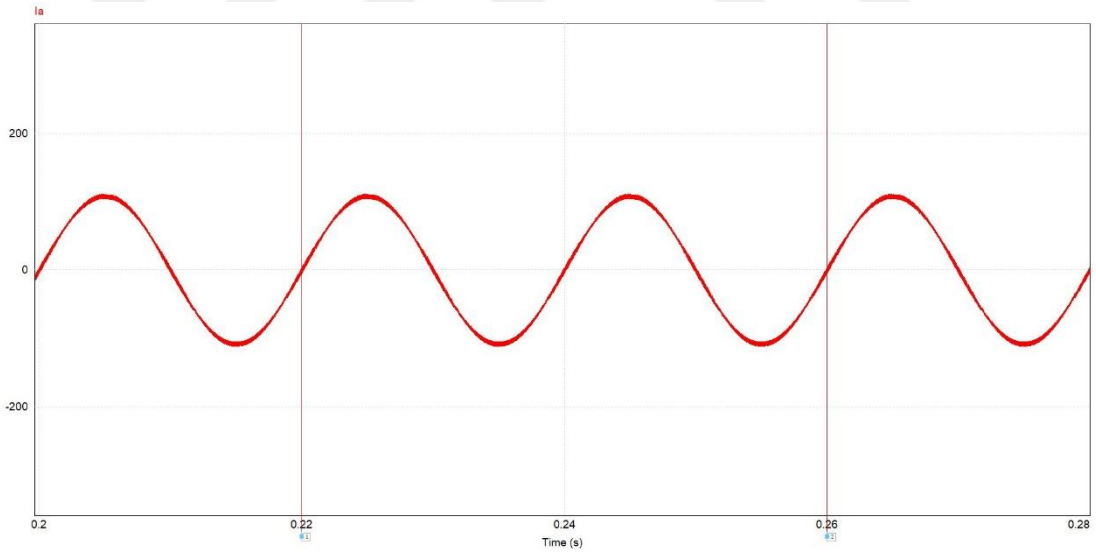

	x1	x2	Δ	THD
Time	2.20000e-001	2.60000e-001	4.00000e-002	freq=50
Ia	-1.69960e+000	-1.69960e+000	1.70365e-007	2.11702e-002

Figure 3-10 Input current waveform and THD for SVPWM at 20kHz switching frequency

Table 1 *Input current THD values for SPWM and SVPWM at different frequencies*

Frequency (kHz)	*THD – SPWM (%)*	*THD - SVPWM (%)*
1	29.85	10.39
2	22.42	9.94
5	9.31	7.75
10	4.56	4.52
15	3.04	2.87
20	2.29	2.11

Simulations conducted at low switching frequencies also implies that IGBTs have high input current harmonics considering their conventional switching frequency range of 2-3 kHz at the output power level of this study, therefore higher THD. Moreover, because the switching frequency is lower for systems with IGBTs compared to systems with SiC MOSFETs, the filtering elements are bigger in size, so the volume of the system is larger. IGBTs have higher switching losses and similar conduction losses, therefore efficiency is lower for these systems.

3.4. Determining the Switching Frequency

After explaining the modes and operation of the Three Phase PWM Rectifier, the All SiC Three Phase PWM Rectifier built for this work will be described.

The distinguished and the most important part of the used PWM Rectifier is the switching elements. Switching elements of the Three Phase PWM Rectifier in this work consist of new technology SiC MOSFETs which are discussed in the introduction section. The chosen SiC MOSFETs are CREE CAS300M17BM2. These transistors have the specifications in Table 2.

Table 2 *Specifications of the MOSFET used in Three Phase PWM Rectifier*

Parameter	*Value*	*Unit*
Drain - Source Voltage (Vds)	1700	V
Gate - Source Voltage (Vgs)	-5/20	V
Drain Current (Id)	325 @ Tc=25°C 225 @ Tc=90°C	A
Diode Forward Current (If)	556 @ Tc=25°C 353 @ Tc=90°C	A
Junction Temperature (Tjmax)	-40 to +150	°C
On-state Resistance (Rds(on))	8.0 @ Vgs=20V, Id=300A	mΩ
Rise Time	72	ns
Fall Time	56	ns

As it can be seen from *Table 2*, these SiC MOSFET has fast switching characteristics with having a rise time of 72 ns and fall time of 56 ns. This feature makes it have less switching losses compared to the Si based MOSFET counterparts at high switching frequencies such as 10-20 kHz. The other reason for choosing CREE CAS300M17BM2 is being only commercially available SiC MOSFET that has 1700 V continuous drain-source voltage level. In our application in Traction Systems R&D Laboratory, the transient voltages can extent 1200V so the other manufacturers' available SiC MOSFET options were not considered. CREE CAS300M17BM2 SiC MOSFET can be observed in Figure 3-11.

Figure 3-11 CAS300M17BM2 SiC MOSFET from CREE

As it is mentioned above CREE CAS300M17BM2 SiC Power MOSFET can have switching frequencies as high as 10-20 kHz. In order to determine the switching frequency for this application of All SiC Three Phase PWM Rectifier, simulations are conducted with Wolfspeed SpeedFit Design Simulator. The starting point of the design process is the maximum junction temperature of the SiC Power MOSFETs. In the datasheet maximum junction temperature (Tj) is given as 150°C. However, in order to extend the lifetime of SiC Power MOSFETs and operate in safe limits, the maximum junction temperature is specified as 120°C. Furthermore, possible bonding weaknesses in the chip are also considered for determining the maximum allowable junction temperature.

The necessary parameters for the simulations are line inductance and heatsink thermal resistance values. The line inductance in our application is 0.5mH. The value of heat sink thermal resistance is given in the datasheet of heatsink as a curve changing with respect to the length of the heatsink which can be observed in Figure 3-12 (Fischer Elektronik SK 461 400 SA). Length of the heatsink in the PWM Rectifier is 400mm and forced cooling is performed. Therefore, according to the curve thermal resistance is 0.018 °K/W.

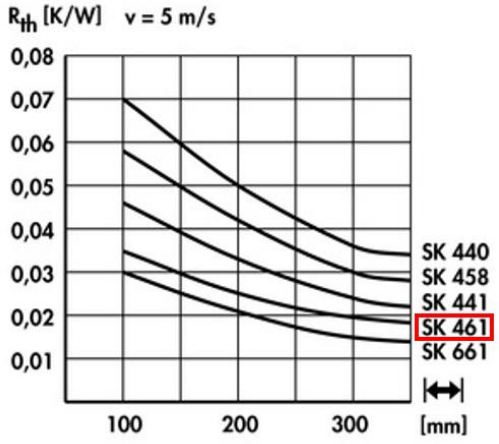

Figure 3-12 Thermal Resistance Curve of the Heatsink

The simulations are conducted by taking the above values into consideration to determine the proper switching frequency for All SiC Three Phase PWM Rectifier. An example of the simulation is presented in Figure 3-13. In this simulation, for 1000V output DC voltage at 20kHz switching frequency, junction temperature reaches 120°C at 143kW output power. It can be observed that at 20kHz switching frequency, the switching losses goes higher than 1kW for 143kW output power.

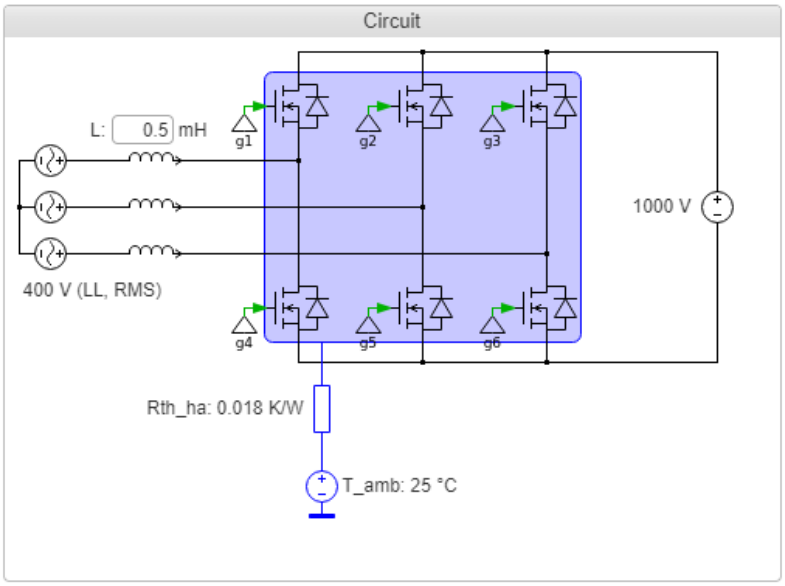

System overview

Input Voltage	Actual Output Power	Switching Frequency	Efficiency
400 V	143.0 kW	20 kHz	98.62 %

Device overview

	Switching	Conduction	Combined Losses	Junction Temperature
MOSFETs	1.017 kW	951.20 W	1.968 kW	120 °C
Diodes				
Converter Losses			1.968 kW	

Figure 3-13 SpeedFit Simulation for 1000V output DC voltage at 20kHz

This simulation is repeated at 10, 15 and 20kHz switching frequencies for various output dc voltage levels such as 625V, 750V, 800V, 900V and finally 1000V. The results showing the effects of switching frequency on maximum output power at junction temperature of 120°C is presented in Figure 3-14. It can be concluded that

maximum output power changes with the output DC voltage level, i.e. as the output voltage increases, the maximum output power decreases for the specified junction temperature level. This heavily depends on the fact that switching losses increase with the rising drain to source voltage of MOSFETs.

The effect of switching frequency change is the crucial result of Figure 3-14, since the maximum output power that can be received from All SiC PWM Rectifier falls with rising switching frequency because of the increasing switching losses. In our system, the ability to deliver high output power is desirable, therefore 10kHz switching frequency is more suitable.

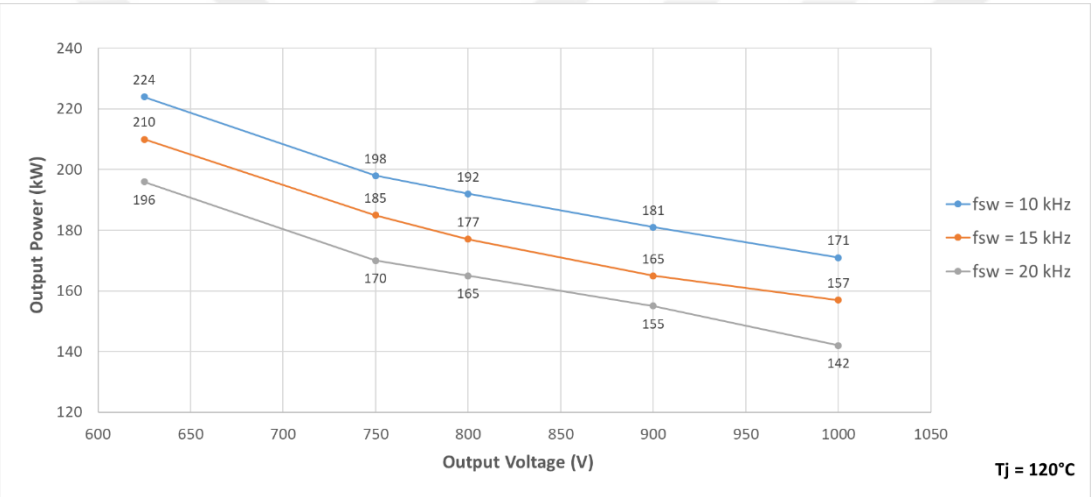

Figure 3-14 Output power comparison at different switching frequencies for Tj=120°C

In Figure 3-15 the comparison of efficiency for changing output voltage levels at different switching frequencies is studied while the maximum junction temperature 120°C condition is satisfied. This graph indicates that efficiency of All SiC Three Phase PWM Rectifier decreases with rising switching frequency. Therefore, it also confirms the choice of 10 kHz switching frequency for our system.

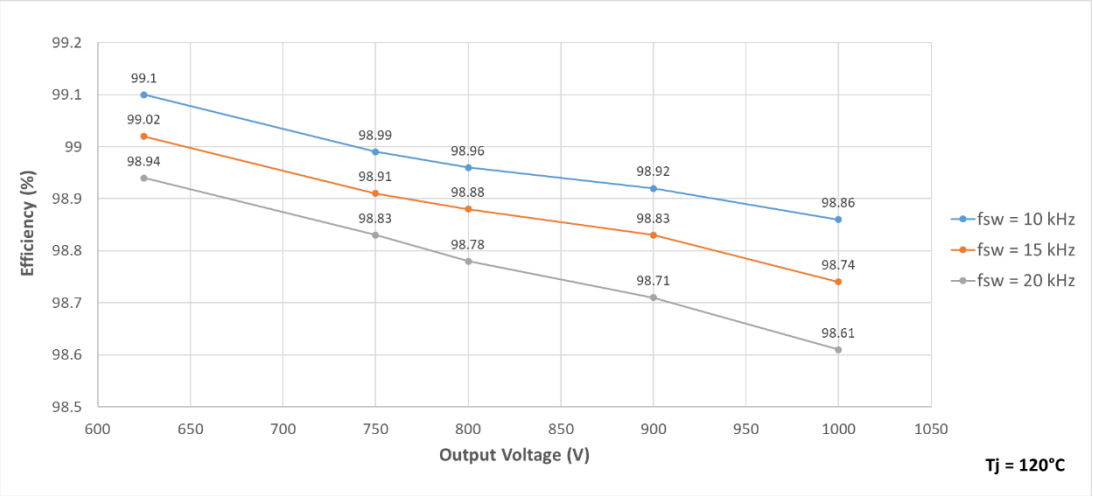

Figure 3-15 Efficiency comparison at different switching frequencies for Tj=120°C

Audible hearing range is another effect of switching frequency. Although it changes according to age and gender, hearing is most sensitive in the 2000 - 5000 Hz frequency range. Therefore, choosing the system frequency as 10000 Hz will reduce the audible noise during the operation of the Three Phase All SiC PWM Rectifier.

3.5. THD and Efficiency Analysis

Up to this point, we have investigated the output and efficiency values for the boundary junction temperature to understand the limits of the PWM Rectifier and to operate it in safe limits. In this part, we are going to analyze the effect of frequency change on THD for 750V constant output voltage at 50kW and 100kW output powers. In SPWM-SVPWM comparison topic, frequency change of SVPWM at 50kW output power is already examined. In *Table 3*, the THD variation on these power levels are given and in Figure 3-16, the graph is presented. As it is expected, the THD values fall as the switching frequency increases and for every frequency 100kW case has less THD than 50kW case, therefore less input current harmonics.

Table 3 *THD for changing frequencies at 50 and 100kW output power*

Frequency (kHz)	*50kW- THD(%)*	*100kW - THD(%)*
2	9.94	5.06
5	7.75	4.01
10	4.52	1.73
15	2.87	1.50
20	2.11	1.12

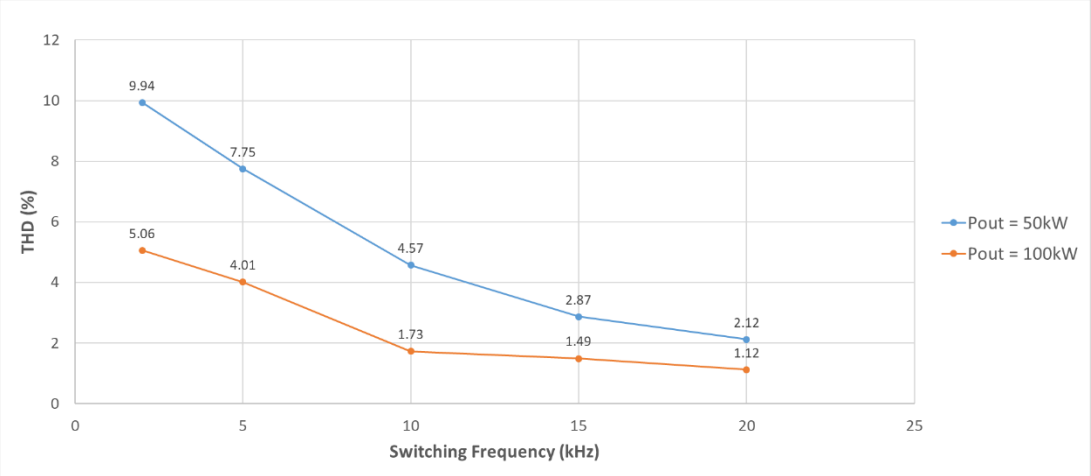

Figure 3-16 THD for changing frequencies at 50 and 100kW output power

The impact of changing output power is noticed in the simulations above; however, we can investigate further by expanding the output power range. For that reason, input current THD variation is simulated for different output power levels from 25kW to 150kW at 750V output DC voltage, 10kHz switching frequency. In Figure 3-17 and Figure 3-18, the input current waveforms and THD values are given for 25kW and 150kW output power respectively. In *Table 4*, THD and efficiencies are presented at 6 different output power from 25 to 150kW and their graph can be seen in Figure 3-19. It can be concurred that efficiency is decreasing with rising output power for fixed output voltage, since switching and conduction losses increase. Moreover, rising output current makes conduction losses dominant which can be observed in *Table 5*.

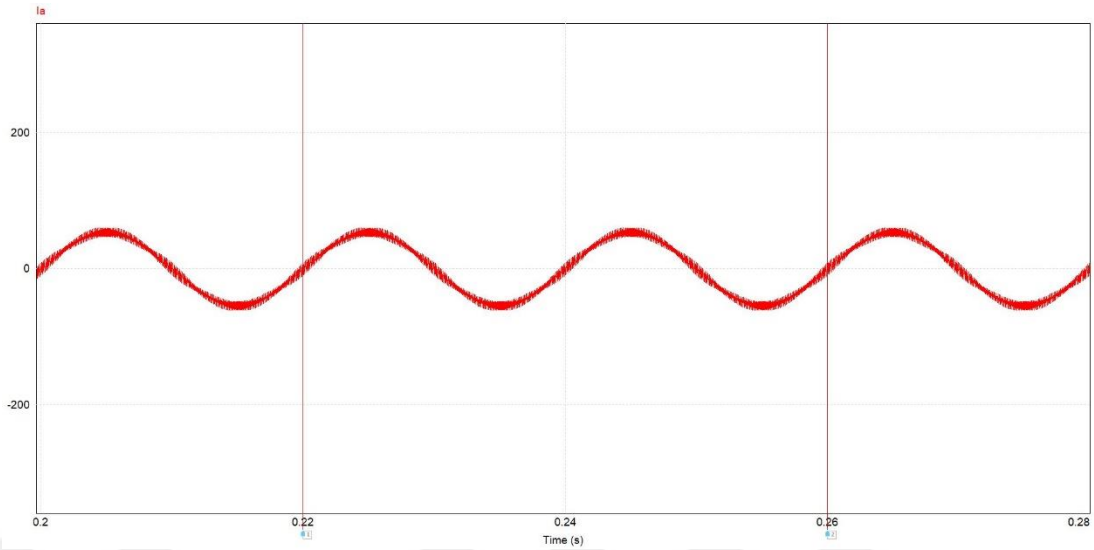

	x1	x2	Δ	THD
Time	2.20000e-001	2.60000e-001	4.00000e-002	freq=50
Ia	-5.63231e+000	-5.63231e+000	-3.48452e-006	8.99668e-002

Figure 3-17 Input current waveform and THD for 25kW output power

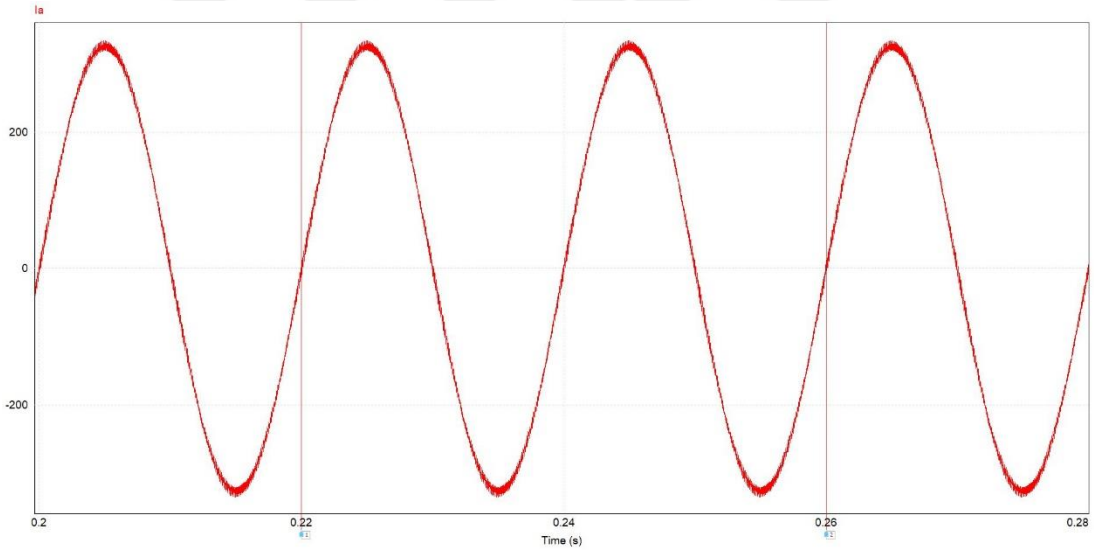

	x1	x2	Δ	THD
Time	2.20000e-001	2.60000e-001	4.00000e-002	freq=50
Ia	-8.15439e+000	-8.15439e+000	1.32656e-008	1.67750e-002

Figure 3-18 Input current waveform and THD for 150kW output power

Table 4 *THD and efficiency values for different output power levels*

Output Power (kW)	*THD(%)*	*Efficiency(%)*
25	8.99	99.63
50	4.58	99.53
75	3.09	99.45
100	2.36	99.38
125	1.96	99.31
150	1.68	99.23

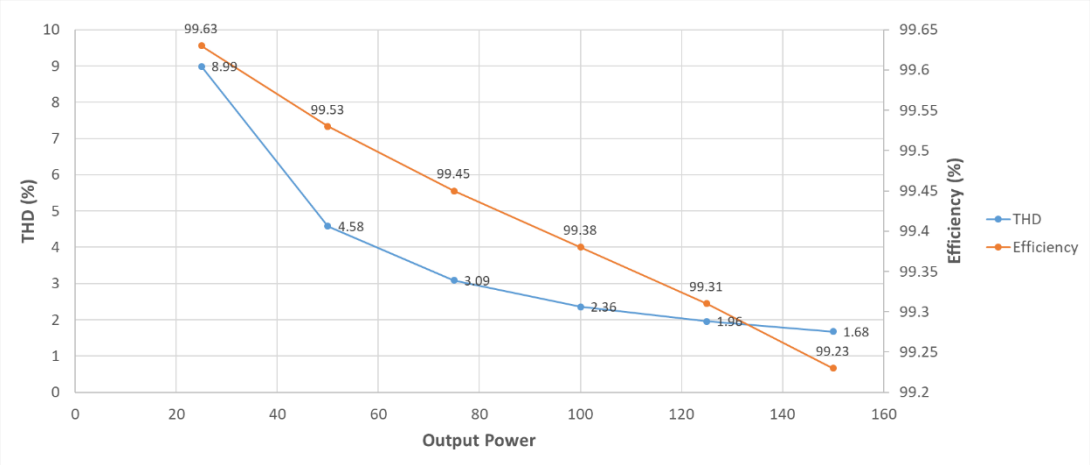

Figure 3-19 THD and efficiency values for different output power levels

Table 5 *Switching and conduction losses for different output power levels*

Output Power (kW)	*Switching Loss (W)*	*Conduction Loss (W)*	*Combined Loss(W)*	*Junction Temperature(°C)*
25	62.95	26.04	89.00	29
50	128.18	102.86	231.04	36
75	191.84	212.25	404.09	44
100	253.33	358.64	611.97	54
125	335.92	553.37	869.29	66
150	379.59	804.95	1185	81

Lastly, effect of different output voltage levels on the input current THD and efficiency is investigated for 100kW output power, 10kHz switching frequency. In *Table 6*, THD and efficiency for different output voltage levels are presented and its graph can be seen in Figure 3-20. This time the switching frequency is dominant with the rising output voltage level which can be deduced from the simulation results in *Table 6*. Therefore, the efficiency falls as the output voltage increases. THD makes a bottom at the 750V output DC voltage. The reason can be presumed as follows: PI controllers of the All SiC PWM Rectifier are optimized for the 750V output voltage, thus the least harmonics are achieved at that voltage level.

Table 6 *THD and efficiency values for different output voltage levels*

Output Voltage (V)	*THD(%)*	*Efficiency(%)*
625	2.04	99.46
750	1.73	99.39
800	2.49	99.36
900	2.69	99.31
1000	2.86	99.24

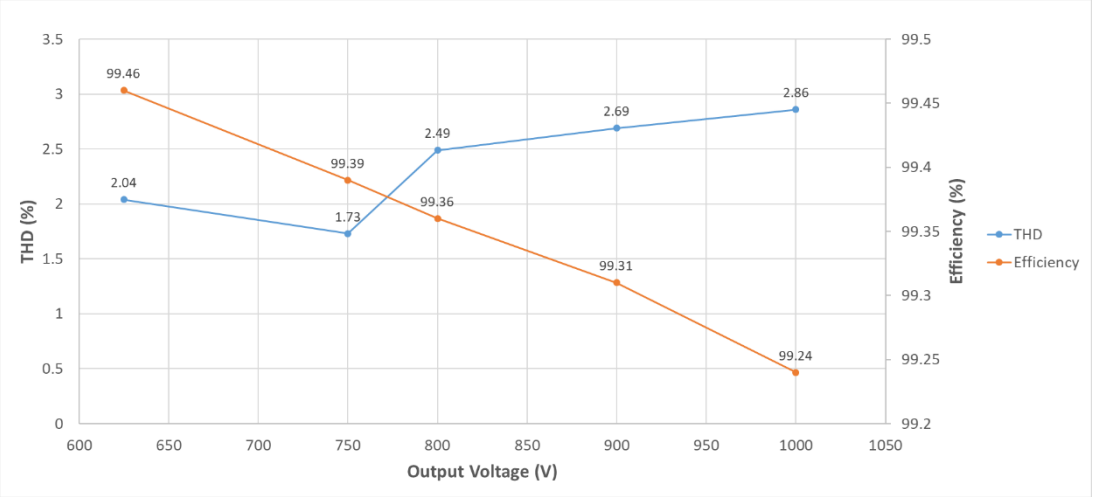

Figure 3-20 THD and efficiency values for different output voltage levels

Table 7 *Switching and conduction losses for different output voltages*

Output Voltage (V)	*Switching Loss (W)*	*Conduction Loss (W)*	*Combined Loss(W)*	*Junction Temperature(°C)*
625	211.44	333.02	544.45	51
750	253.33	358.64	611.97	54
800	270.07	367.23	637.31	55
900	303.85	382.41	686.26	58
1000	358.83	397.05	755.89	61

3.6. Simulation Results

Simulations for the All SiC Three Phase PWM Rectifier is performed on PSIM 9.0 power electronics simulation software. The schematic of the simulation for rectification can be observed in Figure 3-21.

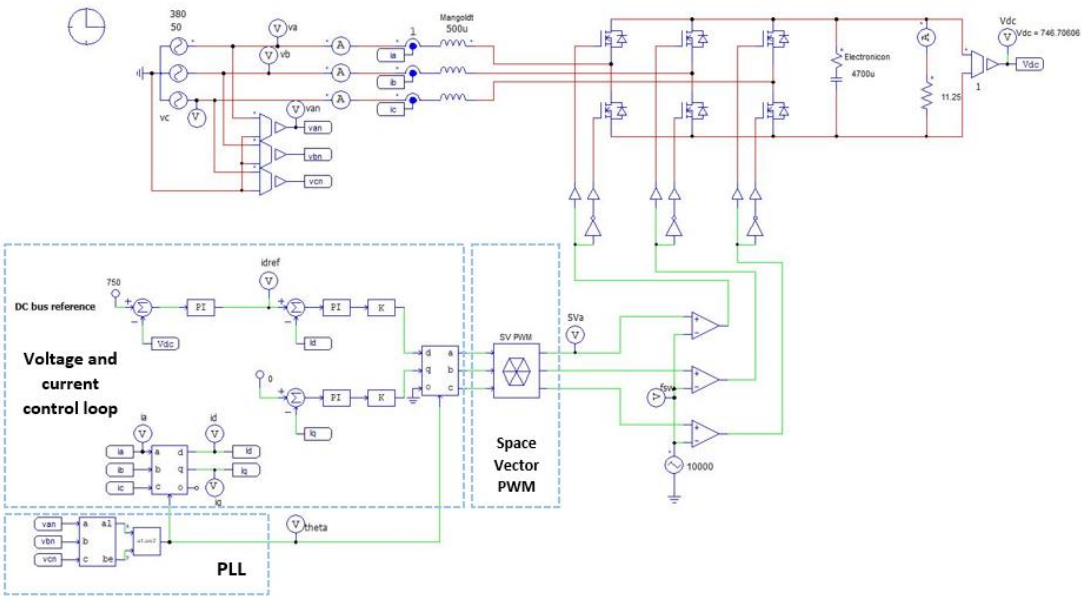

Figure 3-21 Schematic of Three Phase PWM Rectifier

The lower voltage limit for Three Phase PWM Rectifier arise from the fact that anti-parallel diode rectifies the voltage even if MOSFETs are blocked for conduction.

Therefore, the system behaves as three phase diode bridge rectifier with dc-link capacitor which has high capacitance (4700uF). The limit is approximately the peak of line-to-line input voltage (565V). The schematic and the simulation for the circuit can be seen in Figure 3-22 and Figure 3-23 respectively.

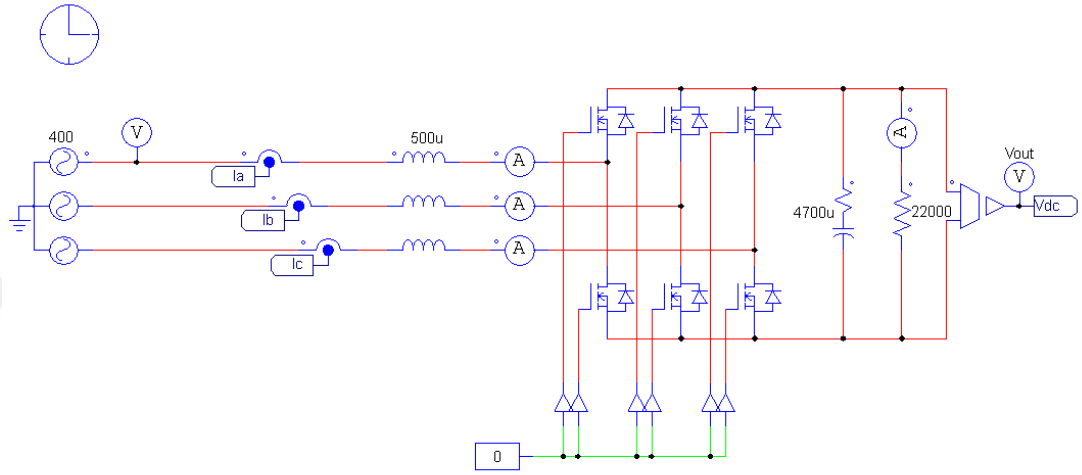

Figure 3-22 Schematic of Three Phase PWM Rectifier with gates of MOSFETs blocked

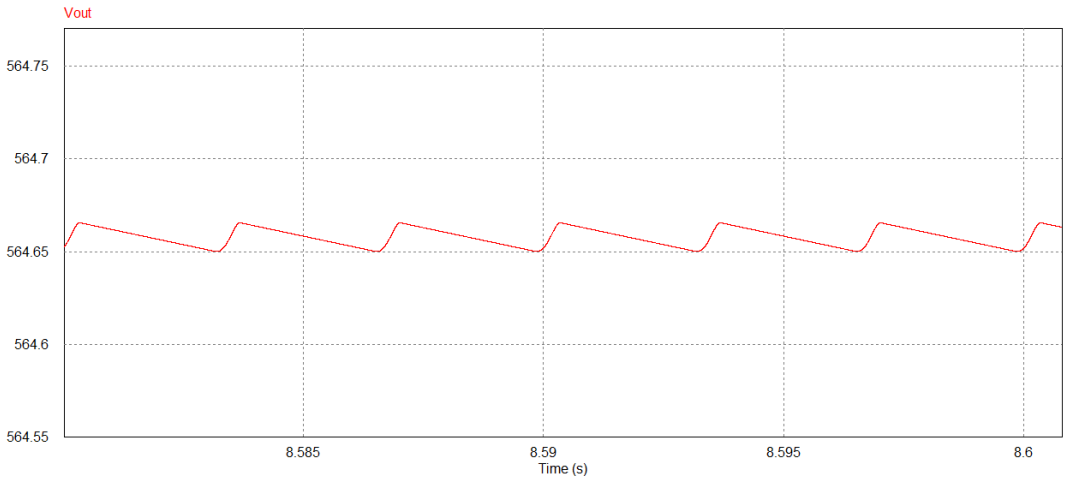

Figure 3-23 Output DC voltage of the rectifier when gates of MOSFETs are blocked for conduction

The average output voltage of this circuit without the dc-link capacitor can be calculated from this formula:

$$Vdc = V_m * \frac{3\sqrt{3}}{\pi} \tag{3.10}$$

Where Vm is the peak of line-to-neutral input voltage. It can also be written as:

$$Vdc = \frac{\sqrt{2}}{\sqrt{3}} V_{l-l} * \frac{3\sqrt{3}}{\pi} \cong 1.35 * V_{l-l} \tag{3.11}$$

The simulations are conducted for 625V, 750V, 800V, 900V and 1000V output dc voltage levels. The load is chosen as 4.5Ω resistive load. The variations of input current waveforms and output dc level voltage can be observed between Figure 3-24 and Figure 3-28. In all simulations unity power factor is achieved.

The three phase AC input current waveforms and output dc voltages are demonstrated in the same figure for each output voltage level.

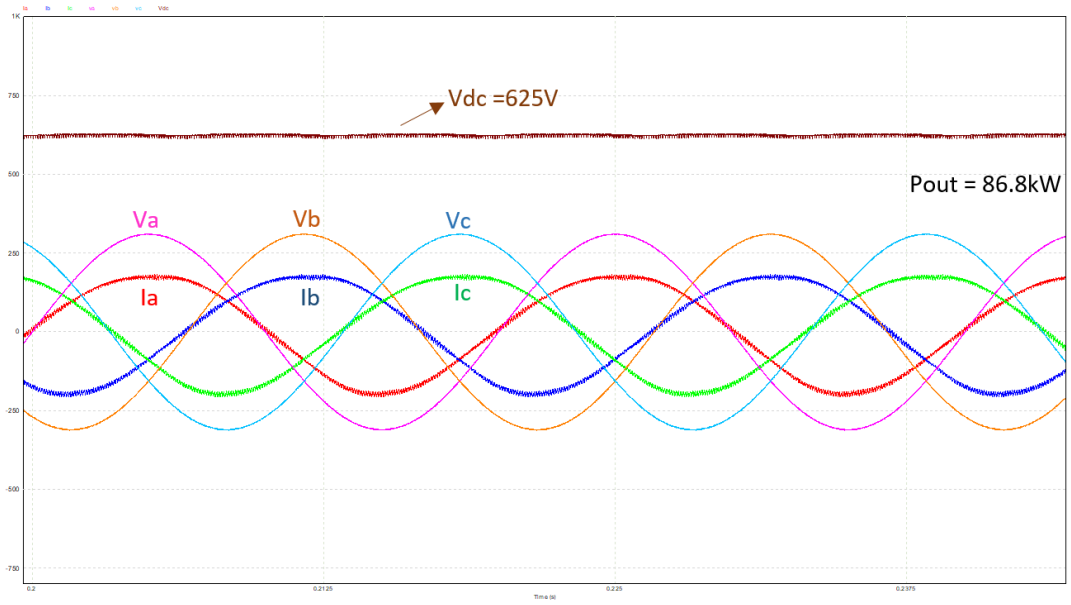

Figure 3-24 AC input currents and DC output voltage waveforms for 625Vdc

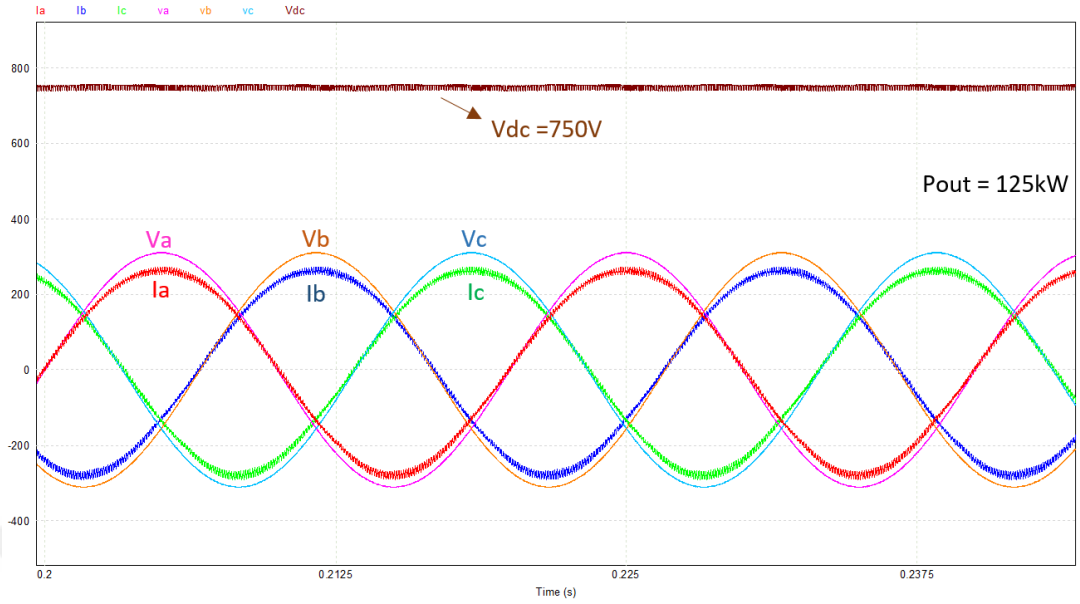

Figure 3-25 AC input currents and DC output voltage waveforms for 750Vdc

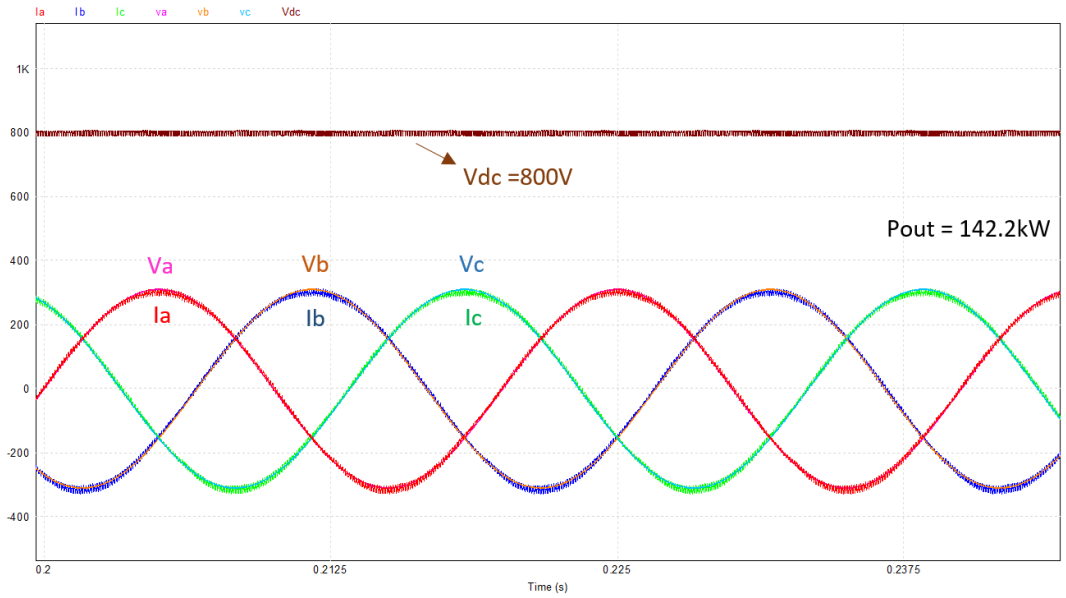

Figure 3-26 AC input currents and DC output voltage waveforms for 800Vdc

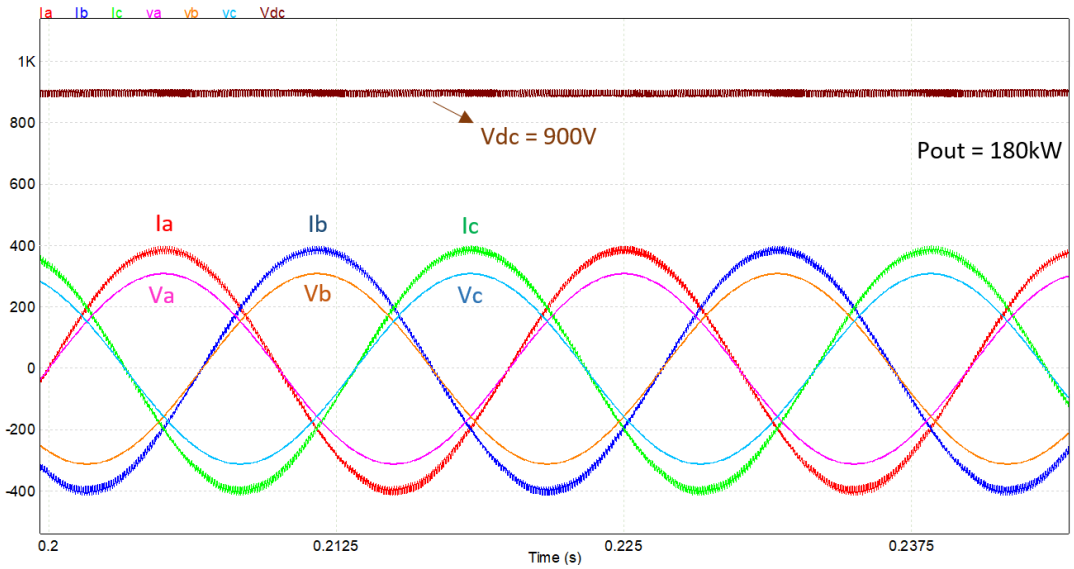

Figure 3-27 AC input currents and DC output voltage waveforms for 900Vdc

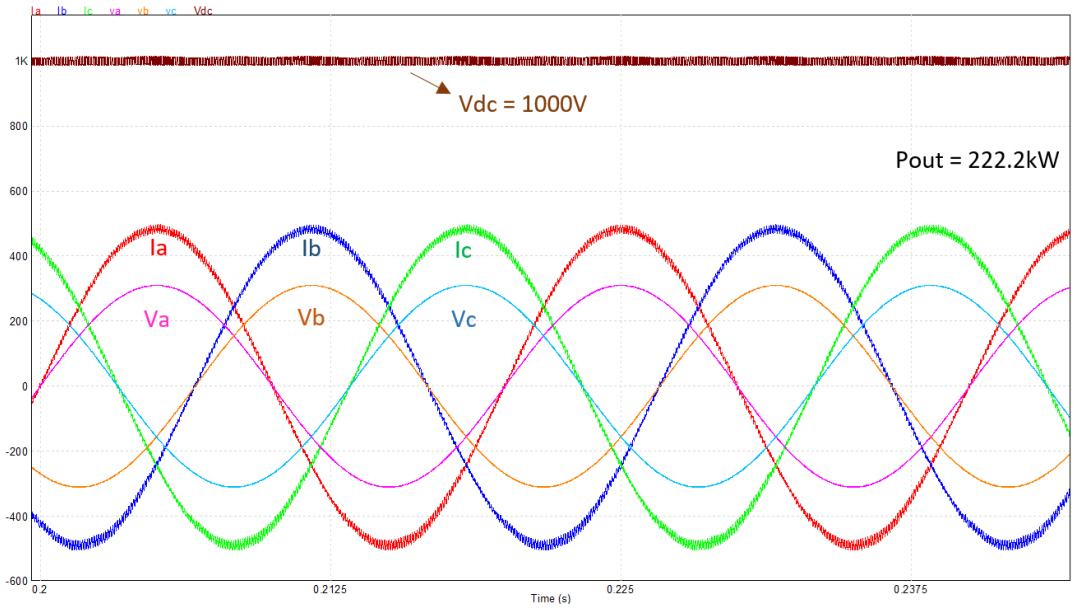

Figure 3-28 AC input currents and DC output voltage waveforms for 1000Vdc

Inversion operation is also examined. For the inversion the following schematic shown in Figure 3-29 is formed. From the dc link side, a 1000V dc voltage source is connected and the dc link control reference value is set to 750Vdc. The result of the

simulation demonstrating the output dc value and phase-A current and voltage waveforms can be observed in Figure 3-30.

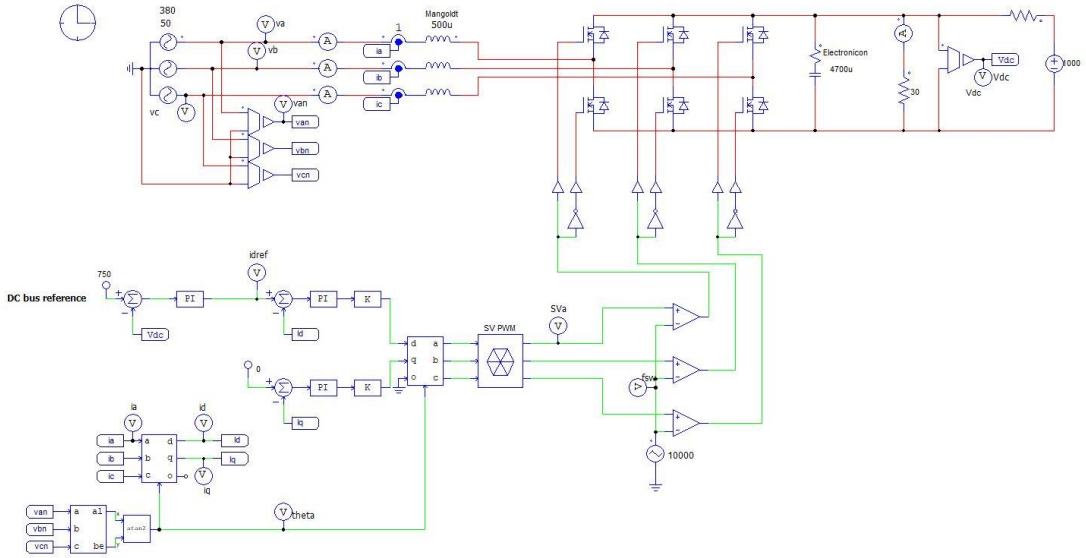

Figure 3-29 Schematic for inversion operation

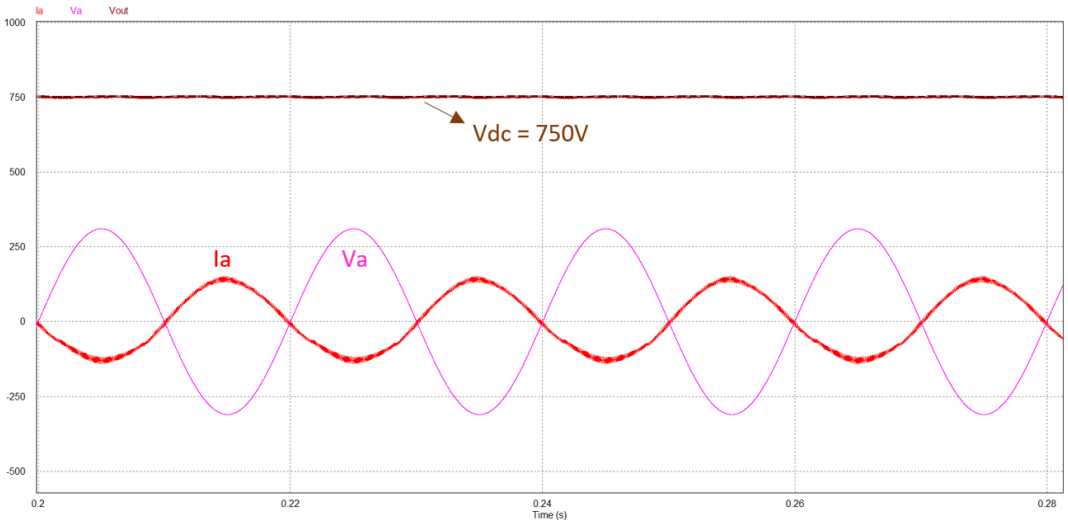

Figure 3-30 Output dc value and phase-A current and voltage waveforms

Transient response of the Three Phase PWM Rectifier also studied in simulations. Peak voltage is observed at 6.05 milliseconds and settling time as 51.43 milliseconds

at 750 V output DC value by adjusting the gain and time constant of voltage and current PI controllers. The control system has a fast response and settles quickly to the desired output voltage value. The response can be seen in Figure 3-31.

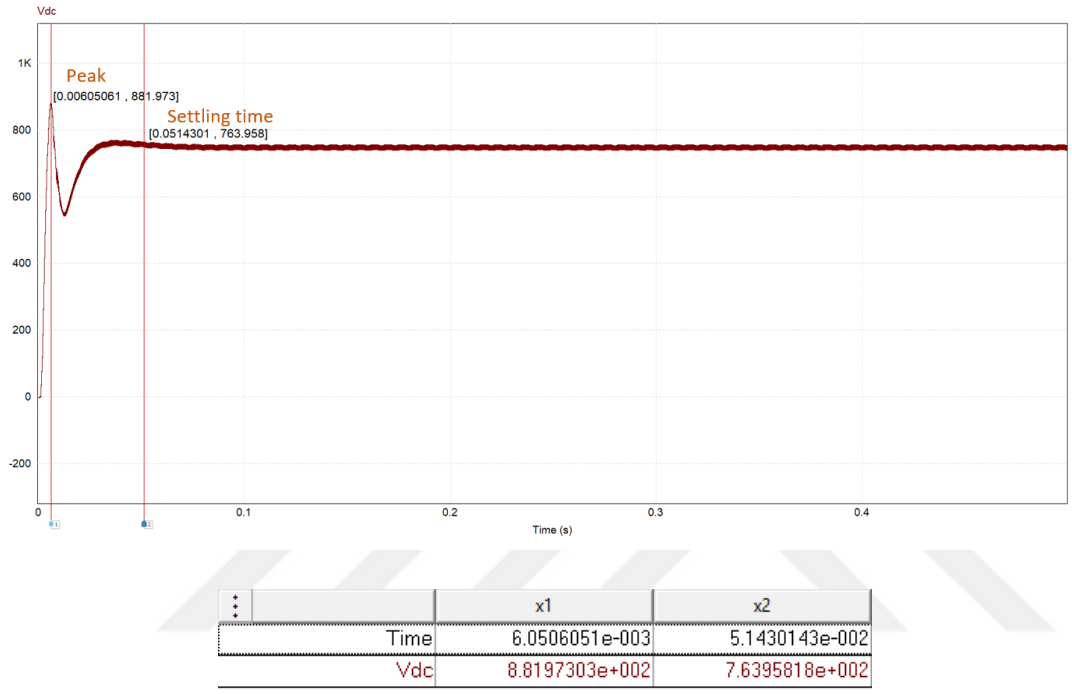

	x1	x2
Time	6.0506051e-003	5.1430143e-002
Vdc	8.8197303e+002	7.6395818e+002

Figure 3-31 DC output voltage transient response for 750Vdc output dc voltage – underdamped response

Lastly, the dynamic response of the Three Phase PWM Rectifier is studied, i.e. during the operation of PWM Rectifier the load resistance level is changed so that the response of the system can be examined.

At the start of the simulation, 30Ω resistor is connected to the dc link of the PWM Rectifier. After 2.5 seconds, the load is changed to 4.5 Ω. As it can be seen from Figure 3-32, Vdc and Iload reach their final values after the dynamic response time.

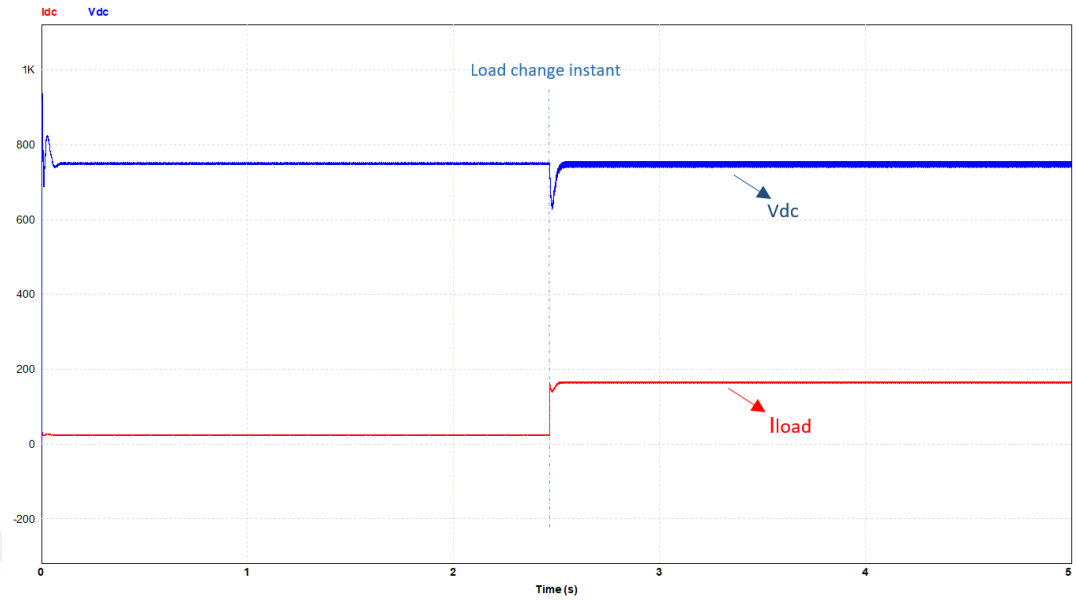

Figure 3-32 Dynamic response of Three Phase PWM Rectifier

3.7. Implementation of All SiC Three Phase PWM Rectifier

All SiC Three Phase PWM Rectifier is given in Figure 3-33. The components it consists of are clarified on the figure. How the materials are chosen for this application of All SiC Three Phase PWM Rectifier are explained thoroughly in [11].

In Table 8 Nominal values of components in All SiC Three Phase PWM Rectifier and their manufacturer part numbers are presented.

In Figure 3-33, the picture of the All SiC Three Phase PWM Rectifier built in the laboratory and all materials used in the rectifier are given. To manufacture the PWM Rectifier cabinet, the drawings of cabinet are implemented in SolidWorks software. In Appendix A, these drawings can be observed. In Figure 3-34, from AC to DC side the materials used in the rectifier can be seen in schematic form.

The close-up picture of power, control, DSP PCBs and SiC MOSFET drivers are shown in Figure 3-35. The PCBs were manufactured in ASELSAN UGES for traction

converters and their functionality was already proven in field. Therefore, it only required coding for DSP in order to use it in All SiC Three Phase PWM Rectifier.

Table 8 *Nominal values of components in All SiC Three Phase PWM Rectifier*

Component	*Manufacturer- Part Number*	*Nominal Value*	*Unit*
Line Boost Inductor	Mangoldt - 1042215	0.5	mH
Voltage Transducer	LEM - LV25-1000	1000	V
Current Transducer	LEM - LF500S	500	A
Soft-start Resistor	REO – BW 154/200	1000	Ω
		200	W
Soft-start Contactor	ABB TAL 26-30-10	690	V
Main Contactor	SCHNEIDER LC1F300	440	V
		330	A
SiC MOSFET	CREE - CAS300M17BM	1700	V
		300	A
MOSFET Driver	CREE - PT62SCMD17	+20/-6	V

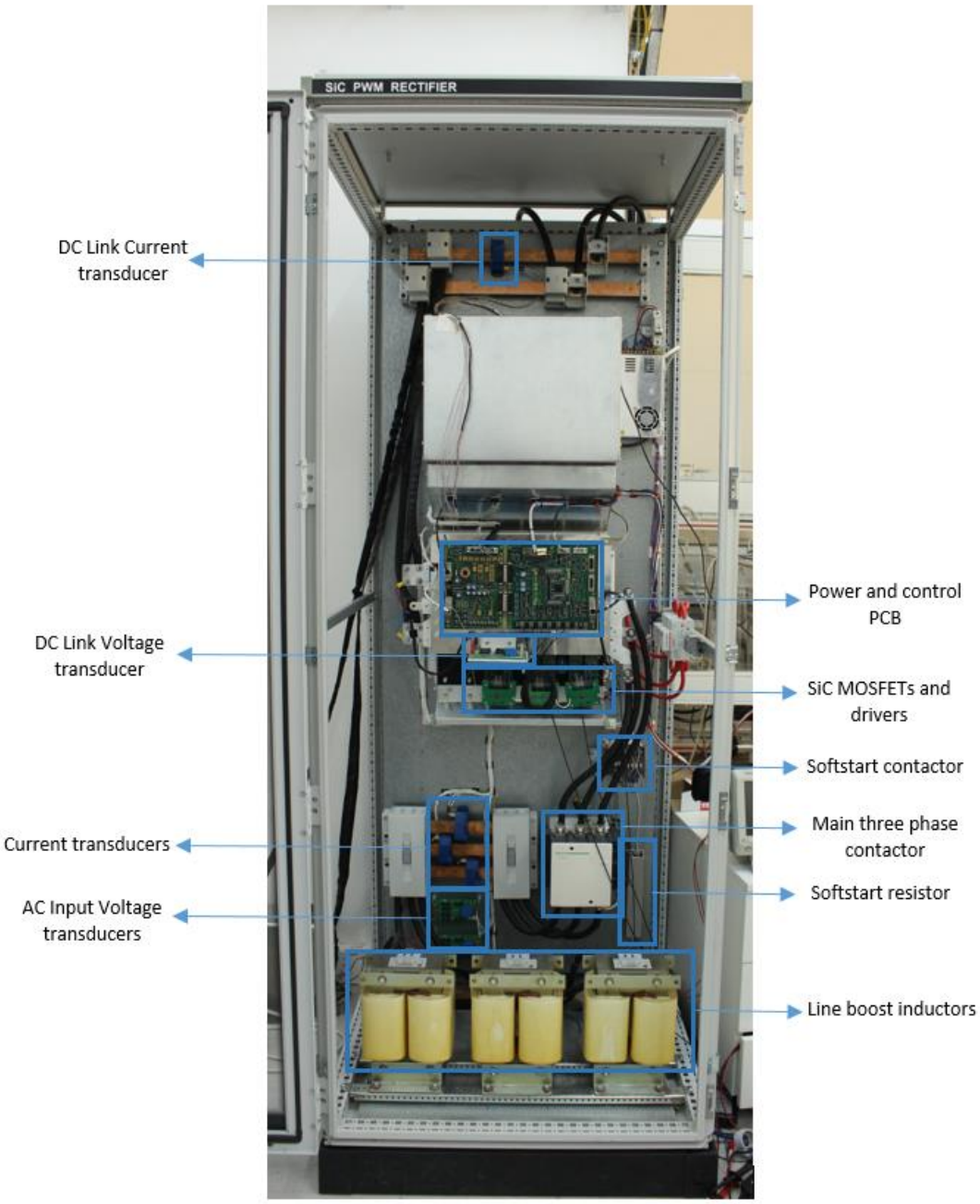

Figure 3-33 All SiC Three Phase PWM Rectifier built in laboratory and used components

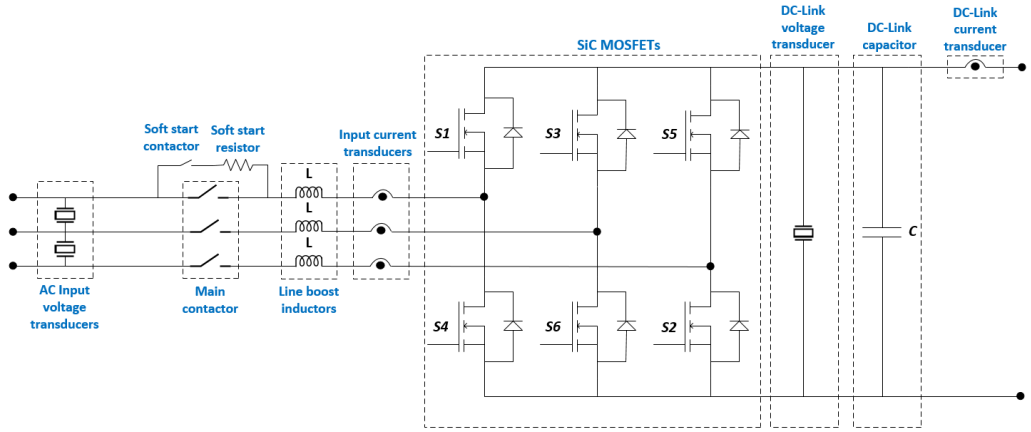

Figure 3-34 All SiC Three Phase PWM Rectifier schematic and used components

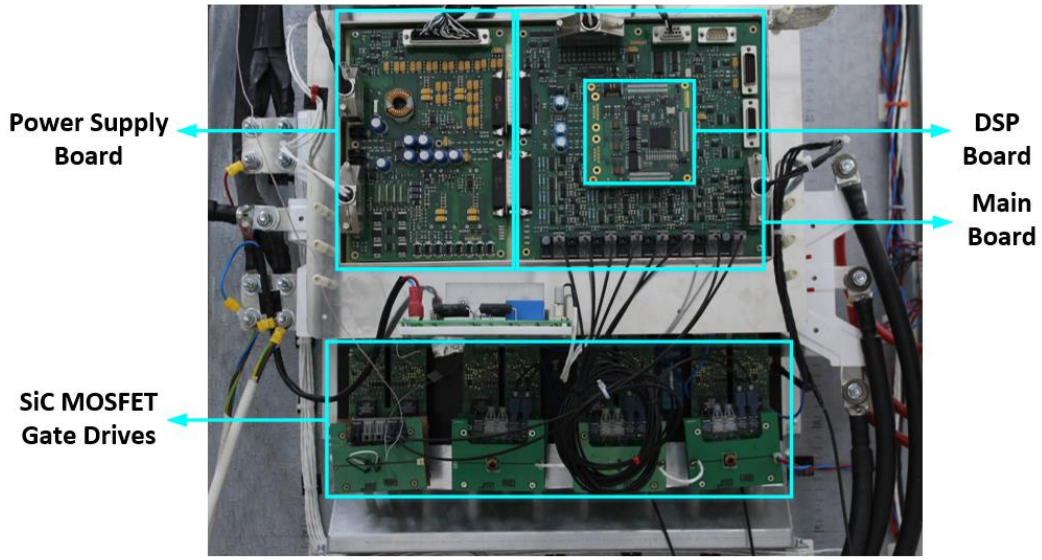

Figure 3-35 Close up picture of boards and SiC MOSFET Gate Drives

In Figure 3-35 the boards are placed on top of the power stage of the All SiC PWM Rectifier which are all self-designed. In Figure 3-36, layers of the power stage are shown from the heat sink to metal film DC link capacitors. First, three half bridge SiC MOSFETs placed on heatsink with thermal paste. Then laminated DC bus with DC

link capacitors is assembled on the MOSFETs. After that, three phase AC bus is placed on top of the DC bus with plastic spacers. Electrical connection between AC bus and the MOSFETs are accomplished by conductive copper spacers.

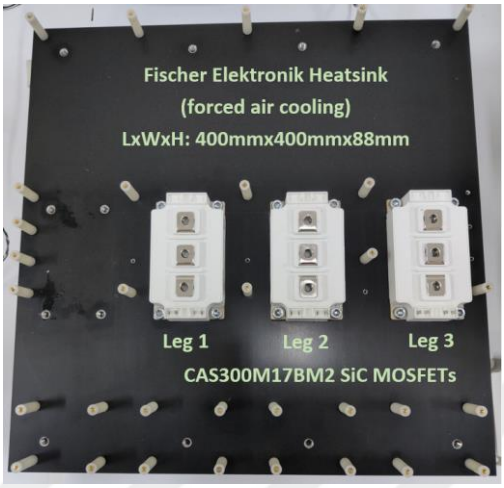

(a)

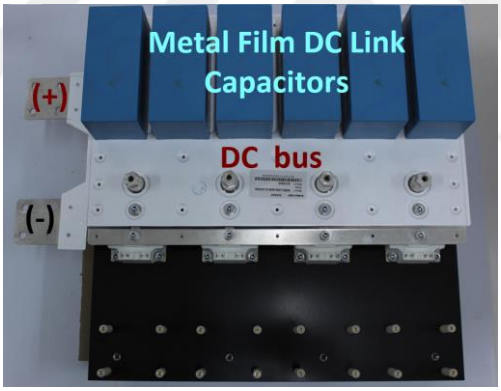

(b)

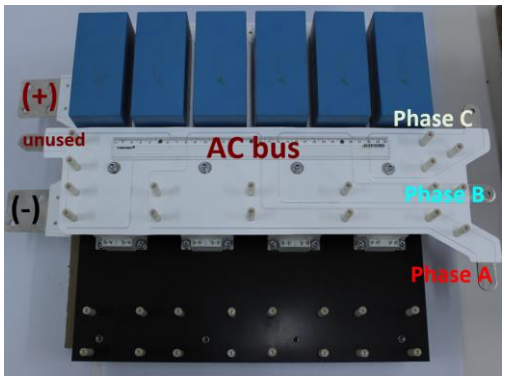

(c)

Figure 3-36 Layers of power stage of All SiC Three Phase PWM Rectifier (a) SiC MOSFETs on heatsink (b) DC Bus with DC Link Capacitors (c) Three phase AC bus

3.8. Discussion

Space Vector PWM modulation technique when compared the Sinusoidal PWM through various frequency levels showed that SVPWM results in less input current harmonic components, thus THD. Determining the switching frequency carried out by considering the thermal limits i.e. junction temperature of switching element. Simulations on different output voltages for the limit junction temperature demonstrated that PWM rectifier has higher output power capacity at 10 kHz switching frequency compared to 15 kHz and 20 kHz. The parameters affecting the input current THD and efficiency are investigated as well. The simulations revealed that THD gets lower as the switching frequency increases. Rising output power at constant output voltage leads to reduced efficiency and THD. Efficiency decreases since conduction losses increase with square of current, therefore they become dominant as the output power rises. When we keep the output power constant and increase the output voltage level, efficiency decreases. This time switching losses become more dominant with rising drain to source voltage on SiC MOSFETs.

CHAPTER 4

EXPERIMENTAL WORK

In experimental work chapter, laboratory experimental setup, experimental results for both rectification and inversion, efficiency and finally harmonic spectrum of the system are investigated. Each application discussed in chapter 2 demands different output power and output voltage. For instance, battery charger application demands narrow output voltage ranges for different periods of its operation. At the beginning of the charging, low voltage and high current, at the end of charging period high voltage and low current is needed. In AC Motor Drive, output voltage is constant whereas output power transferred to inverter is changing. For resistive furnaces, rectifier output voltage, thus power is varied. DC Motor Drive needs variable output voltage and Synchronous Motor Field Exciter needs boosting action of output voltage for stability. Consequently, experiments are conducted for various output power ratings for each output voltage level.

4.1. Experimental Setup

In this part, experiments conducted on the laboratory setup are presented. These results are obtained from the implemented All SiC Three Phase PWM Rectifier cabinet shown in Chapter 3. In this setup, the Three Phase PWM Rectifier is energized from the Distribution Panel constructed for this work which gives three phase line-to-line 400VAC 50Hz voltage to the PWM Rectifier. The distribution panel is presented in Figure 4-1. The electric project of the laboratory is drawn in order to construct the experimental setup in the laboratory. The electric project can be seen in Appendix B.

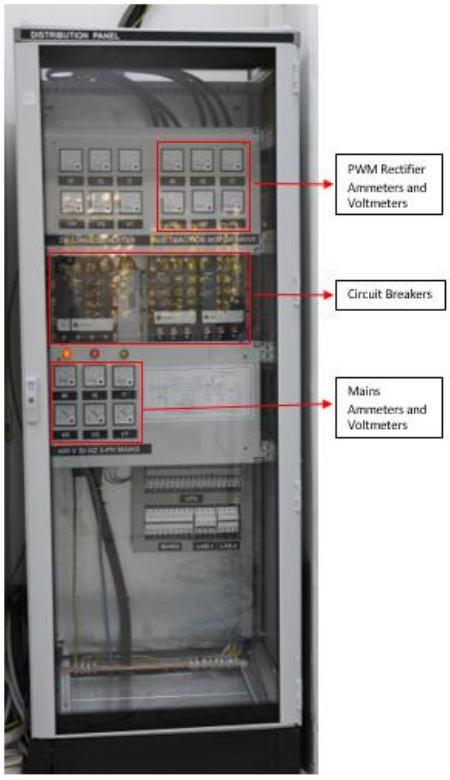

Figure 4-1 Distribution Panel

At the entry of the distribution panel there is a 4-pole circuit breaker connected to the main grid which has line-to-line 400VAC 50Hz voltage. The voltage and current at the input of the circuit breaker is examined via “Mains” ammeters and voltmeters. Output of the 4 pole circuit breaker is connected to two 3-pole circuit breakers. One of them is responsible for the safe transfer of power to the Three Phase SiC PWM Rectifier cabinet. The current and voltage at the output of the circuit breaker is observed via ammeters and voltmeters as well. These measurement and safety devices can be observed in Figure 4-1.

In the experimental procedure, the results are obtained with two different load types. The main load of the All SiC PWM Rectifier is AC Induction Motor. PWM Rectifier feeds the AC Induction Motor through an inverter. Due to the fact that the AC

Induction Motor has rated power of 130 kW, a resistive load is also connected the output of the PWM rectifier so that higher power can be achieved.

The laboratory setup used for this configuration is given in Figure 4-2. The total system consists of Three Phase All-SiC PWM Rectifier, All-SiC Traction Inverter, Induction Motor and Resistive Load. Also, in order to simulate the load on the induction motor, a generator which is driven by a dc-link converter is used. The dc-link converter is commercial motor drive with active front end. There is also a flywheel coupled to the shaft of the motor which is used to simulate the saved and released kinetic energy during induction motor operation.

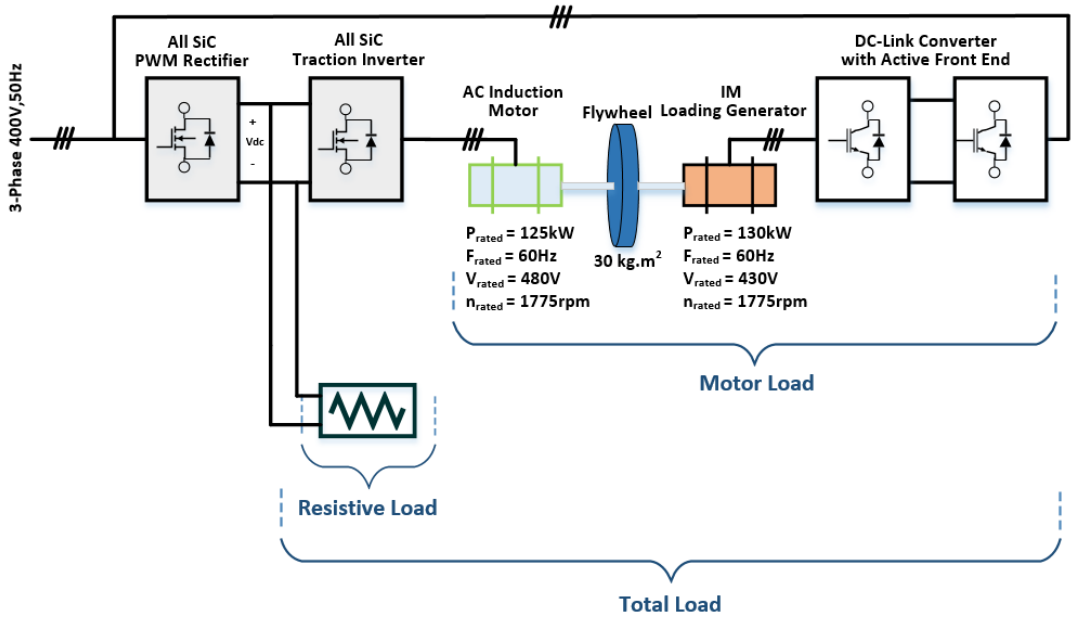

Figure 4-2 System scheme for AC Induction Motor load configuration

The specifications of AC Induction Motor can be seen in Table 9.

Table 9 *Specifications of AC Induction Motor*

Motor Parameters	*Rated (S1)*	*Maximum (S2)*
P [kW]	130	160
U [V]	475	475
fn1 [Hz]	60	60
I1 [A]	200.3	244.5
n [U/min]	1779	1773
Mn [Nm]	670.9	861.9
cosfi	0.8112	0.8527
eta [%]	93.5	93.29

The specifications of Loading Generator which is also an induction motor used in generator mode can be seen in *Table 10*.

Table 10 *Specifications of Loading Generator*

Motor Parameters	*Rated (S1)*	*Maximum (S2)*
P [kW]	125	160
U [V]	430	430
fn1 [Hz]	60	60
I1 [A]	231.9	280.8
n [U/min]	1776	1770
Mn [Nm]	672	862
cosfi	0.80	0.84
eta [%]	93.4	91.4

The parameters represent the following values for motor:

P: Motor power

U: Motor voltage

fn1: Frequency

I1: Current

n: Speed in rpm

Mn: Torque

cosfi: Power factor

eta: Efficiency

The images of All SiC Traction Inverter, AC Induction Motor - Flywheel - Loading Generator system, DC-Link Converter and resistive load can be seen in Figure 4-3.

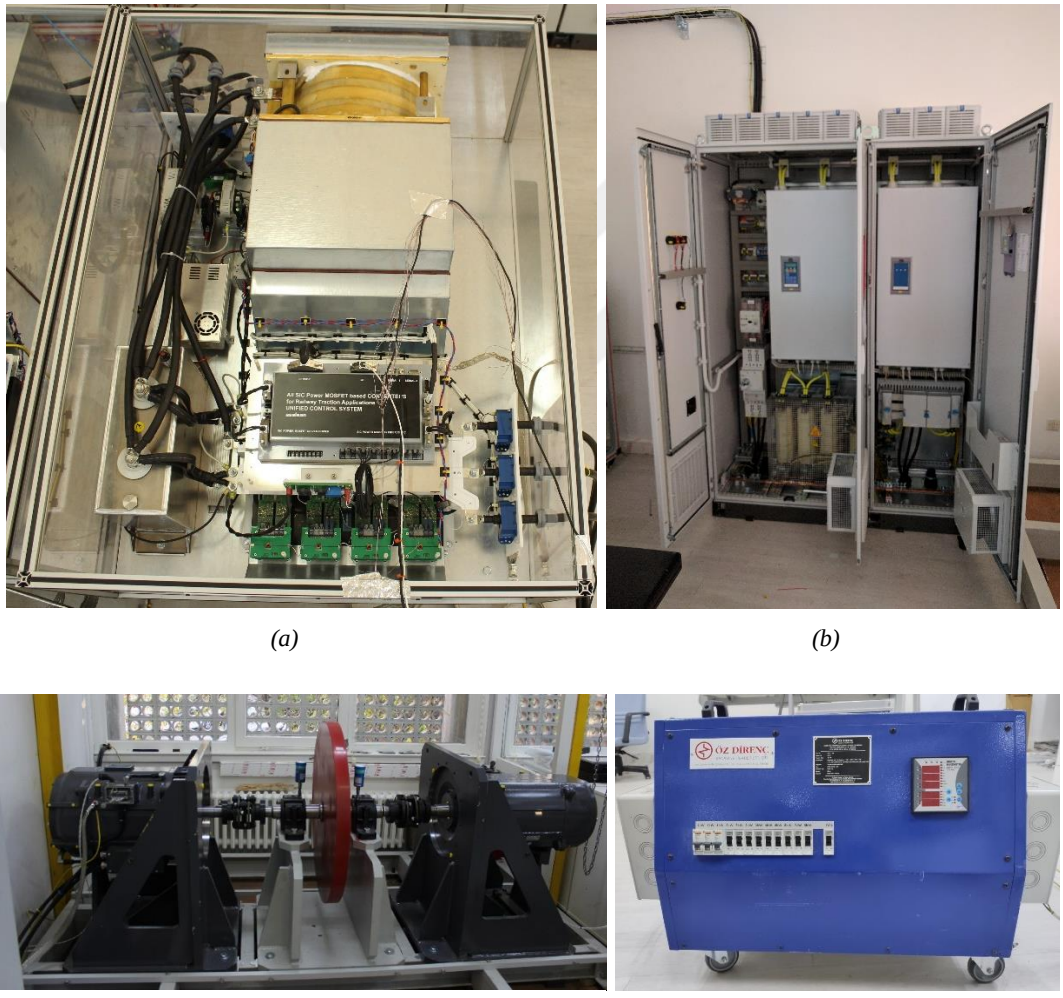

(a) *(b)*

(c) *(d)*

Figure 4-3 (a) All SiC Traction Inverter (b) DC-Link Converter (c) AC Induction Motor – Flywheel – Loading Generator System (d) Resistive Load

The control structure of this system can be seen in Figure 4-4. In this scheme, All-SiC PWM Rectifier and All-SiC Inverter are controlled from MATLAB/Simulink program

on a PC through CAN BUS interface which is converted to USB with a USB/CAN converter. The DC-Link Converter which drives the load generator has a PROFIBUS interface and connected to PLC. PLC communicates with the second desktop PC through Ethernet interface and the control of PLC is maintained with the Codesys software of the Eaton PLC. (XC-CPU202)

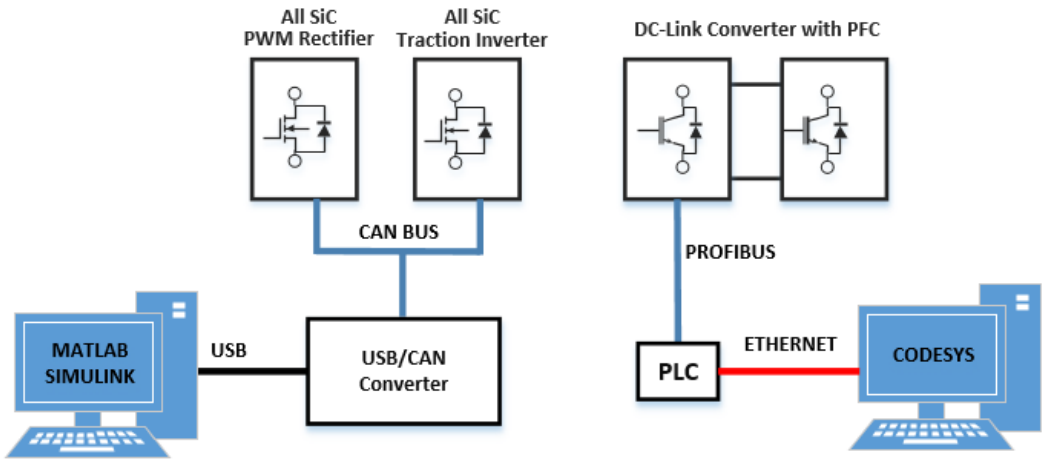

Figure 4-4 Main control of All-SiC PWM Rectifier and All-SiC Traction Inverter on MATLAB/SIMULINK

4.2. Experimental Results

4.2.1. Rectification Mode

As mentioned before, All-SiC Three Phase PWM Rectifier can be used in both Rectification and Inversion Mode. In this part, the results acquired with the systems mentioned in previous section are presented.

All-SiC Three Phase PWM Rectifier operated in various output voltage levels at different loads. These voltage levels include 625V, 750V, 800V, 900V and finally 1000V. It should be emphasized that all results of the experimental work show the unity power factor as aimed for. For the measurements Tektronix MDO 3034 Mixed Domain Oscilloscope is used.

4.2.1.1. Input and Output Waveforms for 625 Vdc Output Voltage Level

Phase A input line to neutral voltage and input current, the DC output current and voltage are presented for rectification mode of operation through Figure 4-5 to Figure 4-9. The experiments are conducted for various load levels.

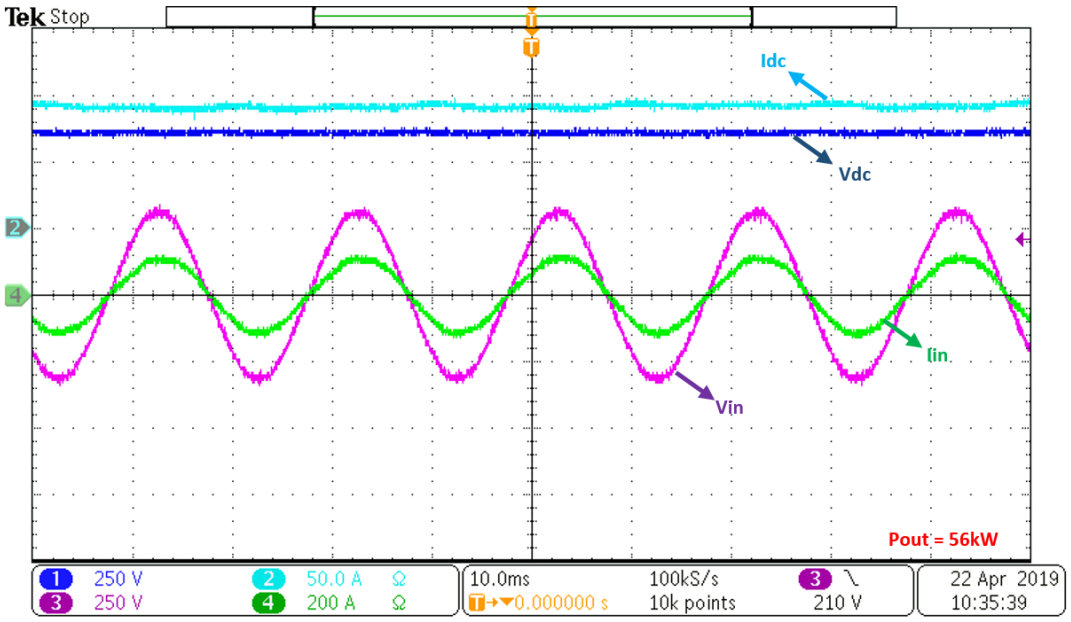

Figure 4-5 Input line to neutral voltage, input current, output dc voltage and output dc current for 56 kW output power

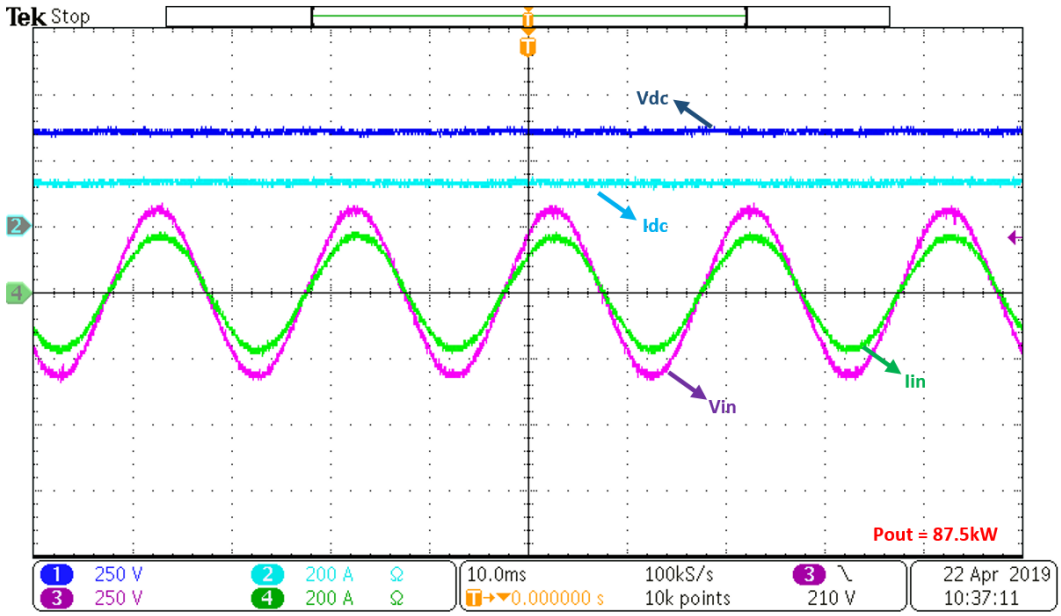

Figure 4-6 Input line to neutral voltage, input current, output dc voltage and output dc current for 87.5kW output power

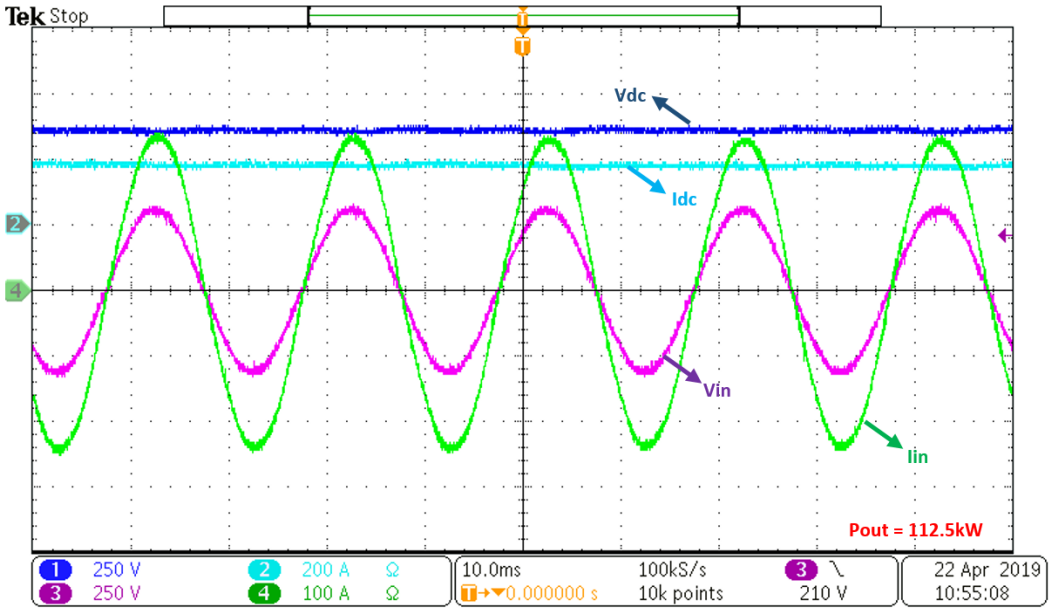

Figure 4-7 Input line to neutral voltage, input current, output dc voltage and output dc current for 112.5kW output power

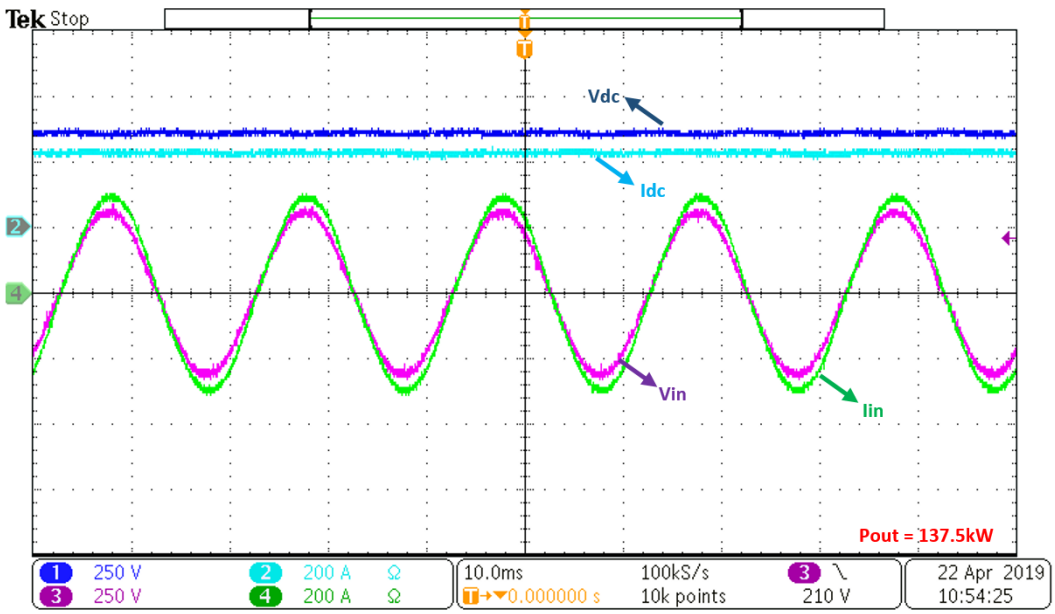

Figure 4-8 Input line to neutral voltage, input current, output dc voltage and output dc current for 137.5kW output power

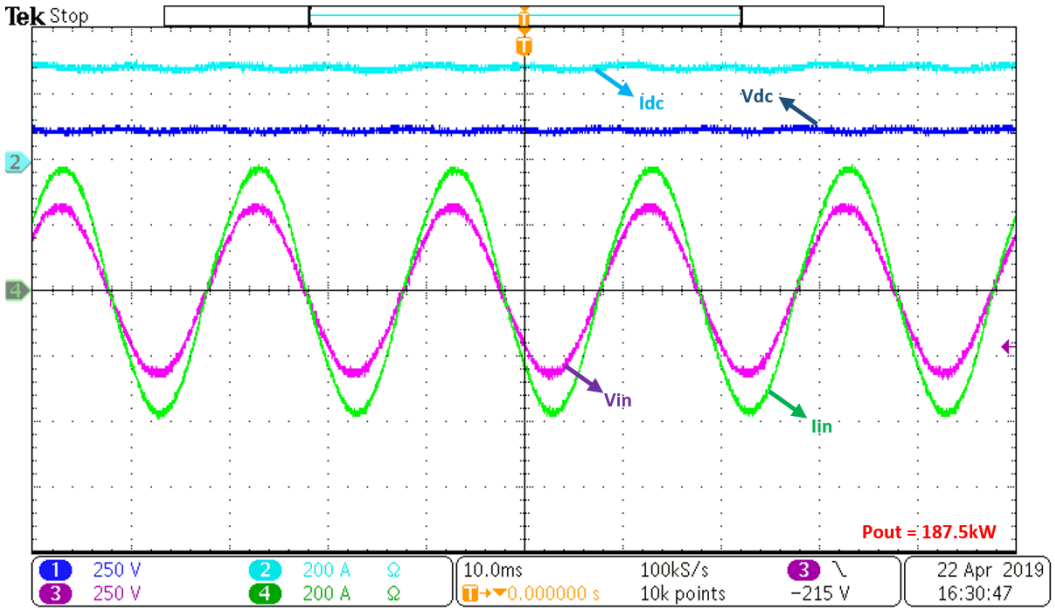

Figure 4-9 Input line to neutral voltage, input current, output dc voltage and output dc current for 187.5 kW output power

4.2.1.2. Input and Output Waveforms for 750 Vdc Output Voltage Level

Input and output waveforms are given for rectification mode of PWM Rectifier for 750 Vdc output voltage through Figure 4-10 to Figure 4-14.

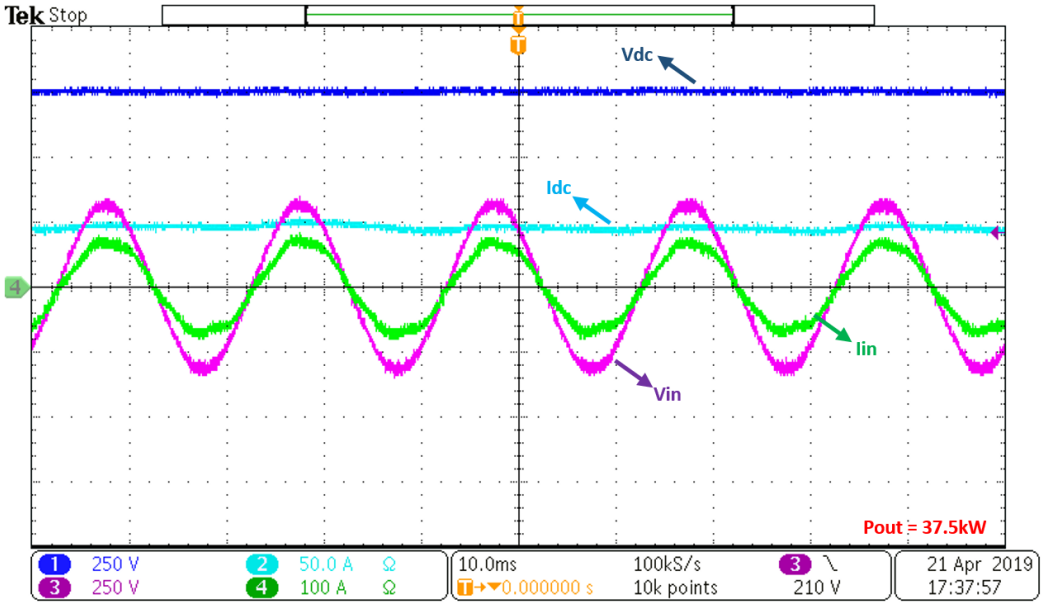

Figure 4-10 Input line to neutral voltage, input current, output dc voltage and output dc current for 37.5kW output power

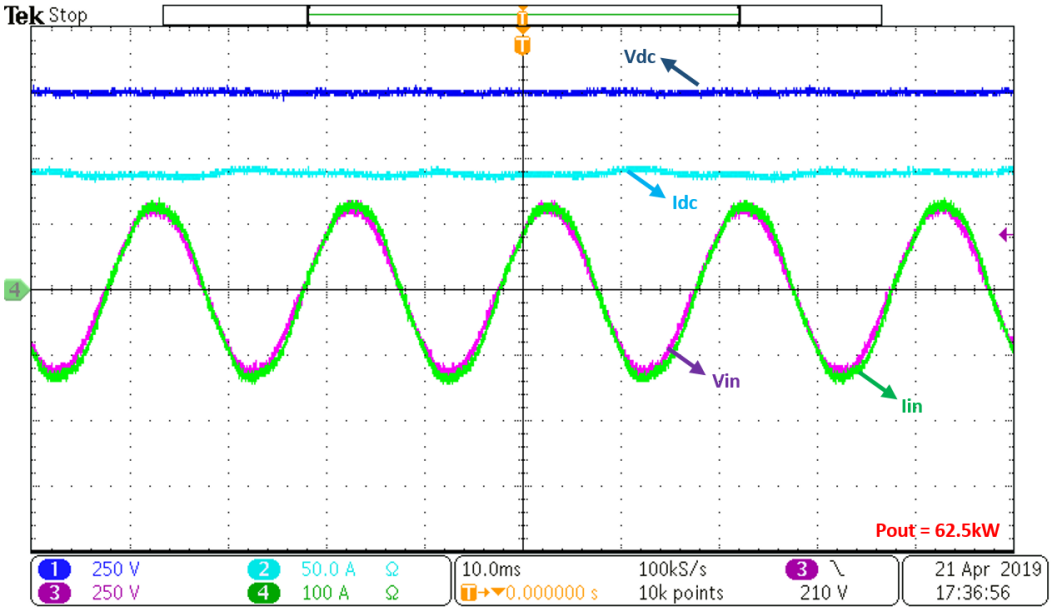

Figure 4-11 Input line to neutral voltage, input current, output dc voltage and output dc current for 62.5kW output power

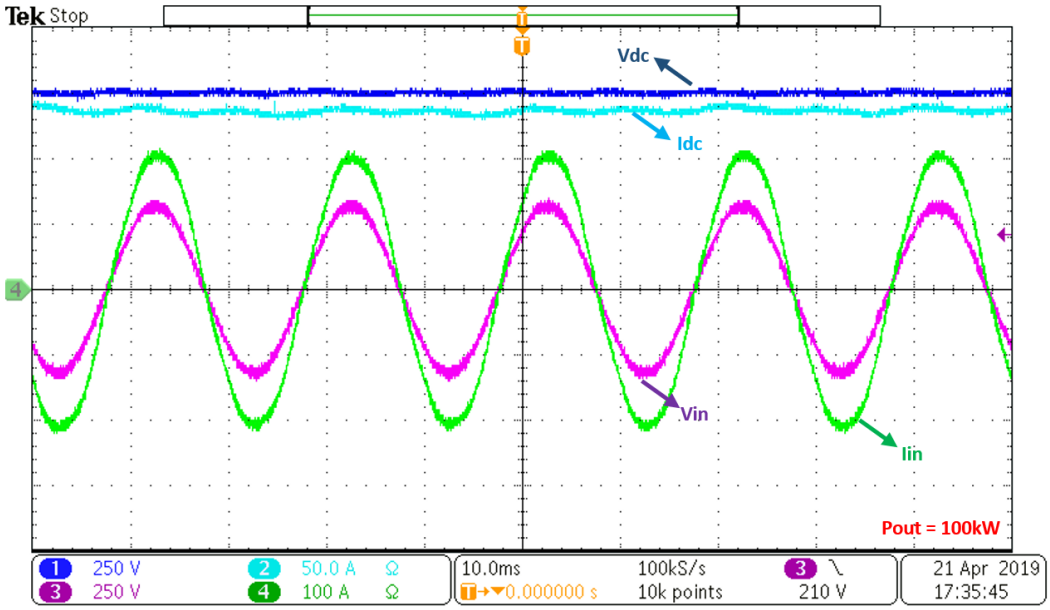

Figure 4-12 Input line to neutral voltage, input current, output dc voltage and output dc current for 100kW output power

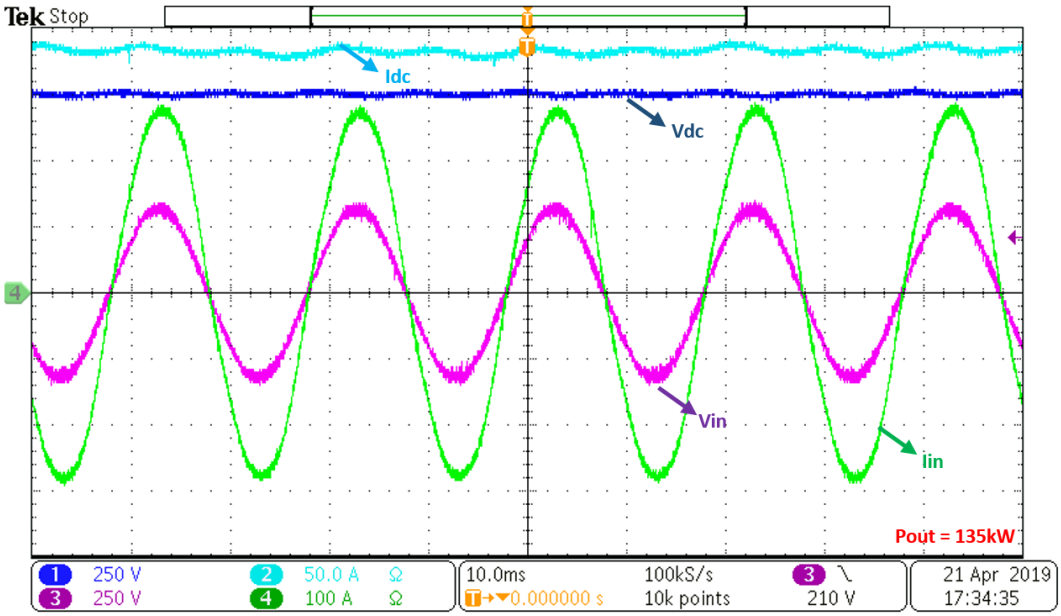

Figure 4-13 Input line to neutral voltage, input current, output dc voltage and output dc current for 135kW output power

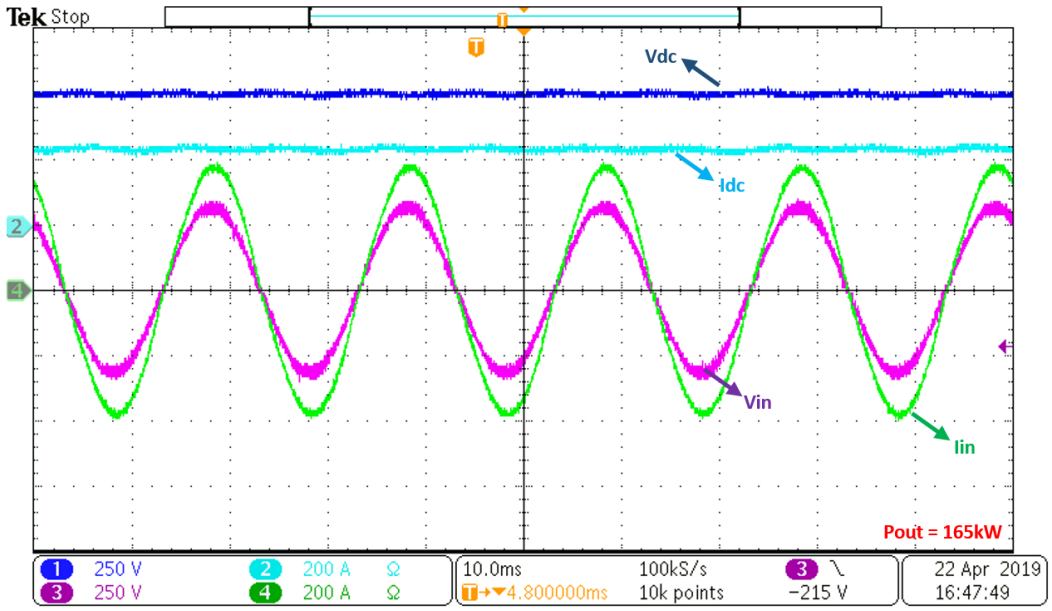

Figure 4-14 Input line to neutral voltage, input current, output dc voltage and output dc current for 165kW output power

4.2.1.3. Input and Output Waveforms for 800 Vdc Output Voltage Level

Phase A input line to neutral voltage and input current, the DC output current and voltage are given for rectification mode of operation through Figure 4-15 to Figure 4-18. The experiments are conducted for various load levels.

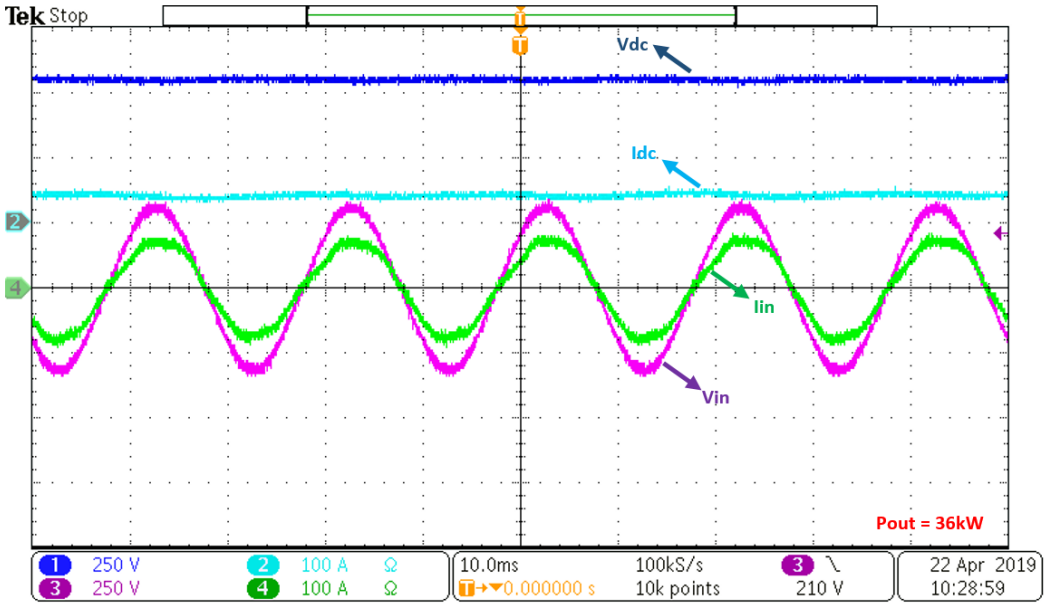

Figure 4-15 Input line to neutral voltage, input current, output dc voltage and output dc current for 36kW output power

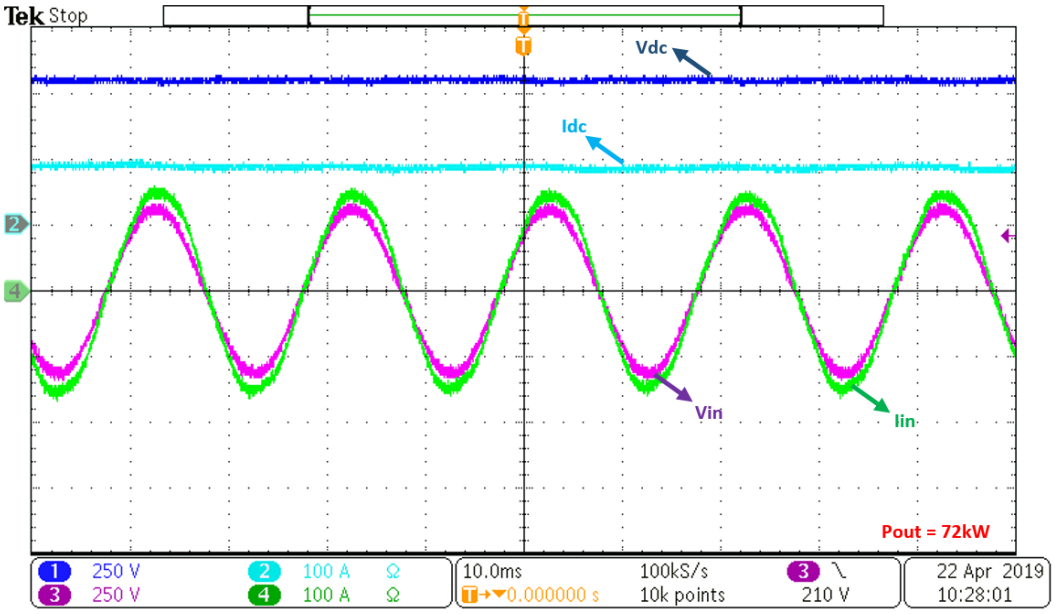

Figure 4-16 Input line to neutral voltage, input current, output dc voltage and output dc current for 72kW output power

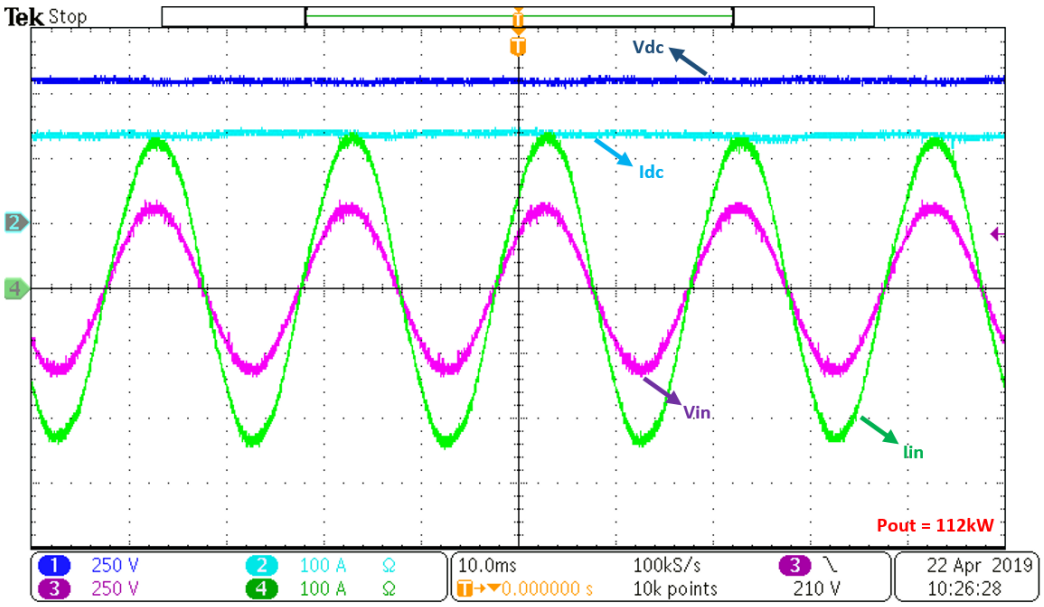

Figure 4-17 Input line to neutral voltage, input current, output dc voltage and output dc current for 112kW output power

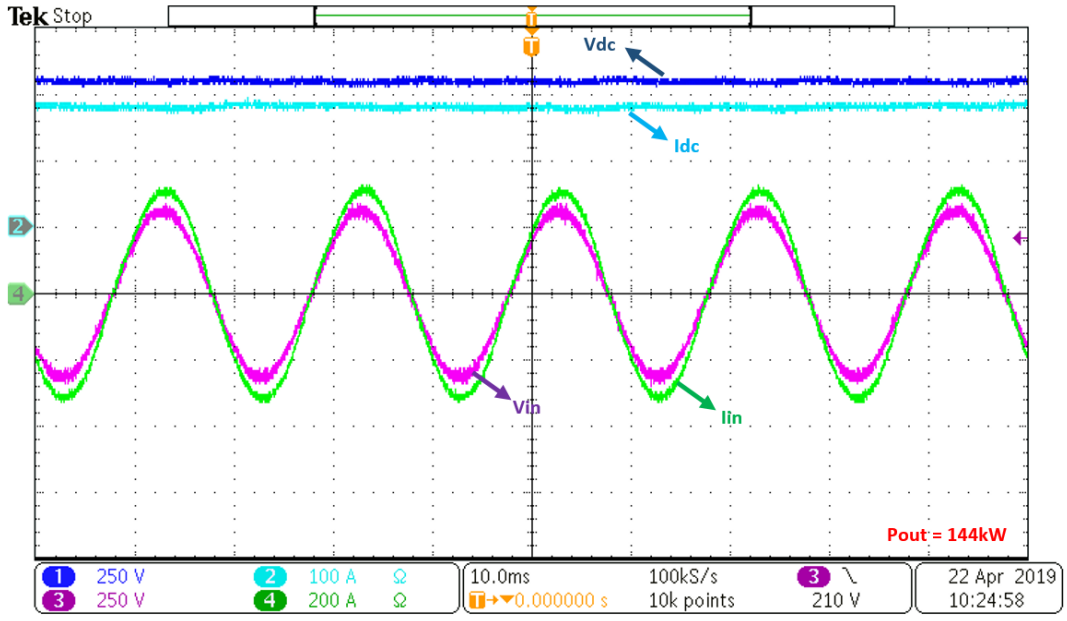

Figure 4-18 Input line to neutral voltage, input current, output dc voltage and output dc current for 144kW output power

4.2.1.4. Input and Output Waveforms for 900 Vdc Output Voltage Level

Input and output waveforms are given for rectification mode of PWM Rectifier for 900 Vdc output voltage from Figure 4-19 to Figure 4-22.

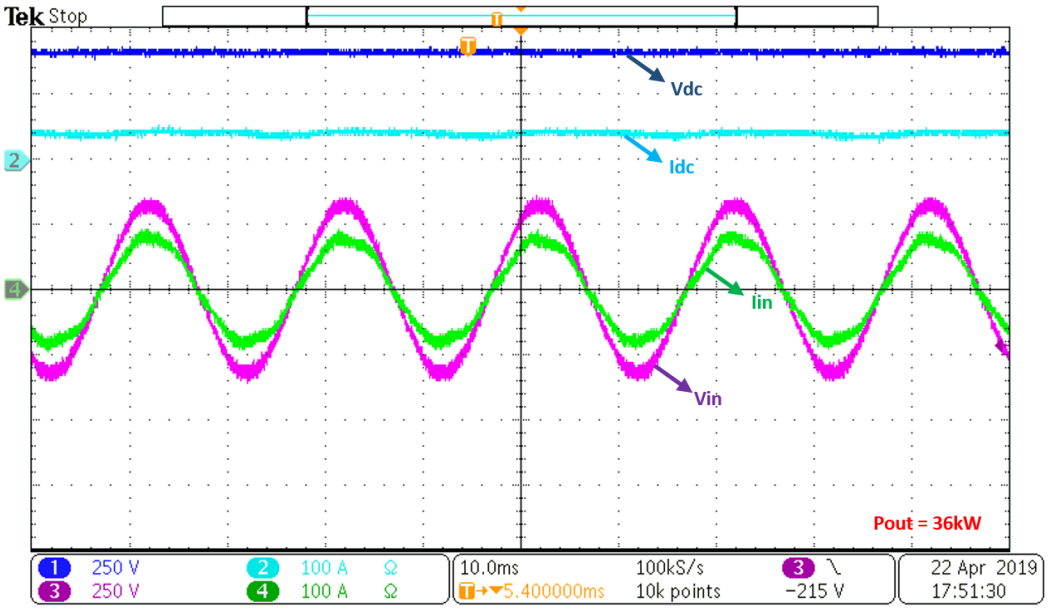

Figure 4-19 Input line to neutral voltage, input current, output dc voltage and output dc current for 36kW output power

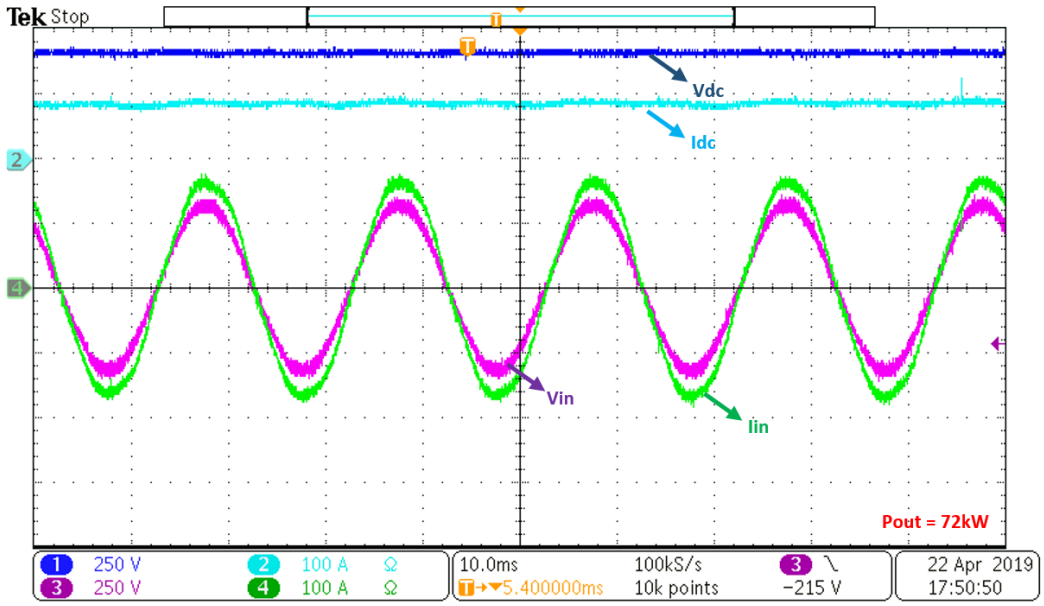

Figure 4-20 Input line to neutral voltage, input current, output dc voltage and output dc current for 72kW output power

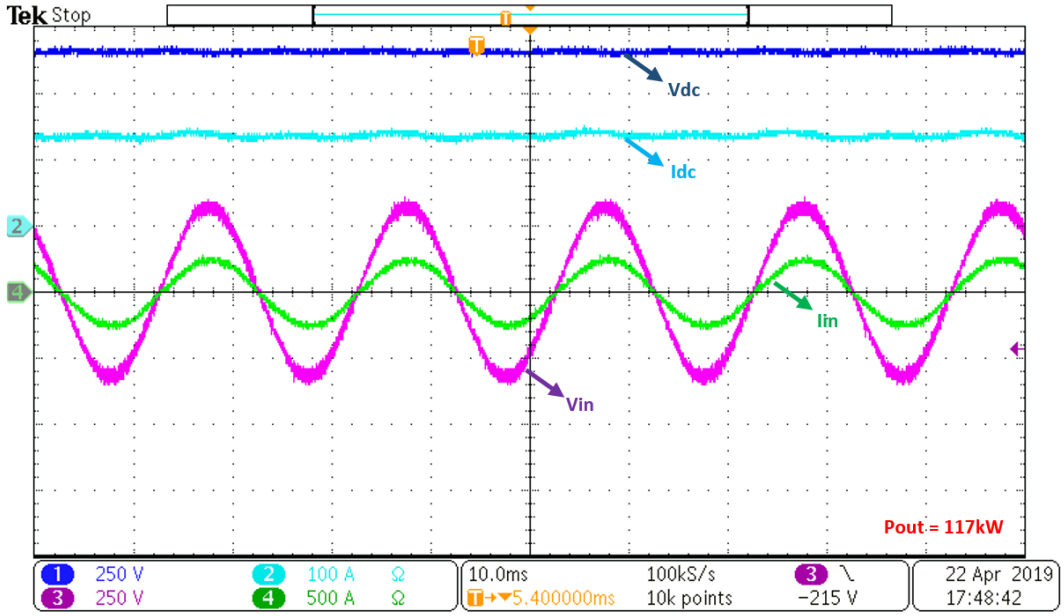

Figure 4-21 Input line to neutral voltage, input current, output dc voltage and output dc current for 117kW output power

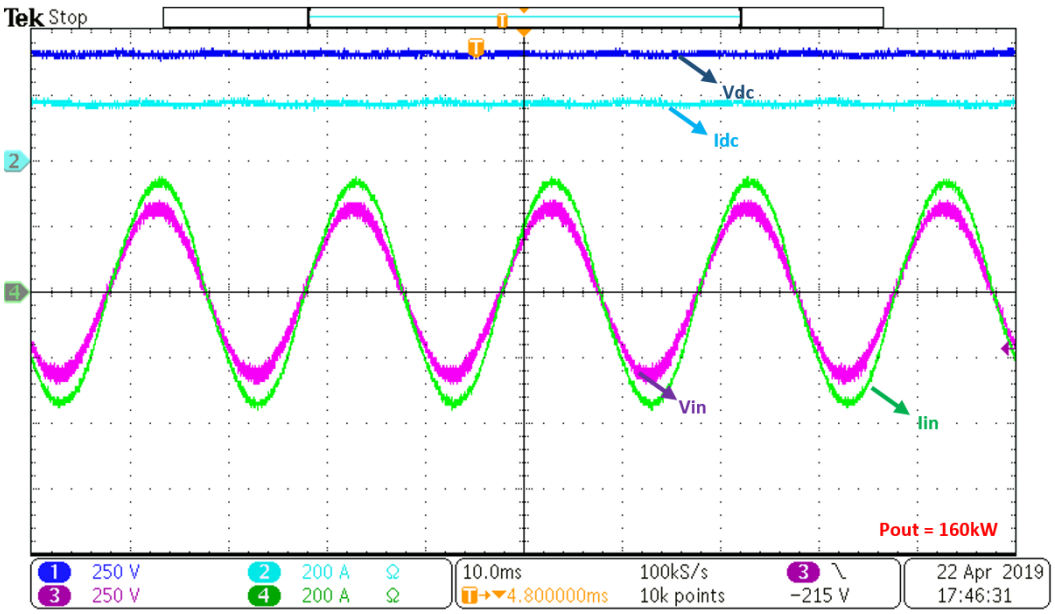

Figure 4-22 Input line to neutral voltage, input current, output dc voltage and output dc current for 160kW output power

4.2.1.5. Input and Output Waveforms for 1000 Vdc Output Voltage Level

Phase A input line to neutral voltage and input current, the DC output current and voltage are given for rectification mode of operation in Figure 4-23 and Figure 4-24.

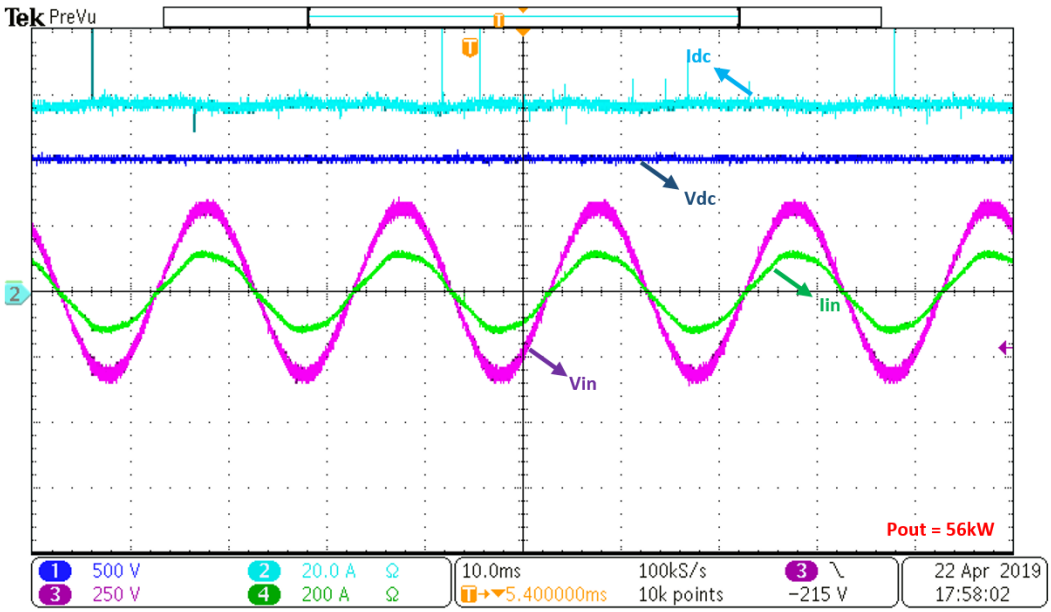

Figure 4-23 Input line to neutral voltage, input current, output dc voltage and output dc current for 56kW output power

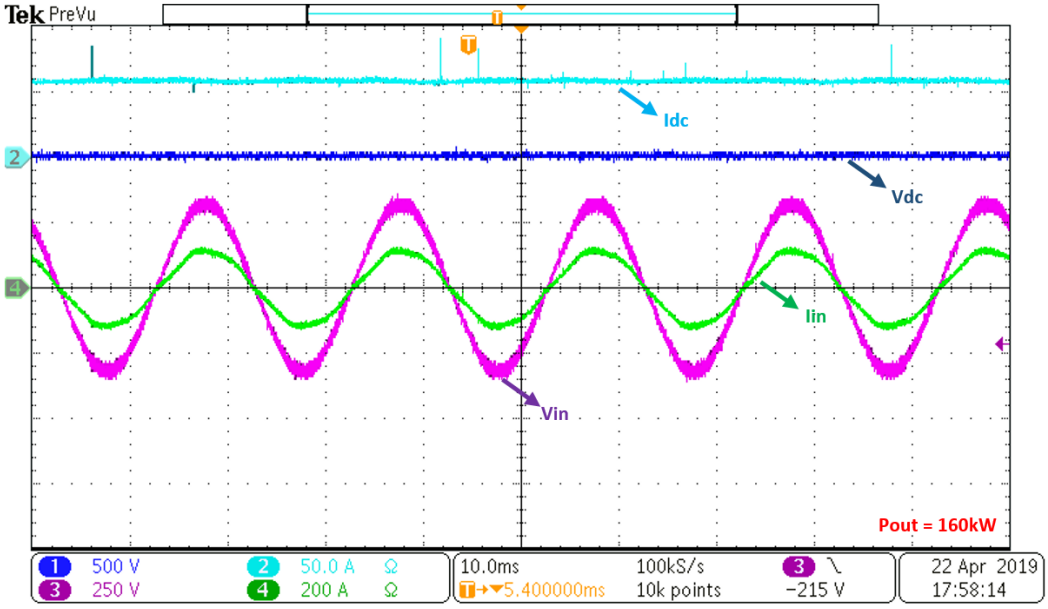

Figure 4-24 Input line to neutral voltage, input current, output dc voltage and output dc current for 160kW output power

4.2.2. Inversion Mode of Operation

Inversion mode of operation achieved by using the AC Induction Motor in generator mode so the power is transferred from the DC side to the AC side of the All-SiC PWM Rectifier and fed to the grid. The scheme can be observed in Figure 4-25.

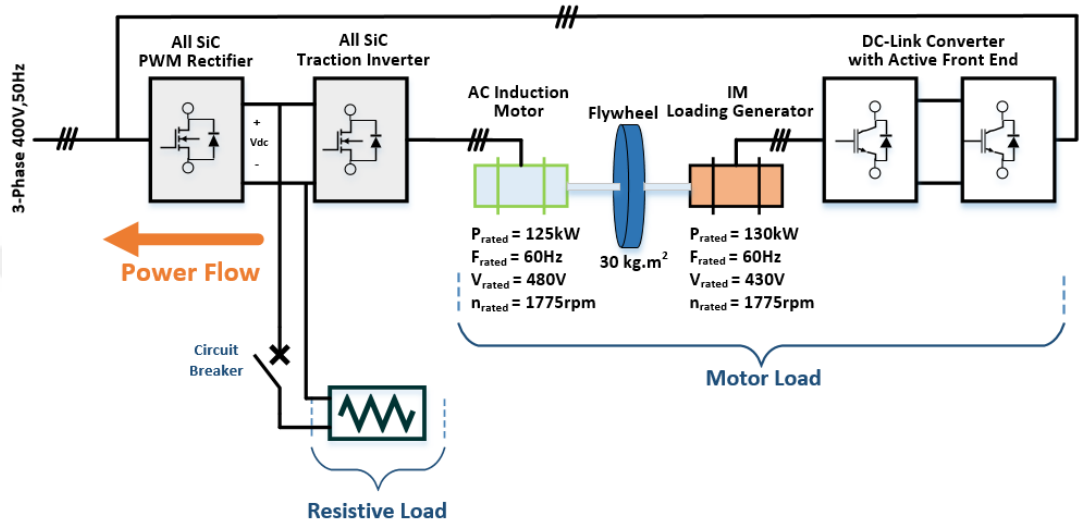

Figure 4-25 Power flow direction on All SiC PWM Rectifier during inversion

The inversion mode of operation is performed in three different voltage levels; 750 V, 800V and 900V.

4.2.2.1. Inversion Input and Output Waveforms for 750Vdc Voltage Level

Input and output voltage and current waveforms of inversion mode of operation can be observed in Figure 4-26 to Figure 4-31.

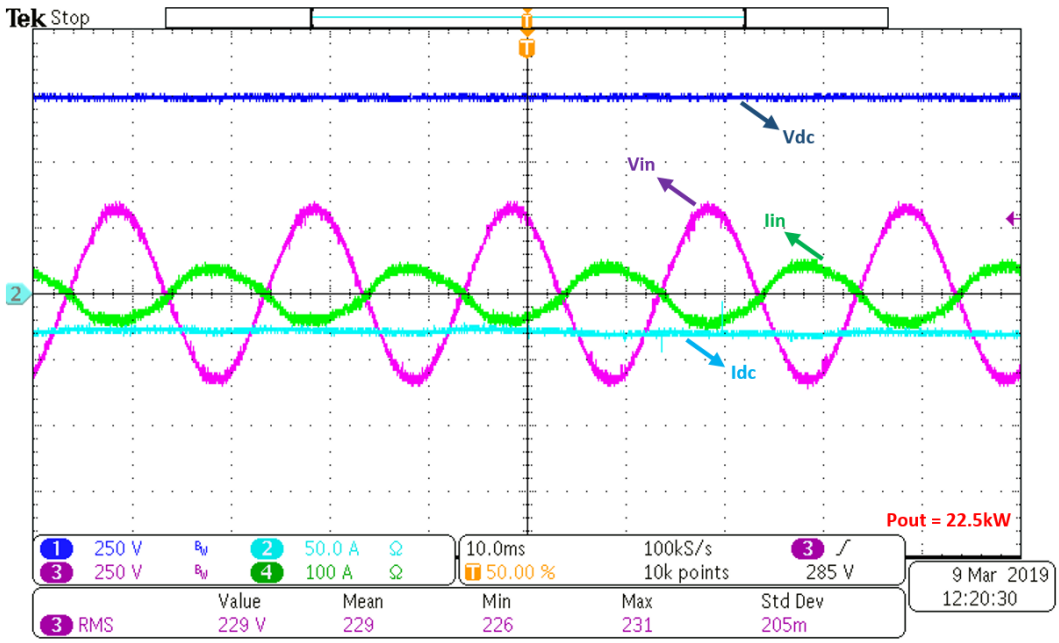

Figure 4-26 Inversion mode input and output voltage and current waveforms for 22.5kW power

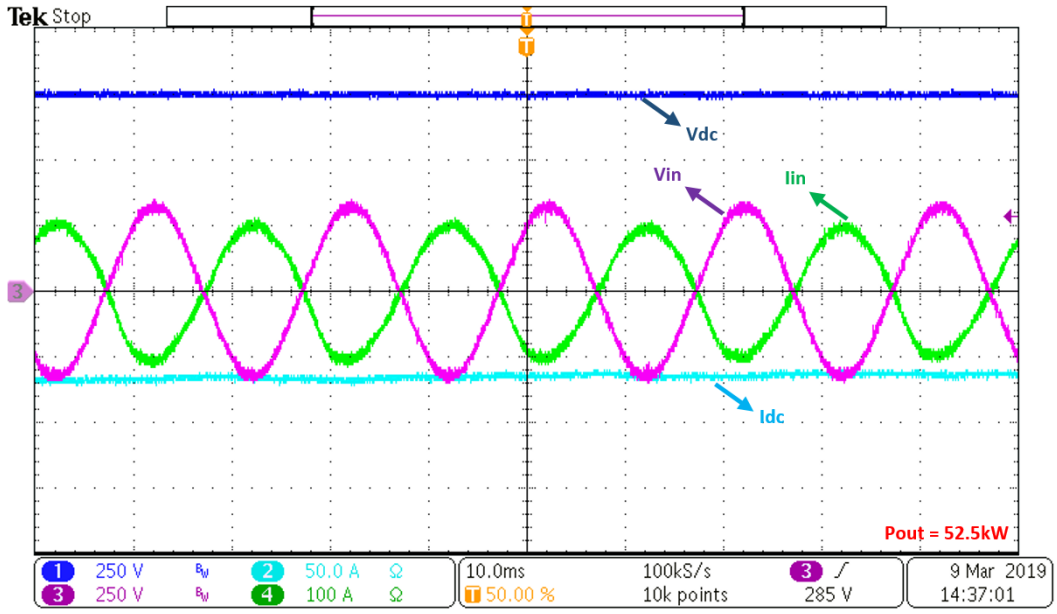

Figure 4-27 Inversion mode input and output voltage and current waveforms for 52.5kW power

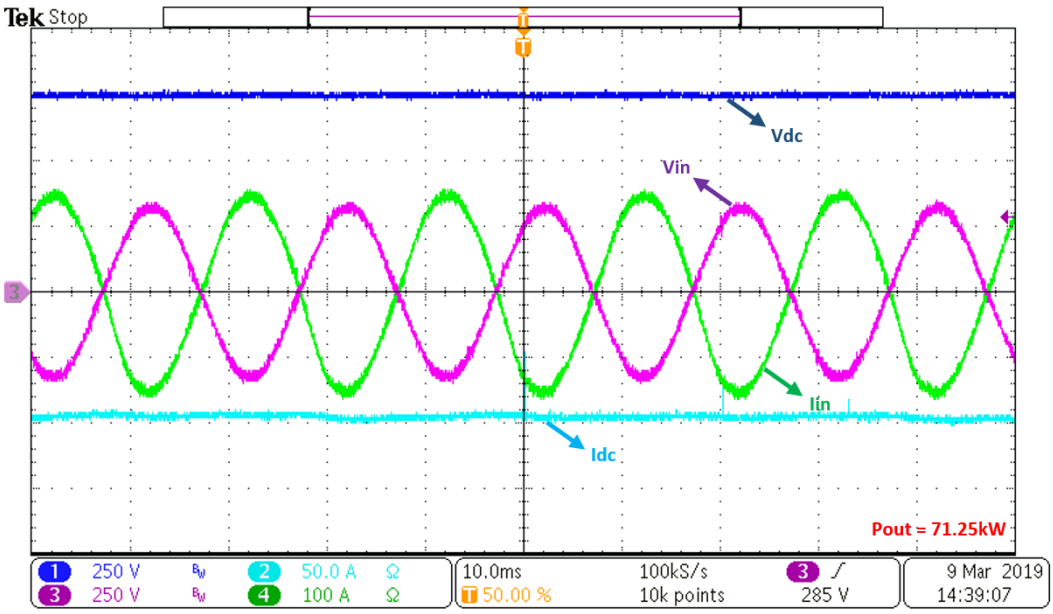

Figure 4-28 Inversion mode input and output voltage and current waveforms for 71.25kW power

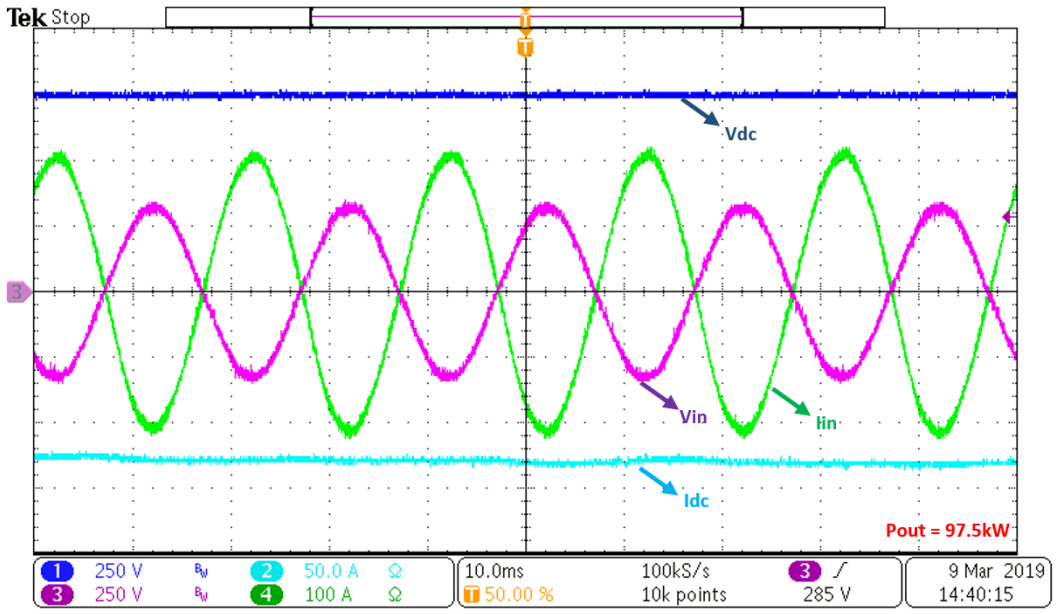

Figure 4-29 Inversion mode input and output voltage and current waveforms for 97.5kW power

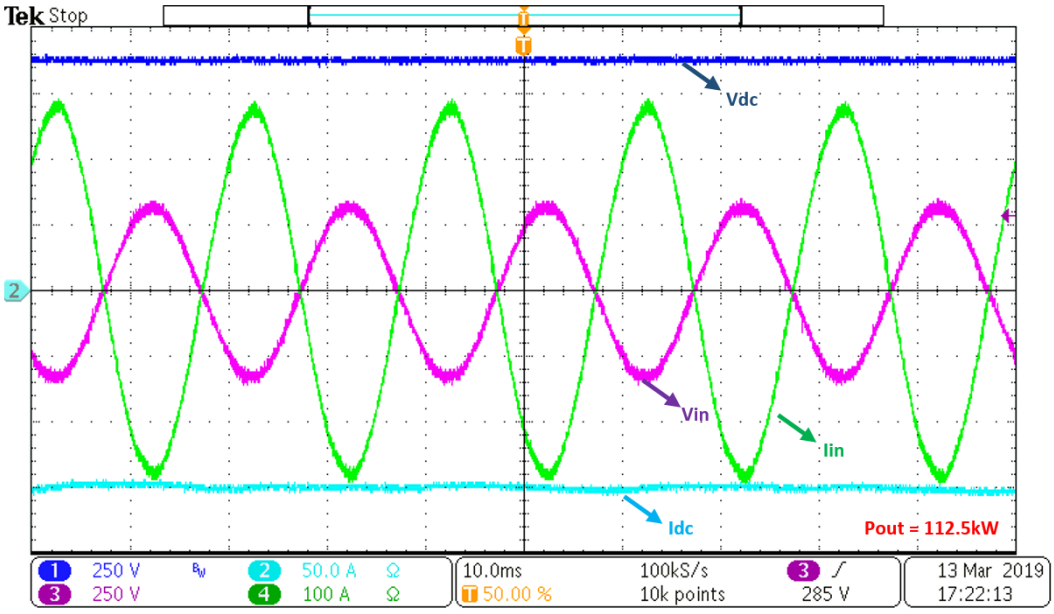

Figure 4-30 Inversion mode input and output voltage and current waveforms for 112.5kW power

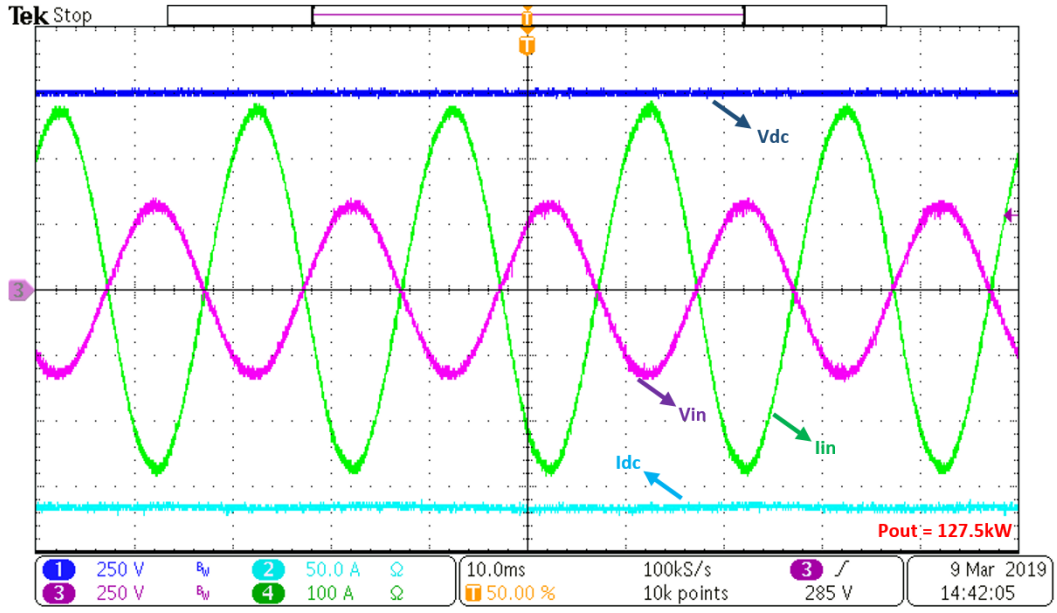

Figure 4-31 Inversion mode input and output voltage and current waveforms for 127.5kW power

4.2.2.2. Inversion Input and Output Waveforms for 800Vdc Voltage Level

Inversion mode input and output voltage and current waveforms for 800Vdc dc-link voltage level are given in Figure 4-32.

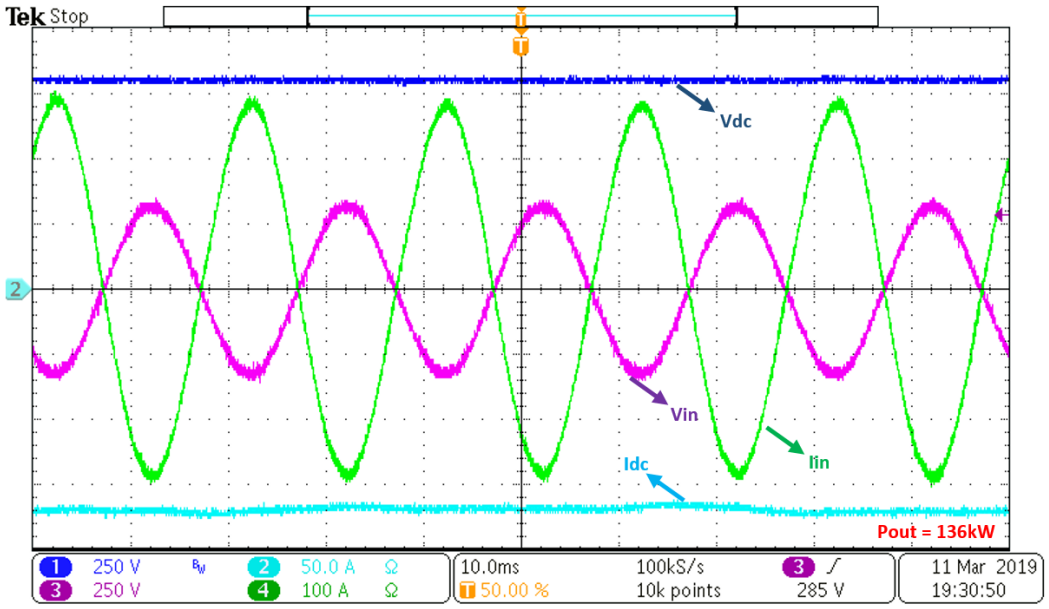

Figure 4-32 Inversion mode input and output voltage and current waveforms for 136kW power

4.2.2.3. Inversion Input and Output Waveforms for 900Vdc Voltage Level

Input and output voltage and current waveforms of inversion mode of operation for 900Vdc can be observed in Figure 4-33.

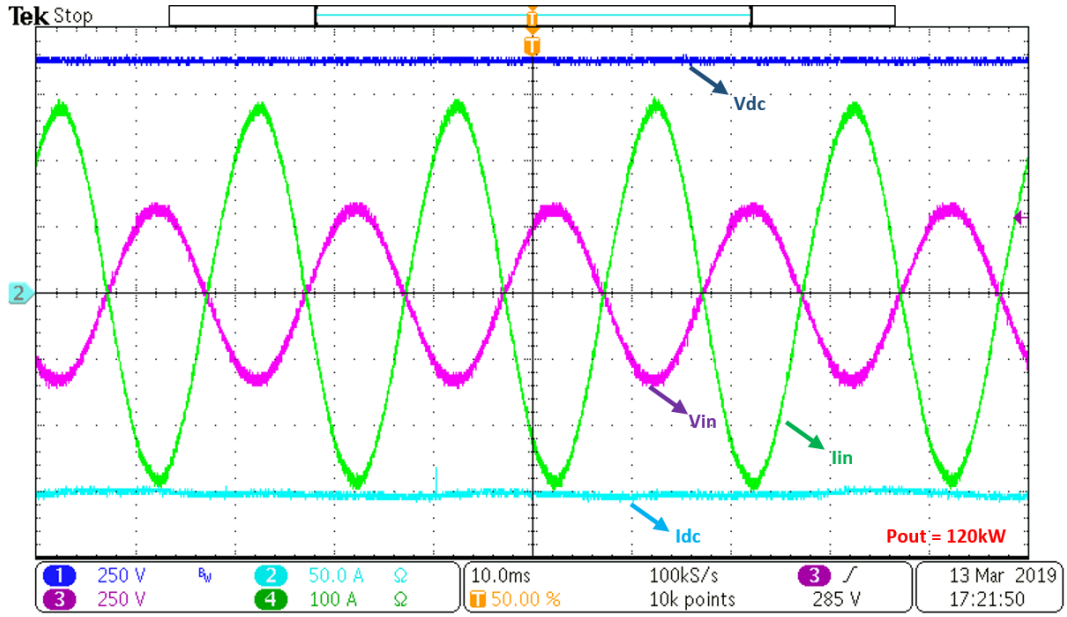

Figure 4-33 Inversion mode input and output voltage and current waveforms for 120kW power at 900Vdc dc-link voltage

4.2.3. Efficiency Calculations for All-SiC Three Phase PWM Rectifier

After obtaining the results of All-SiC Three Phase PWM Rectifier, the efficiencies of the power layer of the rectifier are calculated based on the oscilloscope waveforms. Power layer consists of the switching elements of the PWM Rectifier.

The output power and the input power of the rectifier are calculated and efficiencies are found according to these equations:

$$Pout = Vdc * Idc \tag{4.1}$$

$$Pin = 3 * Vin * Iin \tag{4.2}$$

$$\eta = 100 * \frac{Pout}{Pin} \tag{4.3}$$

In these equations; Pout is the output power, Pin is the input power, Vin is the rms value of input line to neutral voltage, Iin is the rms value of input line current and η is the efficiency.

The method of finding the efficiency from MATLAB by using the oscilloscope waveforms are given in the following procedure.

4.2.3.1. Efficiency Calculation Method

1. The oscilloscope waveform .csv file from which the efficiency will be calculated is imported to MATLAB. Data consist of input current, input voltage, output current and output voltage.
2. The input current and the output current are filtered by a lowpass filter to get rid of high frequency components. The original waveform and filtered waveform can be observed in Figure 4-34 and Figure 4-35.

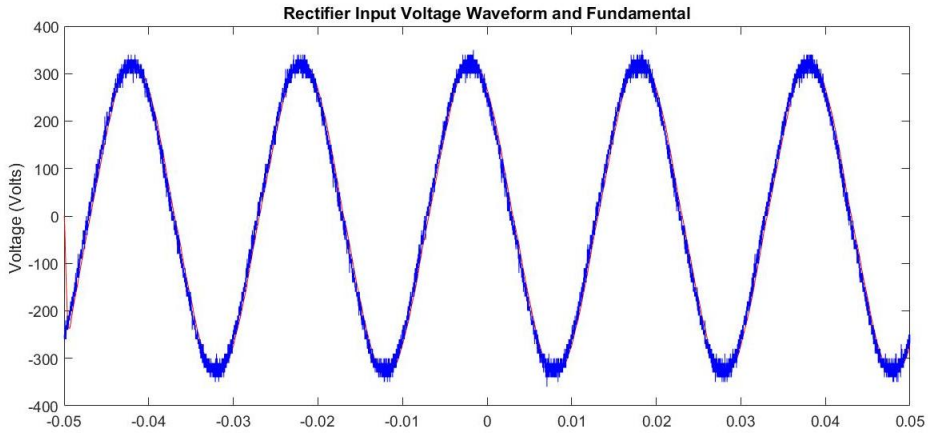

Figure 4-34 Rectifier Input Voltage Waveform and Filtered Waveform

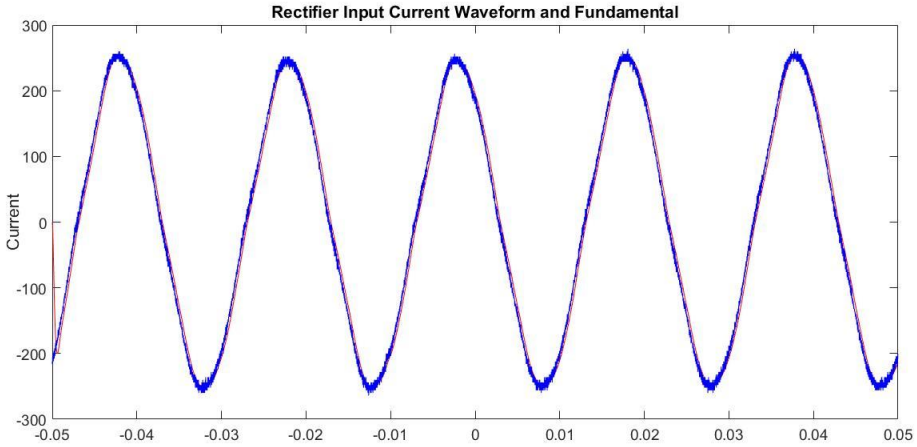

Figure 4-35 Rectifier Input Current Waveform and Filtered Waveform

3. The power factor is calculated from number of data points between the current and voltage waveforms (filter delays are also considered):

   For this waveform:

   The period is: 1994 data points

   The phase difference between voltage and current is: 4 data points

   The phase difference in degrees: (4/1994) * 360 = 0,72°

   The p.f: cos (0,72°) = 0,99992

4. The rms values of the waveforms are calculated.
5. Mean values of the output DC current and voltage are calculated.
6. Input and output power, then efficiency is calculated with the rms and dc values found in previous steps.

   Vrms= 228.2399

   Irms= 172.4420

   pf= 0,99992

   Idc= 155,7231 A

   Vdc= 751,1817 V

   Therefore, the efficiency becomes:

$$100 * (155{,}7231 * 751{,}1817)/(3 * 228{,}2399 * 172{,}4420) = \mathbf{99{,}07}\%$$

In *Table 11* the efficiencies found for rectification and inversion mode of operation are given. In Figure 4-36, the graph is generated from Table 11.

Table 11 *Efficiencies for Rectification and Inversion*

Output kVA	*Rectification Efficiency*	*Inversion Efficiency*
25	99.38	99.35
50	99.32	99.27
75	99.25	99.17
100	99.19	99.08
125	99.07	98.97
150	98.95	98.78

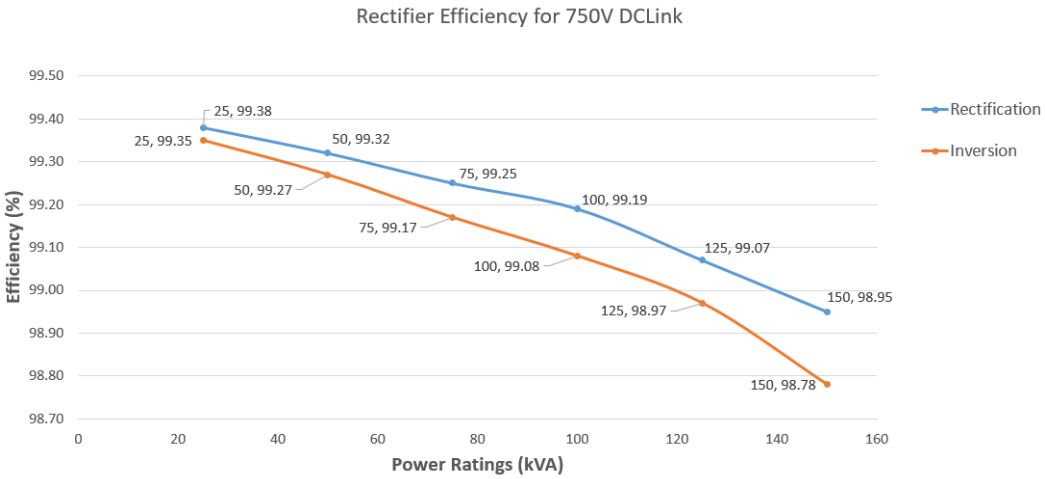

Figure 4-36 Rectification and Inversion Mode Efficiencies

The theoretical efficiencies are also calculated with SpeedFit Design Simulator from the SiC MOSFET manufacturer CREE Wolfspeed website. An example for SpeedFit

Design simulation is demonstrated for 750V output dc voltage and 125kW output power in Figure 4-37 using CAS300M17BM2 SiC MOSFET half-bridge modules. Switching frequency is designated as 10 kHz, same as the experimental setup.

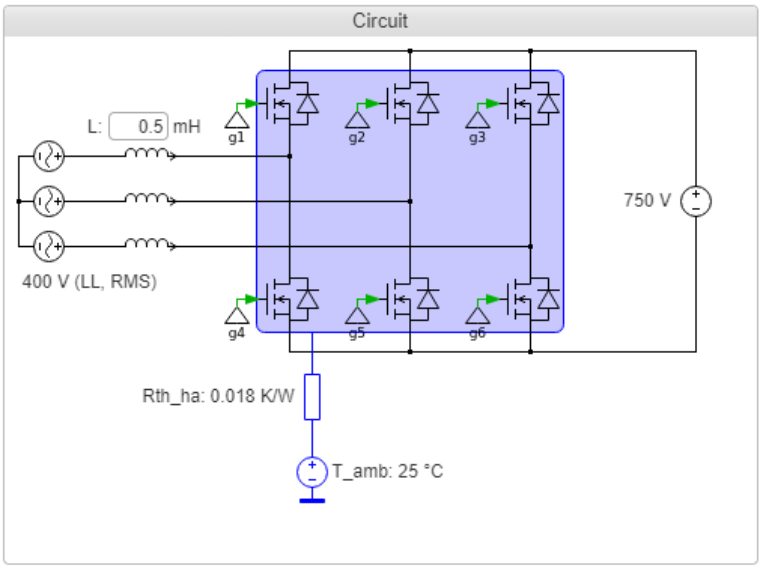

System overview

Input Voltage	Actual Output Power	Switching Frequency	Efficiency
400 V	125.0 kW	10 kHz	99.31 %

Device overview

	Switching	Conduction	Combined Losses	Junction Temperature
MOSFETs	316.14 W	548.04 W	864.18 W	63 °C
Diodes				
Converter Losses			864.18 W	

Figure 4-37 SpeedFit Design Simulation for 125kW output power

The theoretical result is estimated as 99.31% with 316.14W switching, 548.04W conduction losses by the simulator software. In the following table and graphs, the comparison of theoretical and experimental efficiencies is given for rectification and inversion mode of PWM Rectifier.

Table 12 *Theoretical and Experimental Efficiency Comparison for Rectification Mode*

Output kVA	*Experimental Efficiency*	*Theoretical Efficiency*
25	99.38	99.63
50	99.32	99.53
75	99.25	99.45
100	99.19	99.38
125	99.07	99.31
150	98.95	99.23

Table 13 *Theoretical and Experimental Efficiency Comparison for Inversion Mode*

Output kVA	*Experimental Efficiency*	*Theoretical Efficiency*
25	99.35	99.6
50	99.27	99.5
75	99.17	99.3
100	99.08	99.2
125	98.97	98.9
150	98.55	98.6

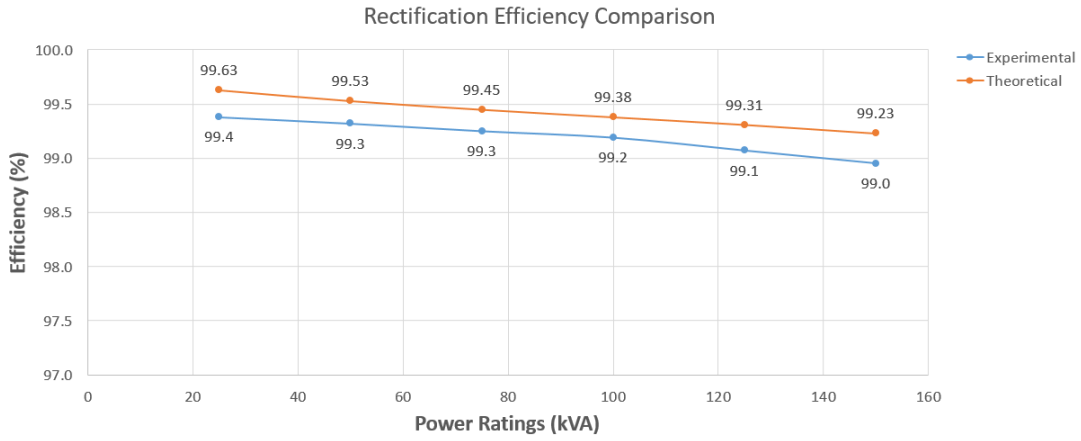

Figure 4-38 Theoretical and Experimental Efficiency Comparison for Rectification Mode

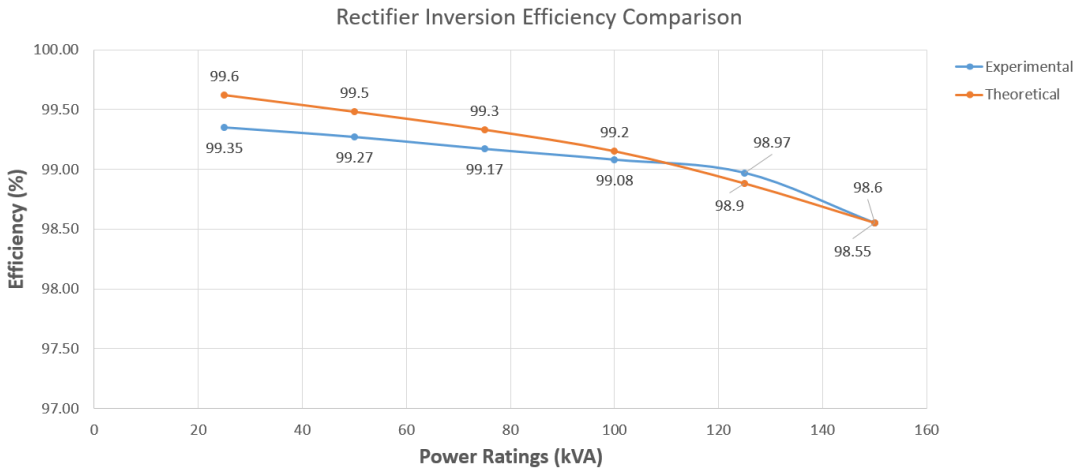

Figure 4-39 Theoretical and Experimental Efficiency Comparison for Inversion Mode

Experimental measurements are obtained with Tektronix MDO 3034 Mixed Domain Oscilloscope using following instruments.

- AC and DC currents:

  Tektronix TCP404XL High Current Probe

  (Accuracy, Typical ≤ 1%, Warranted ≤ 3%)

- AC and DC voltages:

  Tektronix PS205A High Voltage Differential Probe

  (Accuracy, Typical ≤ 2%)

At this point, the accuracies above stated by the Tektronix company should also be minded when evaluating the results. If we visit the calculation at the beginning of the topic and apply the maximum accuracies, the following result is obtained:

Vrms= 228.2399 ± 4.5648 V
Irms= 172.4420 ± 1.7244 A
Idc= 155.7231 ± 1.5572 A
Vdc= 751.1817 ± 15.0236 V

In order to get minimum limit of the efficiency, maximum input power and minimum output power is calculated:

pf= 0.99992

Pin= 121630.55

Pout= 113490.45

η = 93.31%

General expression for calculating minimum accuracy of efficiency (for 2% voltage, 1% current accuracy):

$$\boldsymbol{\eta_{min}} = \eta * \frac{0.99*0.98}{1.01*1.02} = \eta * 0.9418$$

The corresponding power and efficiency accuracy values with respect to given current and voltage accuracy of probes summarized in *Table 14*.

Table 14 *Accuracy values of power and efficiency*

	Current	Voltage	Power	Efficiency
Accuracy	1%	2%	~3%	~6%

1. Measurements can be improved in order to obtain efficiency that is more accurate. First, a power analyzer, which has better accuracy levels provided by the manufacturer should be chosen for the measurements. For instance, Yokogawa WT3000 offers following accuracies:
    - Current and voltage measurements: 0,01% of reading
    - Power measurements: 0,02% of reading
2. The other important feature offered by power analyzer is ability to acquire simultaneous measurements for input and output. By using same instrument, the error occurs from using two different device is eliminated. The efficiency is more accurate than using individual current and voltage meters.

3. Thermal steady state condition is another factor that should be ensured in order to obtain accurate efficiency. Thermal steady state can be achieved by defining a settling time for the system then waiting settling time to be reached before taking measurements.
4. The current and voltage should be measured directly from the terminals of the device so that losses originated from wiring and contact resistant is avoided.
5. Ability to take sequential measurements of current and voltage, then obtaining their average value and multiplying to calculate power would also provide more accurate efficiency value.
6. Calibration of the measurement instrument should be performed on predetermined periods.
7. Sampling frequency of the device should be higher than twice of the measured signal. As the sampling frequency gets higher, the accuracy of the measurements gets better. Therefore, sampling frequency should be as high as it can get.

However, in order the examine the measurements, a test setup is implemented for the voltage and current probes. Differential voltage probe is examined by taking measurements of 1000V DC voltage with Tektronix PS205A and LEM LV25-1000 voltage transducer at the same time from the same power supply which is presented in Appendix D. A high precision 10Ω measuring resistance is connected to the output of LEM LV25-1000 voltage transducer which has 1000V:25mA ratio. The measurements are observed on the Tektronix MDO 3034 Mixed Domain Oscilloscope screen.

Current probe is examined by taking measurements of 250A DC current with Tektronix TCP404XL High Current Probe and LEM LF 510-S current transducer (Appendix D). Output of the transducer is 50mA when 250A DC current passes

through the primary side. A high precision 10Ω measuring resistance is connected to the output of the transducer. The measurements are observed on the Tektronix MDO 3034 Mixed Domain Oscilloscope screen. Devices are also calibrated before taking the measurements for the efficiency calculations. Furthermore, in order to place the cable in the center of clamp, cable is wrapped with an anti-static pad.

In conclusion, according to accuracies provided by measurement instrument manufacturer, the measurement uncertainty is high for determining the system efficiency. This is because, the efficiency of the system is expected to be around 99% and the accuracy range of probes results in wide margins on the calculated experimental efficiency. However, examining the measurements of probes by comparing them to measurements of voltage and current sensors and theoretical results being close and consistent to the experimental results shows the experimental efficiency is realistic and provides insight about the system efficiency.

4.2.4. Harmonic Spectrum of the Input

During the tests conducted in the laboratory harmonic spectrum of the input current and input voltage are recorded with Hioki PW3198 Power Quality Analyzer for 125kW input power. The input voltage and current waveforms and power level are recorded as well.

Current and voltage waveform, power level, current and voltage harmonic spectrum can be observed in Figure 4-40 to Figure 4-45.

In Figure 4-44 it can be seen that the voltage THD is 1.16%. In IEEE Std 515, the THD upper limit for general applications are defined as 5%. All SiC Three Phase PWM Rectifier is clearly under this limit.

In Figure 4-45 current total harmonic distortion i.e. ITHD is measured as 3.83%. The current harmonics are under limits as well according to current distortion limits in IEEE Std 519 which states that up to 11th harmonic, their percentage should be smaller

than 4%. In Figure 4-45, 3rd harmonic is 2.82 and 5th harmonic is 2.45, therefore the PWM Rectifier is operating in limits of regulations.

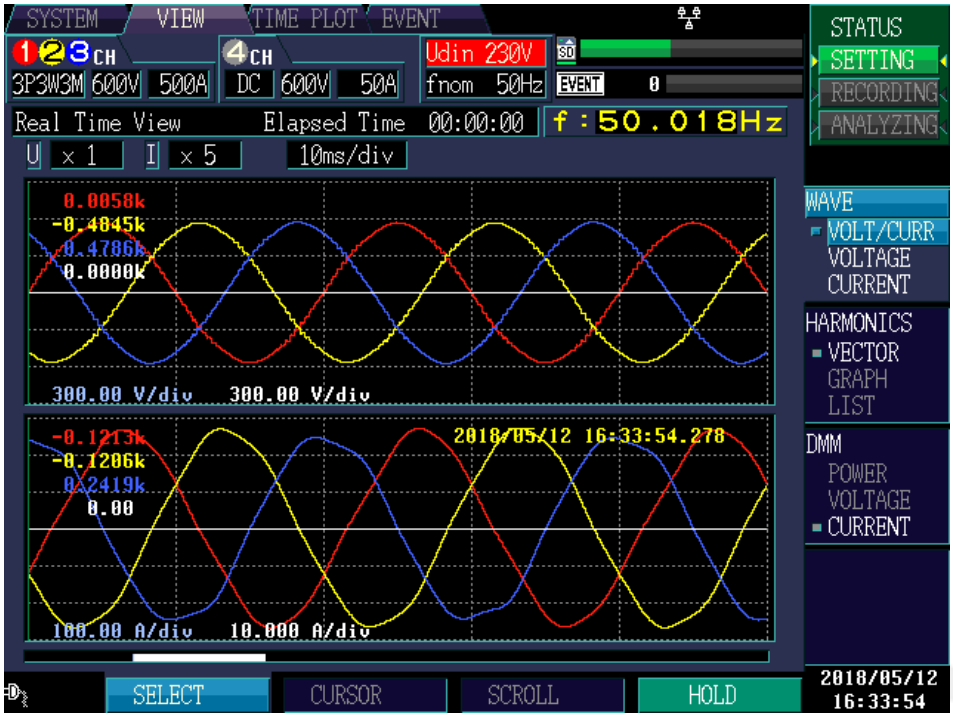

Figure 4-40 Input current and voltage waveforms observed at 125kW input power

Figure 4-41 Line-to-line voltages, line currents, power drawn from the grid, and power factor

Figure 4-42 Input line-to-line voltages and their THD values

Figure 4-43 Input line currents and their THD values

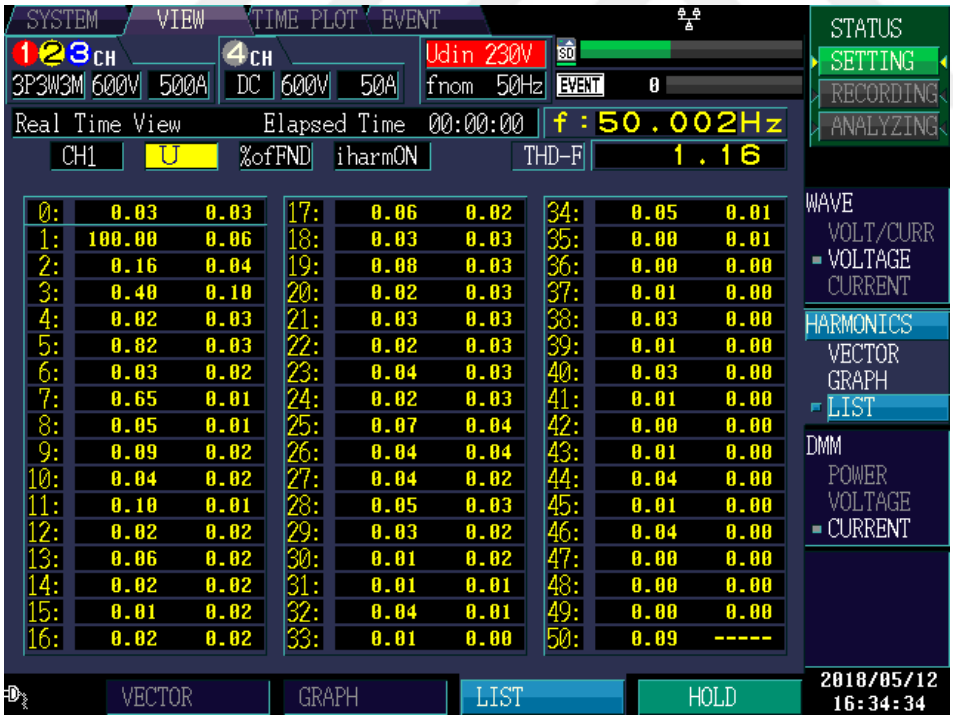

Figure 4-44 Harmonic spectrum of input voltage and THD value

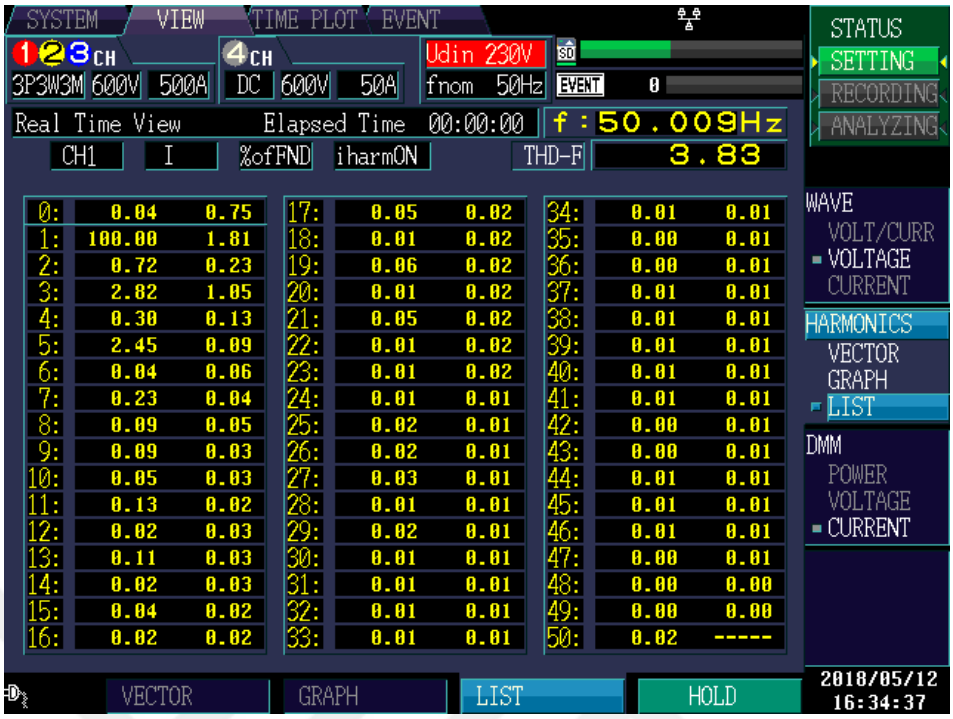

Figure 4-45 Harmonic spectrum of the input current and THD level

FFT of the AC side current waveform also recorded with oscilloscope and calculated with short MATLAB code by importing csv file. Similar results are acquired. The FFT spectrum, 2nd, 3rd and 5th harmonic values are given in Figure 4-46. MATLAB m file code presented in Appendix E.

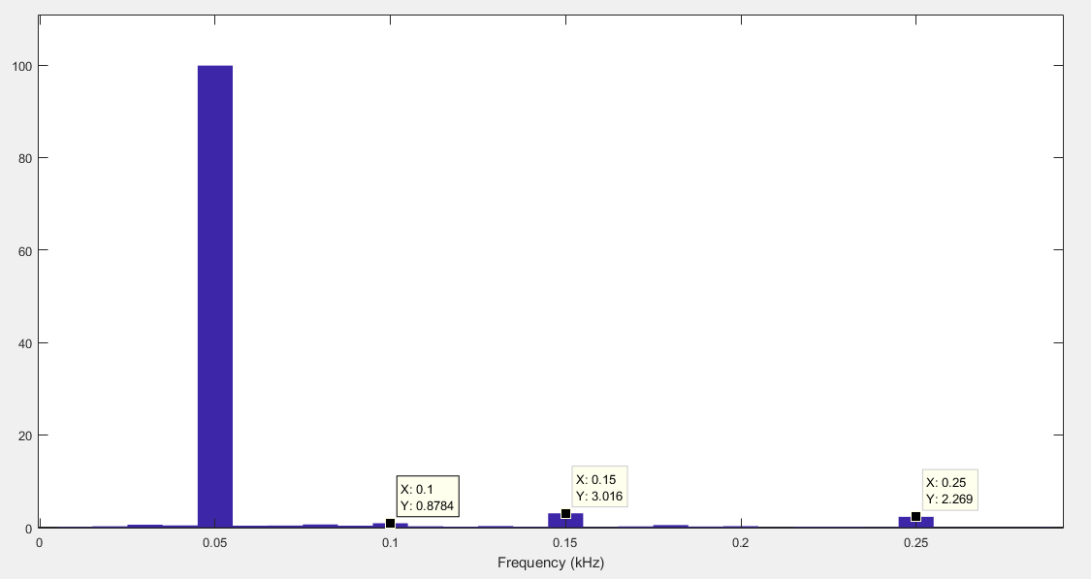

Figure 4-46 Harmonic spectrum of the AC current waveform

4.3. Discussion

Experimental work showed that All SiC Three Phase PWM Rectifier is capable of providing various output power levels on output voltage range from 625V to 1000V. Both rectification and inversion operations are implemented keeping the unity power factor. Result of harmonic spectrum analysis demonstrated that input current THD is 3.83% at 750V output DC voltage, 125kW output power level. This THD value seems a little higher than expected when compared to the result of simulation in *Table 4* which is 1.96%. 3.83% is under the limits; however, as we have deduced from the analysis in Chapter 3, input current THD gets higher when the output power decreases. Therefore, reducing this value would be beneficial for the system. This value can be decreased by improving the control parameters, applying harmonic elimination methods or increasing the switching frequency by paying regard to switching device thermal limitations.

CHAPTER 5

CONCLUSION

All SiC Three Phase PWM Rectifier with variable output voltage levels is studied in this thesis work. Due to advantages of SiC such as high thermal conductivity and high melting point, SiC Power MOSFETs can work in high temperatures and high electron velocity contributes to working in high switching frequencies. These benefits of SiC power MOSFETs let us build converters that have high efficiency and high power density. In Traction Systems R&D Laboratory converters with SiC Power MOSFETs are designed and implemented. In this work All SiC Three Phase PWM Rectifier with variable output voltage is explained. Due to controllable variable output voltage, the All SiC Three Phase PWM Rectifier can be used in many areas in the industry. These areas are summarized as:

- Resistive furnaces; Electric heating
- DC Motor Drive
- Synchronous Motor Field Exciter
- Battery Charger
- Supercapacitor/Battery Energy Storage Systems
- Variable Frequency AC Motor Drives

After the field of use, sample switching pattern is presented and operation modes are explained. Effect of SPWM and SVPWM modulation methods on THD are investigated. The reasons of choosing 10kHz switching frequency is studied. The change of input current THD is observed for different output power and output voltage levels. Using PSIM power electronics simulation software, the input and output voltage waveforms are drawn. Then, response of the rectifier control is mentioned as well.

After that, the implementation of All SiC PWM Rectifier is explained with schematics and the used components.

In the last chapter, results of the experiments conducted in the Traction Systems R&D Laboratory with AC Motor and resistor loads showed the over 99% efficiency of the All SiC PWM Rectifier. Furthermore, experiments are done from 625V to 1000V output voltages in vastly varied output power levels from 37.5 to 187.5kW.

The conclusion of the conducted work can be summarized as follows:

1. Boost type PWM Rectifier is designed and implemented by employing SiC Power MOSFETs
2. It can be supplied from 400V 50Hz 3-phase utility grid.
3. DC output voltage of SiC Three Phase PWM Rectifier is adjustable theoretically in the range from 565V to 1000V. Experimentally 625V to 1000V is implemented successfully.
4. SVPWM technique cause less input current harmonics compared to SPWM.
5. Input current harmonics, thus THD is reduced as output power increases.
6. Input current harmonics, thus THD is reduced as the switching frequency rises.
7. Efficiency of the system decreases as the output power increases for a fixed output voltage due to dominant conduction losses.
8. Efficiency of the system decreases as the output voltage increases for a fixed output power due to dominant switching losses.
9. It can deliver adjustable power to its load. Maximum value of power output is 224kW at 625V output DC voltage.
10. Limit value of the power output at fixed switching frequency depends on Vdc i.e. as Vdc is reduced, Po(max) increases.
11. Compared to 15kHz and 20kHz switching frequencies, 10kHz switching frequency has more power capacity for the system.
12. The implemented system has a very high efficiency in rectification (99.38%) and inversion (99.35%) modes.

13. Harmonic distortion of the current waveforms on the AC side is very low. (3.83% at 125kW output power, 750V output DC voltage)
14. It is also worth to know that THD of line-to-line supply voltage waveforms is also very low, although grid is slightly distorted.

Three Phase All SiC PWM Rectifier can be used to supply different loads such as batteries. Fast charger schemes can be implemented with variable output voltage. Since 10kHz switching frequency is chosen for this work, in the following experiments switching frequencies up to 20kHz can be set for the SiC MOSFETs.

In the medium term, it is expected that All SiC PWM Rectifiers will be developed at much higher output voltage and power ratings with the advances in SiC Power MOSFET technology. As far as the author knows 3300V 1500A SiC power modules are under development and will be commercially available in near future.

REFERENCES

[1] P. Godignon and X. Perpi, "A Survey of Wide Bandgap Power," *IEEE Trans. Power Electron.*, vol. 29, no. 5, pp. 2155–2163, 2014.

[2] R. Wang *et al.*, "A High-Temperature SiC Three-Phase AC – DC Converter Design for > 100 ◦ C Ambient Temperature," *IEEE Trans. Power Electron.*, vol. 28, no. 1, pp. 555–572, 2013.

[3] S. M. Two-level, "Design Considerations and Performance Evaluation," *IEEE Trans. Ind. Appl.*, vol. 52, no. 5, pp. 4257–4268, 2016.

[4] I. Si-, A. Merkert, S. Member, T. Krone, S. Member, and A. Mertens, "Characterization and Scalable Modeling of Power Semiconductors for Optimized Design of Traction," *IEEE Trans. Power Electron.*, vol. 29, no. 5, pp. 2238–2245, 2014.

[5] F. Xu *et al.*, "Development of a SiC JFET-Based Six-Pack Power Module for a Fully Integrated Inverter," *IEEE Trans. Power Electron.*, vol. 28, no. 3, pp. 1464–1478, 2013.

[6] B. Ozpineci *et al.*, "A 55-kW Three-Phase Inverter With Si IGBTs and SiC Schottky Diodes," *IEEE Trans. Ind. Appl.*, vol. 45, no. 1, pp. 278–285, 2009.

[7] P. Roussel, "SiC market and industry update," presented at the Int. SiC Power Electron. Appl. Workshop, Kista, Sweden, 2011.

[8] T. Funaki *et al.*, "Power Conversion With SiC Devices at Extremely High Ambient Temperatures," *IEEE Trans. Power Electron.*, vol. 22, no. 4, pp. 1321–1329, 2007.

[9] B. Shi and H. Sundstrand, "Design Considerations for Reactive Elements and Control Parameters for Three Phase Boost Rectifiers," *IEEE Int. Conf. Electr. Mach. Drives, 2005.*, pp. 1757–1764, 2005.

[10] J. R. Rodríguez et al., "PWM Regenerative Rectifiers : State of the Art," *IEEE Trans. Ind. Electron.*, vol. 52, no. 1, pp. 5–22, 2005.

[11] B. Singh et al., "A Review of Three-Phase Improved Power Quality AC – DC Converters," *IEEE Trans. Ind. Electron.* vol. 51, no. 3, pp. 641–660, 2004.

[12] T. PUL, "Design and implementation of a 130KW, 750VDC Bidirectional PWM Rectifier Supplied from 400V, 50HZ Grid," METU, 2019.

[13] D. Yıldırım, M. H. Akşit, C. Yolaçan, T. Pul, C. Ermiş, B. H. Aghdam, I. Çadırcı, M. Ermiş, "Full-Scale Physical Simulator of All SiC Traction Motor Drive with On-

Board Supercapacitor ESS for Light-Rail Public Transportation.", Early Access Article

[14] T. Ma, V. Scaini, "High Current DC Choppers in the Metals Industry", Conference Record of the 2000 IEEE Industry Applications Conference. Thirty-Fifth IAS Annual Meeting and World Conference on Industrial Applications of Electrical Energy, vol. 4, 2000.

[15] I. Wallace, A. Bendre, J. P. Nord, and G. Venkataramanan, "A Unity-Power-Factor Three-Phase PWM SCR Rectifier for High-Power Applications in the Metal Industry," IEEE Trans. Ind. Appl., vol. 38, no. 4, pp. 898–908, 2002.

[16] M. H. Dc, M. Drive, H. F. Bilgin, K. N. Köse, G. Zenginobuz, and M. Ermis, "A Unity-Power-Factor Buck-Type PWM Rectifier for," *IEEE Trans. Ind. Appl.*, vol. 38, no. 5, pp. 1412–1425, 2002.

[17] D. Yildirim, S. Öztürk, I. Çadirci, and M. Ermiş, "All SiC PWM rectifier-based off-board ultrafast charger for heavy electric vehicles," IET Power Electron., no. August, pp. 1–15, 2019.

APPENDICES

A. All SiC Three Phase PWM Rectifier Drawings

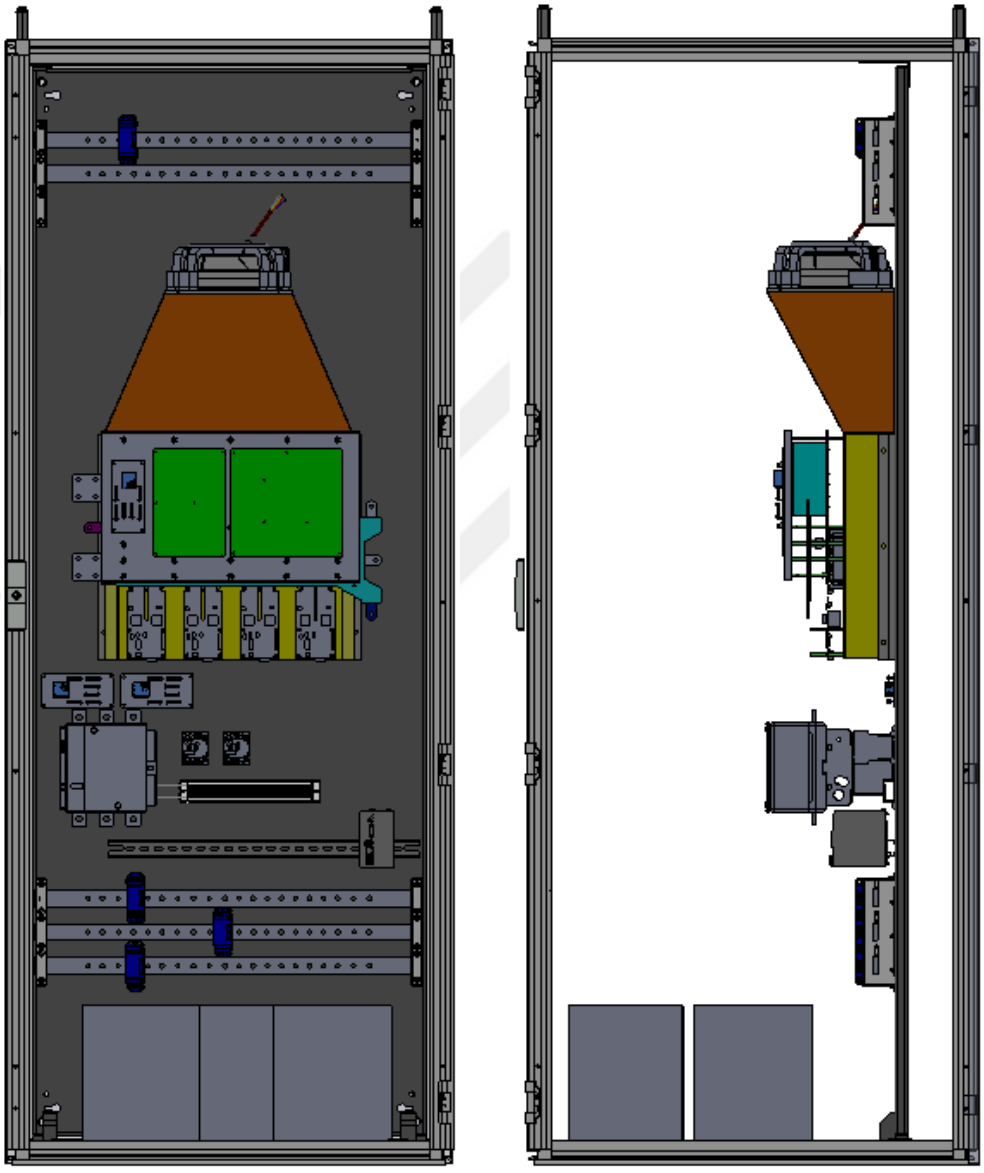

Figure A 1 All SiC Three Phase PWM Rectifier Model on SolidWorks

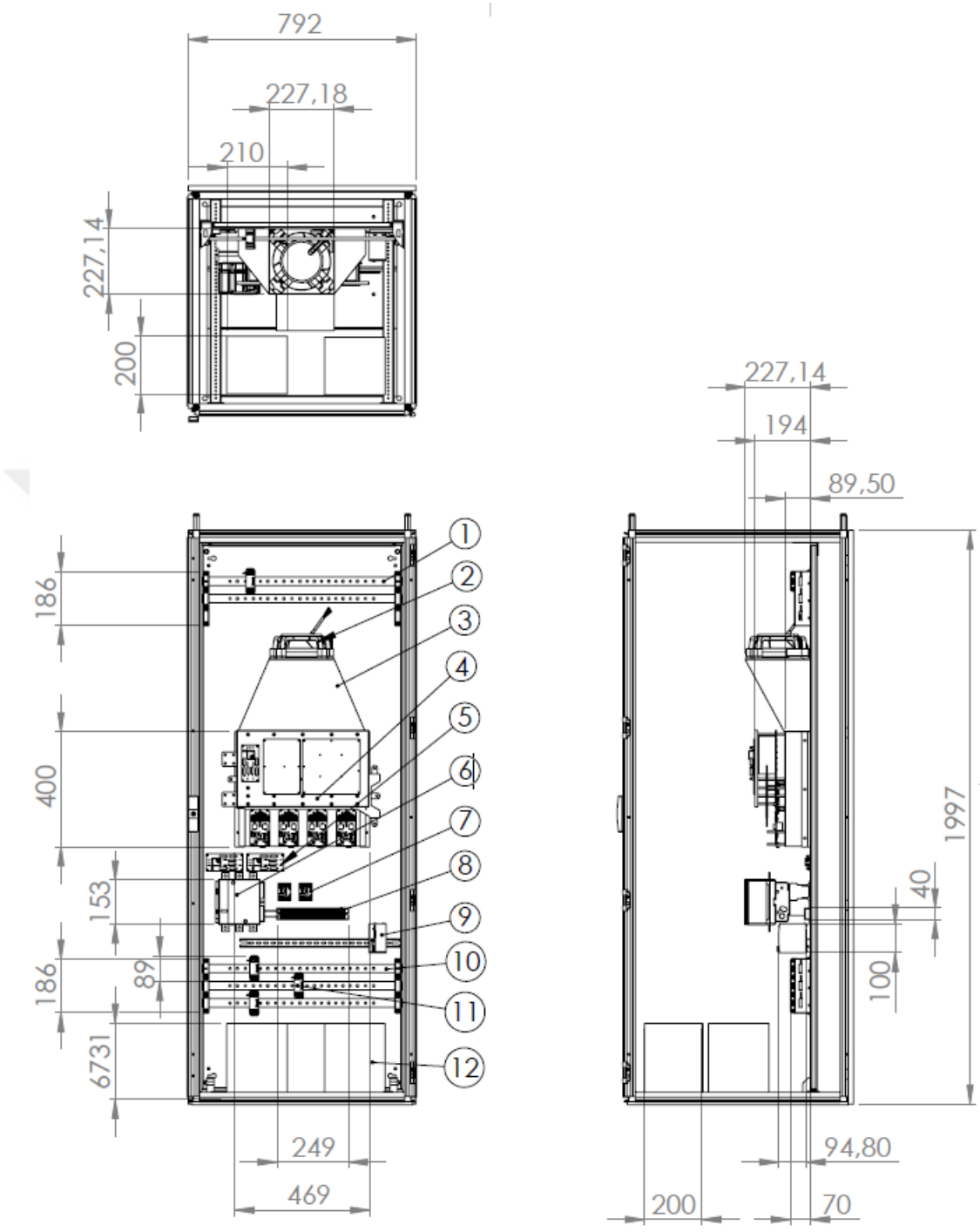

Figure A 2 All SiC Three Phase PWM Rectifier Drawing on SolidWorks

PWM Rectifier Cabinet Reference Material List:

1. DC Busbars
2. Fan (K3G200BD4604)
3. Range Hood
4. PWM Rectifier Power Block
5. Voltage Sensor x 2 (LV25-1000)
6. 3 Phase Contactor (LC1F330M7)
7. Soft Start Contactor x 2 (3RT1017-1KB41)
8. Soft Start Resistor (R154-200)
9. PLC (XC-CPU202)
10. 3-Phase AC Busbar
11. Current Sensors x 3 (LF510-S)
12. Boost Reactor x 3 (Mangoldt 1042215)

B. Traction Systems R&D Laboratory Electric Project

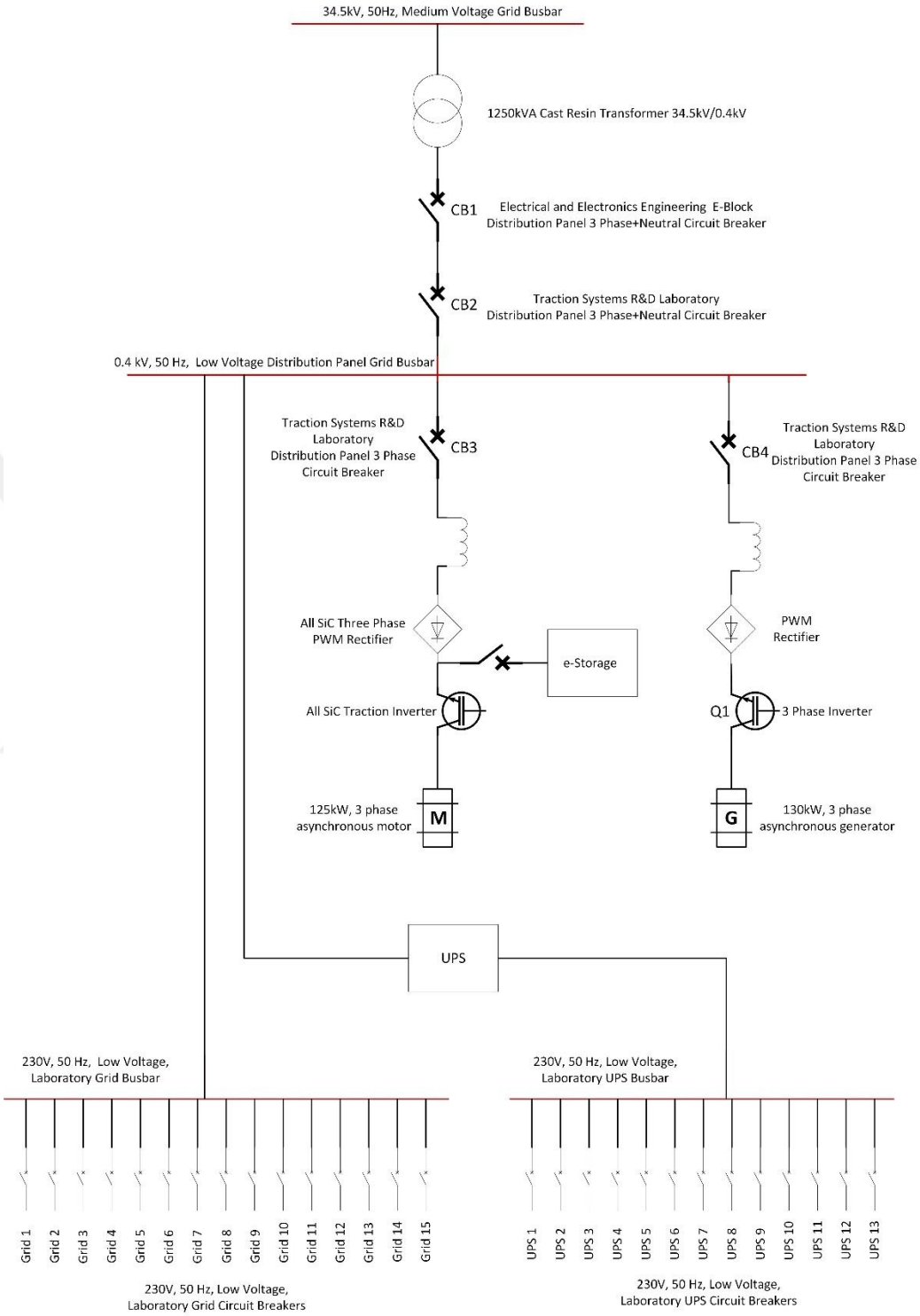

C. MATLAB Code for Efficiency Calculation

```
close all

fs=100000;
N = 2;                                                  %first order
cutoff_Hz = 1000;
[b,a]=butter(N,cutoff_Hz/(fs/2),'low');                 %a lowpass filter
Filtered_Vout_1800_vol2 = filter(b,a,V1(:,1));
plot(VerticalUnits,Filtered_Vout_1800_vol2,'r' );
hold on
plot(VerticalUnits,V1, 'b');
 title('Rectifier Input Voltage Waveform and Fundamental')
ylabel('Voltage (Volts) ')

figure;
[b,a]=butter(N,cutoff_Hz/(fs/2),'low');                 %a lowpass filter
filtered_I = filter(b,a,A1(:,1));

plot(VerticalUnits,filtered_I, 'r');
hold on
plot(VerticalUnits,A1, 'b');
title('Rectifier Input Current Waveform and Fundamental')
ylabel('Current')


Vrms=rms(Filtered_Vout_1800_vol2(1000:10000));
Irms=rms(filtered_I(1000:10000));

Vdc=mean(V);
Idc=mean(A);

Pout=Vdc*Idc;
Pin= pf*Vrms*Irms*3;

Eff=Pout/Pin*100;

```

D. Voltage and Current Probe Examinations

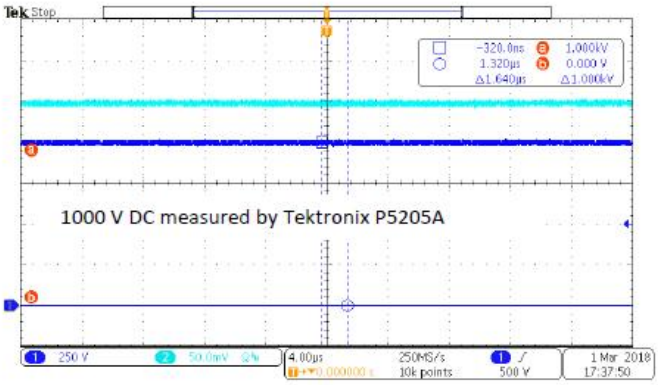

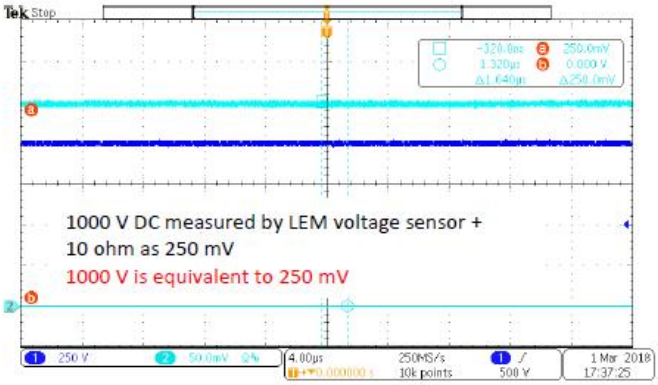

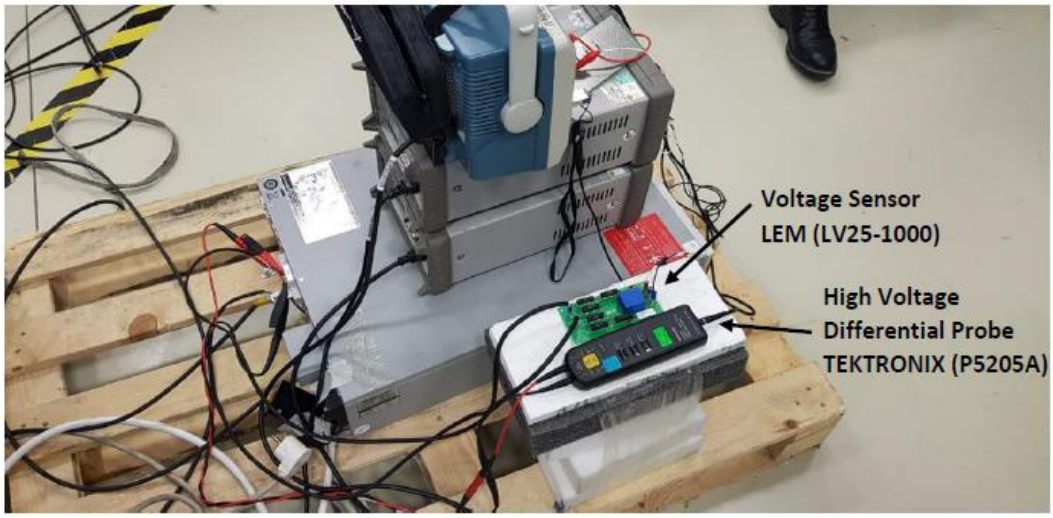

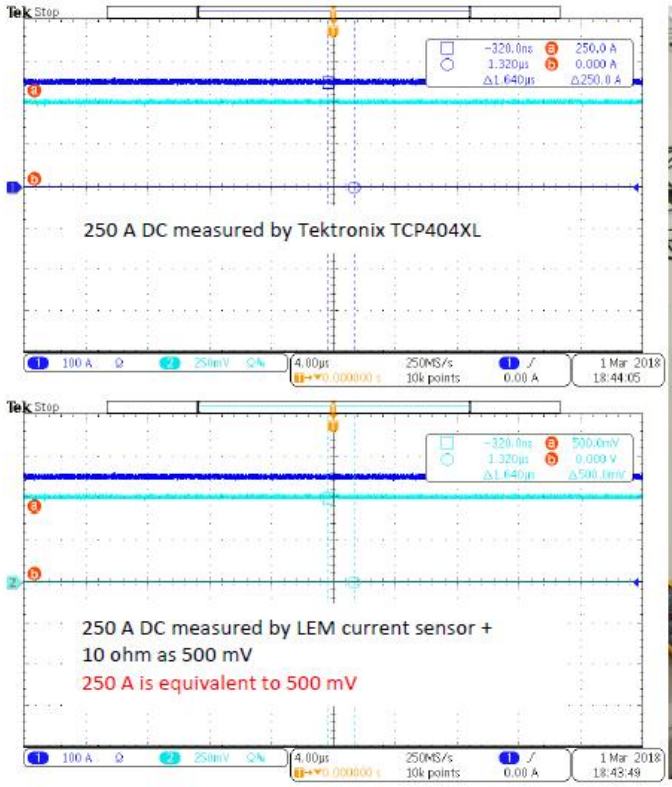
Tek Stop
250 A DC measured by Tektronix TCP404XL
Tek Stop
250 A DC measured by LEM current sensor +
10 ohm as 500 mV
250 A is equivalent to 500 mV

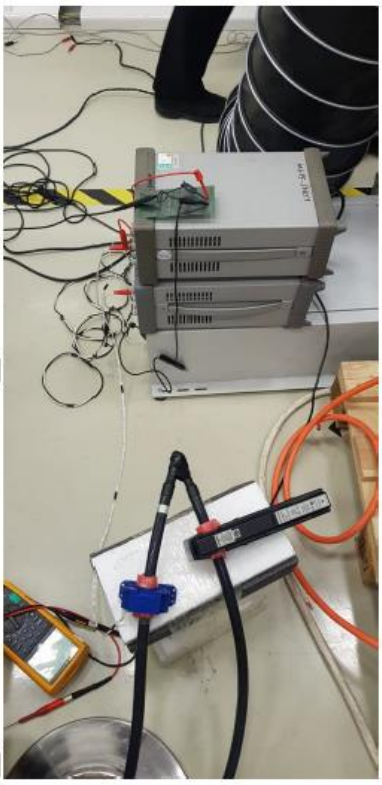

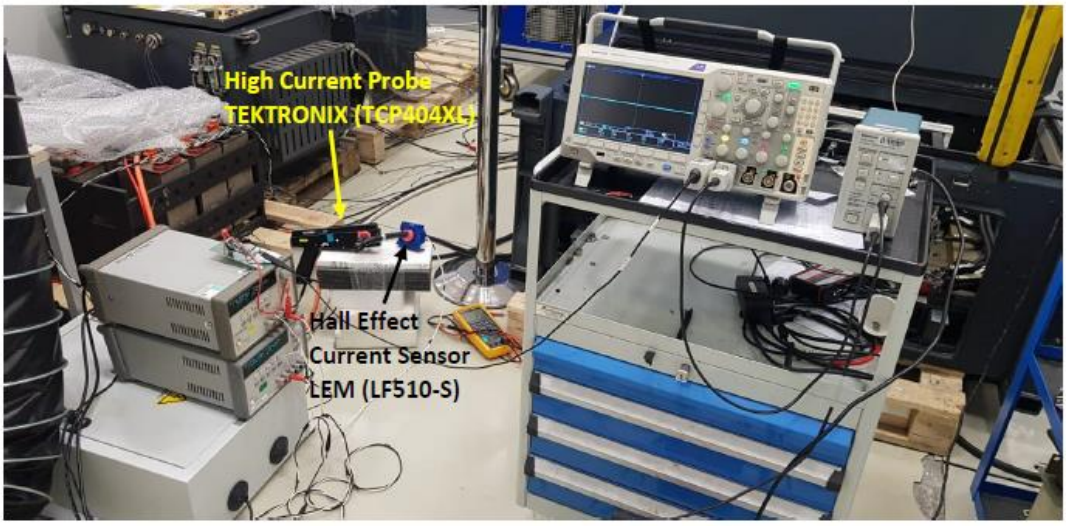
High Current Probe
TEKTRONIX (TCP404XL)
Hall Effect
Current Sensor
LEM (LF510-S)

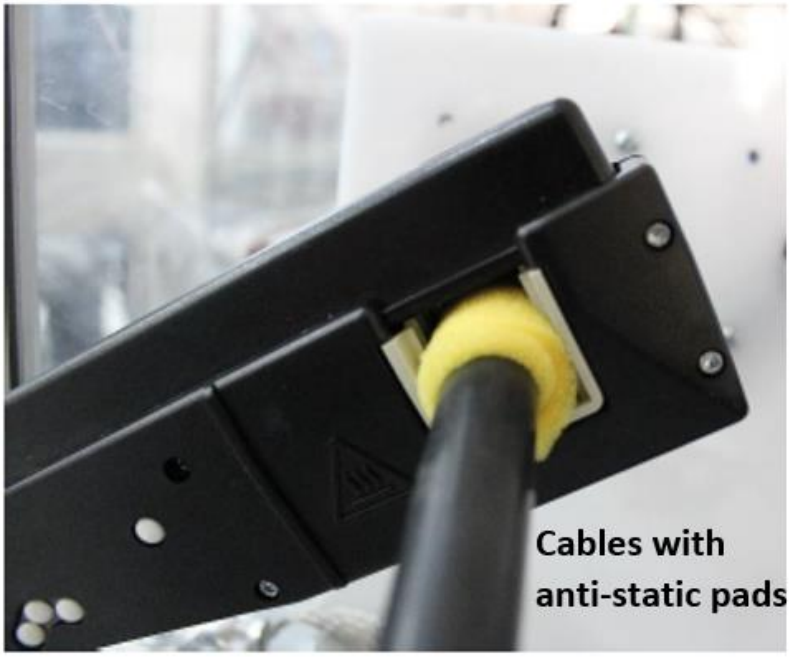
Cables with
anti-static pads


MS-PE-57111
EDM-KKH
SST-ETM
Tektronix
P5205A
100 MHz, High Voltage
Differential Probe

E. MATLAB Code for FFT Analysis

```
1
2 -    SamplingRate=100000;
3 -    SamplingPeriod=1/SamplingRate;
4 -    a = A1;
5 -    figure;
6
7 -    a=a-mean(a);
8 -    fft_cur=1*abs(fft(a)/(length(a)/2));
9 -    fft_cur_100=(fft_cur/(rms(a)*1.41421356))*100;
10 -   l=length(a);
11 -   f_axis=0.001*SamplingRate*(0:length(a)-1)/length(a);
12 -   bar(f_axis(1,1:1e4),fft_cur(1:1e4,1), 'BarWidth',1);
13 -   xlabel('Frequency (kHz)');
14
15 -   figure;
16
17 -   bar(f_axis(1,1:1e4),fft_cur_100(1:1e4,1), 'BarWidth',1);
18 -   xlabel('Frequency (kHz)');
19    %--------------------------------------------------------------------------
```